


2020-01-01

# Life Cycle Studies To Evaluate The Physiological And Biochemical Effects Of Copper Oxide And Surface-Coated Titanium Dioxide Nanoparticles On Green Onion (*allium Fistulosum*) And Carrot (*daucus Carota L.*) Plants: Insights Utilizing Two-Photon Microscopy And Spectroscopy

Yi Wang  
*University of Texas at El Paso*

Follow this and additional works at: [https://scholarworks.utep.edu/open\\_etd](https://scholarworks.utep.edu/open_etd)

 Part of the [Chemistry Commons](#), [Environmental Engineering Commons](#), and the [Environmental Sciences Commons](#)

---

## Recommended Citation

Wang, Yi, "Life Cycle Studies To Evaluate The Physiological And Biochemical Effects Of Copper Oxide And Surface-Coated Titanium Dioxide Nanoparticles On Green Onion (*allium Fistulosum*) And Carrot (*daucus Carota L.*) Plants: Insights Utilizing Two-Photon Microscopy And Spectroscopy" (2020). *Open Access Theses & Dissertations*. 3129.  
[https://scholarworks.utep.edu/open\\_etd/3129](https://scholarworks.utep.edu/open_etd/3129)

This is brought to you for free and open access by ScholarWorks@UTEP. It has been accepted for inclusion in Open Access Theses & Dissertations by an authorized administrator of ScholarWorks@UTEP. For more information, please contact [lweber@utep.edu](mailto:lweber@utep.edu).

LIFE CYCLE STUDIES TO EVALUATE THE PHYSIOLOGICAL AND BIOCHEMICAL  
EFFECTS OF COPPER OXIDE AND SURFACE-COATED TITANIUM DIOXIDE  
NANOPARTICLES ON GREEN ONION (*ALLIUM FISTULOSUM*) AND  
CARROT (*DAUCUS CAROTA* L.) PLANTS: INSIGHTS UTILIZING  
TWO-PHOTON MICROSCOPY AND SPECTROSCOPY

YI WANG

Doctoral Program in Chemistry.

APPROVED:

---

Jorge L. Gardea-Torresdey, Ph.D., Chair

---

Dino Villagran, Ph.D.

---

Geoffrey B Saupe, Ph.D.

---

Jie Xu, Ph.D.

---

Jose Angel Hernandez-Viezcas, Ph.D.

---

Stephen L. Crites, Jr., Ph.D.  
Dean of the Graduate School

Copyright ©

by

Yi Wang

2020

## **Dedication**

This thesis is dedicated to my parents and my husband, for their unconditional love and support.

I admire and love you.

Even with all the hustle and hard times, they let me know I will never walk alone.

LIFE CYCLE STUDIES TO EVALUATE THE PHYSIOLOGICAL AND BIOCHEMICAL  
EFFECTS OF COPPER OXIDE AND SURFACE-COATED TITANIUM DIOXIDE  
NANOPARTICLES ON GREEN ONION (*ALLIUM FISTULOSUM*) AND  
CARROT (*DAUCUS CAROTA* L.) PLANTS: INSIGHTS UTILIZING  
TWO-PHOTON MICROSCOPY AND SPECTROSCOPY

by

YI WANG, B.S.

DISSERTATION

Presented to the Faculty of the Graduate School of

The University of Texas at El Paso

in Partial Fulfillment

for the Requirements

of the Degree of

DOCTOR OF PHILOSOPHY

Department of Chemistry and Biochemistry

THE UNIVERSITY OF TEXAS AT EL PASO

August 2020

## Acknowledgments

I would like to express my gratitude to my advisor, Dr. **Jorge Gardea-Torresdey** of the Chemistry and Biochemistry Department at The University of Texas at El Paso, not only because of pushing me to achieve more goals and many opportunities he gave me, but also his leadership and for caring so genuinely for me in several things. I joined his group in fall 2016, and since then, his advice, encouragement, lessons of life attitude, and support have been never-ending. I believed in him when the first moment I met him. There is no better mentor than the one who helps you and cares about you so much. Thanks to Dr. Gardea for your guidance and patience through all these wonderful years.

I am indebted to **Dr. Jose R Peralta-Videa**, **Dr. Jose Hernandez-Viezcas (Pepe)**, and **Dr. Keni Cota-Ruiz**, for all the time advising and yearlong support my studies. I also want to thank **Dr. Genhua Niu** and **Dr. Youping Sun** from the Texas A&M AgriLife Research center at El Paso, who took care of me when I need anything or any help in the research center. **Dr. Mansor** and **Dr. Jie Xu**, thank for your kindly cooperation. It is my pleasure to work with and learn from you. My committee member, **Dr. Dino Villagran**, **Dr. Jie Xu**, and **Dr. Geoffrey B Saupe**, thank you all. I learn a lot in your class, and your teaching skill really impresses me. Also, thank you for giving me a helping hand all the time. I am truly grateful you have been there for me.

Thanks to my colleagues for lending their helping hand and being my friends: Dr. Wenjuan Tan, Dr. Swati Rawat, Dr. Nubia Zuverza-Mena, Dr. Aidee Medina, Mariana Molina-Hernandez, and Loren Ochoa. You guys make me become not just a better scientist also a better person. and I look forward to continuing to work with you. Thank you for being there for me.

I also want to thank the financial support from the University of Texas at El Paso and its Graduate School, the College of Science and the Department of Chemistry and Biochemistry for the teaching assistantship and funds, also thanks United States Department of Agriculture (USDA),

the University of California- Center for Environmental Implications of Nanotechnology (UC-CEIN), and the National Science Foundation (NSF) for supporting my academic research.

## Abstract

With the recent increase of nanomaterial production, nano copper oxide (nCuO) and surface-modified titanium dioxide nanoparticles (nTiO<sub>2</sub>) are among the most widely applied nanoparticles in industry and daily lives. Their use has resulted in accumulation in soils as a consequence of their direct or indirect release. Hence, these NPs may raise a potential risk to crops cultivated in soils. Moreover, the physiological effects of nCuO on green onion (*Allium fistulosum*) and surface-coated nTiO<sub>2</sub> on full-grown carrot (*Daucus carota* L.) are still unknown. Green onion is characterized by its high content of the antioxidant allicin, and carrot is a worldwide economic and nutritionally important taproot crop. After environmental release, NPs may remain in the soil for a long time and undergo surface chemical/physical changes. Currently, no studies have addressed the soil weathering effects on the chemistry of surface-coated TiO<sub>2</sub> and their implications on belowground carrots. Thus, this research was aimed at evaluating the physiological and biochemical responses of green onion and carrot plants after being exposed to nCuO and surface-coated nTiO<sub>2</sub>, respectively.

This research was performed into three phases. In phase I, green onions were harvested after growing for 80 days in soil treated with nano (nCuO), bulk (bCuO), and CuSO<sub>4</sub> at 75–600 mg/kg]. Two-photon microscopy images confirmed the Cu uptake in nCuO and bCuO-treated roots. Plants cultivated with soils at 150 mg/kg of the Cu-based compounds exhibited a higher root Cu content when treated with nCuO, in comparison to bCuO, CuSO<sub>4</sub>, and control ( $p \leq 0.05$ ). The nCuO increased root Ca and Fe, bulb Ca, and Mg, while bCuO reduced root Ca and Mg, compared with controls ( $p \leq 0.05$ ). At all evaluated concentrations, nCuO and CuSO<sub>4</sub> augmented leaf allicin compared with control. The activity of antioxidant enzymes was differentially affected by the treatments. In phase II, carrots grew in soils amended with nTiO<sub>2</sub> at 0, 100, 200, and 400 mg/kg for 115 days until plant maturity. Three types of nTiO<sub>2</sub> in the form of pristine, hydrophilic, and hydrophobic surface-coated were applied. The fresh biomass of the taproot was significantly decreased by all nTiO<sub>2</sub> forms at 400 mg/kg, compared to control. Remarkably, an abnormal



increase of taproot splitting was found in plants treated with all nTiO<sub>2</sub> forms. It was more significant in plants exposed to pristine nTiO<sub>2</sub> treatments. In carrots treated with the surface-coated nTiO<sub>2</sub>, the accumulation of Ca, Mg, Fe, and Zn increased in leaves; but Mg, Mn, and Zn decreased in taproots. In phase III, surface-coated nTiO<sub>2</sub> were aged in the soil for four months at 0, 100, 200, and 400 mg/kg, and their effect on carrot development was investigated. The aged nTiO<sub>2</sub> with surface coatings improved taproot and leaf fresh biomass, plant height, total taproot length, and taproot top perimeter, compared to control. Hydrophilic and hydrophobic-coated nTiO<sub>2</sub> showed more stimulation effects on plant development. Moreover, changes in surface charges of aged pristine, hydrophilic, and hydrophobic surface-coated nTiO<sub>2</sub> were detected. Additionally, the accumulation of nutrient elements such as Ca, Zn, and K in roots, Fe in leaves, and Mg in taproots was enhanced by aged nTiO<sub>2</sub>.

Overall, our results demonstrated that nCuO improved the nutrient and allicin contents in green onion, which suggests they might be used as a nanofertilizer. Meanwhile, the overall growth of carrots was inhibited by the unaged nTiO<sub>2</sub>, while benefited by the aged nTiO<sub>2</sub>. The future regulation of nTiO<sub>2</sub> release into soils should consider its surface coating properties since plant responses depended on the nTiO<sub>2</sub> outer structure. These studies provide valuable insights into the interaction of nCuO with green onion, and aged and un-aged surface-coated nTiO<sub>2</sub> with carrots.

## Table of Content

Dedication.....	iii
Acknowledgments.....	v
Abstract.....	vii
List of Figure.....	xi
List of Table.....	xiv
Chapter 1: Introduction.....	1
General Objectives.....	6
Research Questions.....	6
Hypothesis.....	7
Chapter 2: Spectroscopic and Microscopic Studies Demonstrate Nutrient Improvement in Green Onion ( <i>Allium fistulosum</i> ) Plants Exposed to CuO Nanoparticles: Its Role as a Potential Nanofertilizer .....	14
2.1 Introduction.....	14
2.2 Materials and Methods.....	16
2.2.1 Preparation of nCuO <sub>2</sub> amended Soil .....	16
2.2.2 Seed germination and plant growth .....	17
2.2.3 Chlorophyll measurement.....	18
2.2.4 Quantification of allicin .....	18
2.2.5 Antioxidant enzymatic activities.....	18
2.2.6 Essential Element Quantification by ICP-OES and Two-photon microscopy sample preparation .....	19
2.2.7 Statistical analysis of the data .....	20
2.3. Result and Discussion.....	20
2.3.1 Uptake of nCuO and bCuO particles .....	20
2.3.2 Copper Content in Roots, Bulbs, and Leaves .....	21
2.3.3 Elements accumulation in tissues .....	24
2.3.3.1 Macronutrient elements in roots .....	24
2.3.3.2 Micronutrients and aluminum in roots.....	27
2.3.3.3 Essential elements in bulbs and leaves .....	29
2.3.4 Plant growth and chlorophyll content.....	30
2.3.5 Allicin content.....	30
2.3.6 Antioxidant defense system in roots and leaves .....	32
2.4. Conclusions.....	33
Chapter 3: Effects of Different Surface-coated nTiO <sub>2</sub> on Full-life Grown Carrot Plants: Impacts on Root Splitting, Essential Elements Accumulation, and Ti Uptake .....	35
3.1 Introduction.....	35

3.2. Materials and Methods.....	37
3.2.1 Preparation of nTiO <sub>2</sub> and soil treatments.....	37
3.2.2 Seed germination and plant cultivation.....	38
3.2.3 Plant harvest and agronomic parameters .....	39
3.2.4 Ti uptake and nutrient element concentration.....	39
3.2.5 Two-photon microscopy .....	39
3.2.6 Statistical analysis.....	40
3.3. Results and discussions.....	40
3.3.1 Ti uptake .....	40
3.3.2 Agronomical parameters.....	43
3.3.2.1 Leaf fresh weight and plant height.....	43
3.3.2.2 Taproot morphology, splitting, and fresh weight.....	45
3.3.3 Two-photon microscopy image of root Ti uptake .....	49
3.3.4 Micro and macro elements in leaf.....	51
3.3.5 Micro and macro elements in secondary roots .....	55
3.3.6 Micro and macro elements in the taproot .....	59
3.4 Conclusion .....	60
Chapter 4: Aging Process as A Sustainable Strategy to Alleviate Phytotoxicity of Nanoparticles: Soil-Aged Surface-Coated nano TiO <sub>2</sub> Improve Full-grown Carrot Physiological Performance .	
4.1 Introduction.....	62
4.2 Materials and Methods.....	64
4.2.1 Preparation of nTiO <sub>2</sub> aging in soil .....	64
4.2.2 Seed germination and plant cultivation.....	65
4.2.3 Plant harvest and agronomic parameters .....	66
4.2.4 Ti uptake and nutrient element concentration.....	66
4.2.5 Sugar and Starch .....	67
4.2.6 Statistical analysis.....	67
4.3. Results and Discussion .....	68
4.3.1 Ti uptake by roots changed along with the zeta potential of aged nTiO <sub>2</sub> .....	68
4.3.2 Taproots fresh biomass were improved by the two aged nTiO <sub>2</sub> with surface coatings.....	71
4.3.3 Leaves fresh biomass and height were improved by aged surface-coated nTiO <sub>2</sub> .....	74
4.3.4 Taproot morphology .....	74
4.3.5 Nutrient element accumulations in roots and leaves.....	77
4.3.6 Nutrient element accumulations in taproot flesh and core.....	80
4.3.7 Biomacromolecule contents.....	83
4.4. Conclusion .....	85
Chapter 5: Conclusion.....	87
Supporting material for Chapter 2-4 .....	89
References.....	96
Vita.....	121

## List of Figure

- Fig. 2.1. Two-photon microscopy images of root samples of control plants (a) and plants treated with (b) CuSO<sub>4</sub>, (d) bCuO and (f) nCuO at 600 mg/kg. The inserted pictures correspond to (c) CuSO<sub>4</sub> in DI water, (e) pure bCuO suspension in DI and (g) pure nCuO suspension in DI. The fluorescence of root cell walls and vascular tissue is shown. Arrows inside the square indicate fluorescence from bCuO (d) or nCuO (f) particles. .... 21
- Fig. 2.2. Copper concentration (mg/kg DW) in scallion roots (a), bulbs (b) and leaves (c) exposed to nCuO, bCuO, and CuSO<sub>4</sub> at 0, 75, 150, 300 and 600 mg/L. Data are the average of three replicates ± standard error (SE). Lowercase letters stand for statistical differences among different compounds at the same concentration. Uppercase letters represent significant differences among different concentrations of the same compound ( $p \leq 0.05$ ,  $n = 3$ ). .... 23
- Fig. 2.3. Concentration (mg/kg DW) of the elements (a) Ca, (b) K, (c) Mg, (d) P, (e) Fe, (f) Mn, (g) Al, and (h) Ni, in scallion roots. Plants were cultivated for 80 days in soil amended with nCuO, bCuO, and CuSO<sub>4</sub> at 0 (control), 75, 150, 300 and 600 mg of Cu/kg of soil. Data are averages of three replicates ± standard error (SE). Lowercase letters stand for statistical differences among different compounds at the same concentration. Uppercase letters represent significant differences among different concentrations of the same compound ( $p \leq 0.05$ ). .... 27
- Fig. 2.4. Concentration (mg/kg DW) of the essential elements (a) Ca, (b) Mg, and (c) Ni in dry bulbs of scallion plants. Green onions were cultivated for 80 days in soil amended with nCuO, bCuO, and CuSO<sub>4</sub> at 0 (control), 75, 150, 300 and 600 mg of Cu/kg of soil. Data are averages of three replicates ± standard error (SE). Lowercase letters represent statistical differences among different compounds at the same concentration. Uppercase letters represent significant differences among different concentrations of the same Cu-based compounds ( $p \leq 0.05$ ). .... 29
- Fig. 2.5. Alliin content (w%) in leaves of plants cultivated for 80 days in soil amended with nCuO, bCuO, and CuSO<sub>4</sub> at 0, 75, 150, 300 and 600 mg/L. Data are averages of three replicates ± standard error (SE). Uppercase letters stand for significant differences among different compounds evaluated at the same concentration. Asterisks (\*) represent statistical differences in treatments compared to control ( $n=3$ ,  $p \leq 0.05$ ). .... 31
- Fig. 2.6. Enzyme activities of CAT, GPOX, SOD, and APOX in the roots and leaves of soil-grown green onion plants. Chinese scallions were exposed to nCuO, bCuO, and CuSO<sub>4</sub> at 0, 75, 150, 300 and 600 mg/L. Data are the average of three replicates ± standard error (SE). Uppercase letters represent statistical differences among different compounds tested at the same concentration. Asterisks (\*) represent statistical differences in treatments compared to control ( $n=3$ ,  $p \leq 0.05$ ). .... 33
- Fig. 3.1. Titanium concentration (mg/kg DW) in carrot roots exposed to pristine, hydrophilic, and hydrophobic coated nTiO<sub>2</sub> at 0, 100, 200 and 400 mg/kg. Data are the average of three replicates ± SE. Lowercase letters stand for statistical differences between different compounds at the same

concentration. Asterisk represent significant differences with respect to control ( $p \leq 0.05$ ,  $n = 3$ ). ..... 42

Fig. 3.2. (A) Leaf fresh biomass (g) and (B) plant height (cm) of carrots exposed to pristine, hydrophilic, and hydrophobic coated nTiO<sub>2</sub> at 0, 100, 200 and 400 mg/kg. Data are the average of three replicates  $\pm$  SE. Lowercase letters stand for statistical differences between different compounds at the same concentration. Asterisk represent significant differences with respect to control ( $p \leq 0.05$ ,  $n = 3$ ). ..... 45

Fig. 3.3. Taproot of control (a), un-coated nTiO<sub>2</sub> treated plants at 100 (b), 200 (c) and 400 (d) mg/kg, hydrophilic coated nTiO<sub>2</sub> treated plants at 100 (e), 200 (f) and 400 (g) mg/kg, and hydrophobic coated nTiO<sub>2</sub> treated plants at 100 (h), 200 (i) and 400 (j) mg/kg..... 48

Fig. 3.4. Taproot fresh biomass (g) of carrots exposed to pristine, hydrophilic, and hydrophobic coated nTiO<sub>2</sub> at 0, 100, 200 and 400 mg/kg. Data are the average of three replicates  $\pm$  SE. Lowercase letters stand for statistical differences between different compounds at the same concentration. Asterisk represent significant differences with respect to control ( $p \leq 0.05$ ,  $n = 3$ ). ..... 49

Fig. 3.5. Two-photon microscopy images of carrot (A) control root and roots treated with (B) pristine, (C) hydrophilic, (D) hydrophobic coated nTiO<sub>2</sub> at 400 mg/kg soil, and. The fluorescence of root cell walls and vascular tissue is shown. Fluorescence from (C) hydrophilic, (D) hydrophobic coated nTiO<sub>2</sub> are pointed out by arrows inside the square. .... 51

Fig. 4.1. Titanium concentration (mg/kg DW) in carrot roots exposed to 4-month-aged pristine, hydrophilic, and hydrophobic coated nTiO<sub>2</sub> at 0, 100, 200 and 400 mg/kg. Data are the average of three replicates  $\pm$  SE. Lowercase letters stand for statistical differences between different compounds at the same concentration. Asterisks represent significant differences between treatments and control ( $p \leq 0.05$ ,  $n = 3$ )...... 70

Fig. 4.2. Effect of pH (ranged from 3-10) on the  $\zeta$ -potential of 4-month-aged (A) pristine, (B) hydrophilic coated and (C) hydrophobic coated nTiO<sub>2</sub> at 400 mg/kg suspended in MW..... 71

Fig. 4.3. (A) Taproot fresh biomass, (B) Leaf fresh biomass (g) and (C) plant height (cm) of carrot exposed to 4-month-aged pristine, hydrophilic, and hydrophobic coated nano TiO<sub>2</sub> at 0, 100, 200 and 400 mg/kg soil. Data are the average of three replicates  $\pm$  SE. Lowercase letters stand for statistical differences between different compounds at same concentration. Asterisks represent significant differences between treatments and control ( $p \leq 0.05$ ,  $n = 3$ ). ..... 73

Fig. 4.4. (A) Taproot total length (cm) and (B) taproot top perimeter (cm) of carrots exposed to 4-month-aged pristine, hydrophilic, and hydrophobic coated nTiO<sub>2</sub> at 0, 100, 200 and 400 mg/kg. Data are the average of three replicates  $\pm$  SE. Lowercase letters stand for statistical differences between different compounds at the same concentration. Asterisks stand for significant differences between treatments and control ( $p \leq 0.05$ ,  $n = 3$ ). ..... 76

Fig. 4.5. Taproot (A) sugar and (B) starch contents of carrots exposed to 4-month-aged pristine, hydrophilic, and hydrophobic coated nTiO<sub>2</sub> at 0, 100, 200 and 400 mg/kg. Data are the average of three replicates ± SE. Lowercase letters stand for statistical differences between different compounds at the same concentration. Asterisks mean statistical differences between treatments and control ( $p \leq 0.05$ ,  $n = 3$ ). ..... 84

Fig. S2.1: Plant height (a), fresh biomass (b), single leaf weight (c) and water content (d) of scallion plants grown under nCuO, bCuO, and CuSO<sub>4</sub> treatments. Data are averages of three replicates ± standard error (SE). Lowercase letters stand for statistical differences between among different compounds at same concentration. Uppercase letters represent significant differences among different concentrations of the same compounds ( $p \leq 0.05$ ,  $n = 3$ )..... 92

Fig. S2.2: Plant leaf chlorophyll *a* (a), chlorophyll *b* (b) and total carotenoid content of scallion plants grown under nCuO, bCuO, and CuSO<sub>4</sub> treatments. Data are averages of three replicates ± standard error (SE). Lowercase letters stand for statistical differences among different compounds at same concentration. Uppercase letters indicate significant differences among different concentrations of the same compounds ( $p \leq 0.05$ ,  $n = 3$ ). ..... 92

Fig. S3.1. Hydrodynamic size distribution of (A) hydrophobic, (B) pristine, and (C) hydrophobic nTiO<sub>2</sub> particles suspended in MW. .... 94

Fig. S3.2. Taproot core diameter (cm) of carrots exposed to pristine, hydrophilic, and hydrophobic coated nTiO<sub>2</sub> at 0, 100, 200 and 400 mg/kg. Data are the average of three replicates ± SE. Lowercase letters stand for statistical differences between different compounds at the same concentration. Asterisk represent significant differences with respect to control ( $p \leq 0.05$ ,  $n = 3$ ). ..... 95

Fig. S3.3. The inserted pictures correspond to (A) pure pristine, (B) pure hydrophilic and (C) pure hydrophobic coated nTiO<sub>2</sub> suspension in DI. .... 95

## List of Table

Table 3.1. Concentration (mg/kg DW) of micro- and macro-elements in carrot leaves (Ca, Mg, Fe, Se and Zn), secondary roots (Zn) and taproots (K, Mg, Mn and Zn). Plants were cultivated for 115 days in soil amended with pristine, hydrophilic and hydrophobic coated nTiO <sub>2</sub> at 0 (control), 100, 200 and 400 mg of Ti/kg of soil. Data are averages of 3 replicates ± Standard Error (SE). .....	56
Table 4.1. Concentration (mg/kg DW) of micro- and macro-elements in carrot leaves (Ca, Mg, Fe, Se and Zn), secondary roots (Zn) and taproots (K, Mg, Mn and Zn). Plants were cultivated for 115 days in soil amended with 4-month-aged pristine, hydrophilic and hydrophobic coated nTiO <sub>2</sub> at 0 (control), 100, 200 and 400 mg of Ti/kg of soil. Data are averages of 3 replicates ± Standard Error (SE). .....	81
Table S2.1: Physiochemical characterization of nCuO and bCuO particles .....	89
Table S2.2: The effect of two main independent variables (compound and concentration) and the respective interactions on the uptake of Cu in roots, bulbs and leaves in plants exposed to nCuO, bCuO or CuSO <sub>4</sub> at 0, 75, 150, 300 and 600 mg/kg. (n = 3).....	89
Table S3.1. Physical characterization of nano-TiO <sub>2</sub> . .....	92

## Chapter 1: Introduction

Innovations in nanoscience have revolutionized technology, becoming one of the fastest developing industry trends of the 21<sup>st</sup> century. The global market of nanotechnology was \$10.6 billion in 2018 and is estimated to achieve \$22.3 billion by 2024 (Tewari and Baul, 2019). Nanoparticles (NPs) are defined by their small size with at least one dimension within  $10^{-9}$  m, which imparts unique physical and chemical properties, compared to larger bulk particles (Zuverza-Mena et al., 2017). Engineered nanoparticles (ENPs) with these properties are designed for specialized applications. The enhanced biocompatibility and reactivity of ENPs have allowed their integration into the industry, consumer goods, medicine, and energy, among others (Abdussalam-Mohammed, 2019; Ahmadi et al., 2019). There are also promising potential applications of ENPs in agriculture (Chhipa, 2019; White and Gardea-Torresdey, 2018). Nano-sized elements can function as fertilizers or pesticides that provide nutrition and combat phytopathogens, respectively, in a variety of plant species (Huang et al., 2015; Liu and Lal, 2015). Nanopesticides and nano fertilizers may be more efficient and might reduce application rates over traditional products (Kah, 2015). Nonetheless, many studies have emerged reporting ENP-induced toxicity. After use, a large number of ENPs are directly or indirectly released into the environment. Soil and bodies of water are considered to be the most massive sinks for ENPs. This may threaten agricultural ecosystems. There exists a need to understand the various effects of ENPs exposure to plants, develop safety protocols for NPs applications and disposal in the agriculture field, and enforce their proper regulation.

By 2010, the manufacturing of copper oxide NPs (nCuO), one of the most extensively applied Cu-based materials, was higher than 200 metric tons per year (Keller et al., 2013a). CuO-based NPs have been widely utilized in batteries, lubricants polymers, pigments, gas sensors, and



catalysts, among others (Anjum et al., 2015). Moreover, the production and use of nCuO in the agrosystem are increasing (European Commission, 2018). The production of nano titanium dioxide (nTiO<sub>2</sub>) is at the top list of the most manufactured ENPs worldwide (Mitrano et al., 2015; Piccinno et al., 2012). The annual production of nTiO<sub>2</sub> would nearly reach 2.5 million metric tons in 2025, which would convert virtually 100% of the total TiO<sub>2</sub> market to nano (Robichaud et al., 2009). Production of TiO<sub>2</sub> is mainly distributed into cosmetics (sunscreens), plastics, and coatings (Piccinno et al., 2012). To improve the performance and to meet the demands from various costumers, surface-modified nTiO<sub>2</sub> surfaces have been widely used (Pancrecius et al., 2018). Better appearance, properties, or advanced functionalities such as corrosion resistance, less catalytic degradation, self-cleaning, and depolluting abilities are achieved in hydrophilic or hydrophobic-coated nTiO<sub>2</sub> (Bergamonti et al., 2015; Calia et al., 2017; Chen et al., 2019; Colangiuli et al., 2019). Based on their exponential production, more massive releases of nTiO<sub>2</sub> to the environment are expected (Keller and Lazareva, 2014). The estimated emissions into soil and water in 2010 were up to 23,130 and 36,664 metric tons/year, respectively (Keller and Lazareva, 2014). Additionally, some wastewater and sewage sludges, which contain TiO<sub>2</sub>, might be used to treat agricultural soils (Cornelis et al., 2014). The interaction between coated nTiO<sub>2</sub> and soil is complicated due to the various soil components, including humic and non-humic compounds, microbial community structure, soil ionic strength, among others (Fig. 1) (Rawat et al., 2018a). Thus, the influence that TiO<sub>2</sub> ENPs have on plants will depend on several factors, which include surface coating properties (surface area, charge, hydrophilicity, and suspension stability), soil type, plant species, growth stage, and exposure method (Tan et al., 2018).

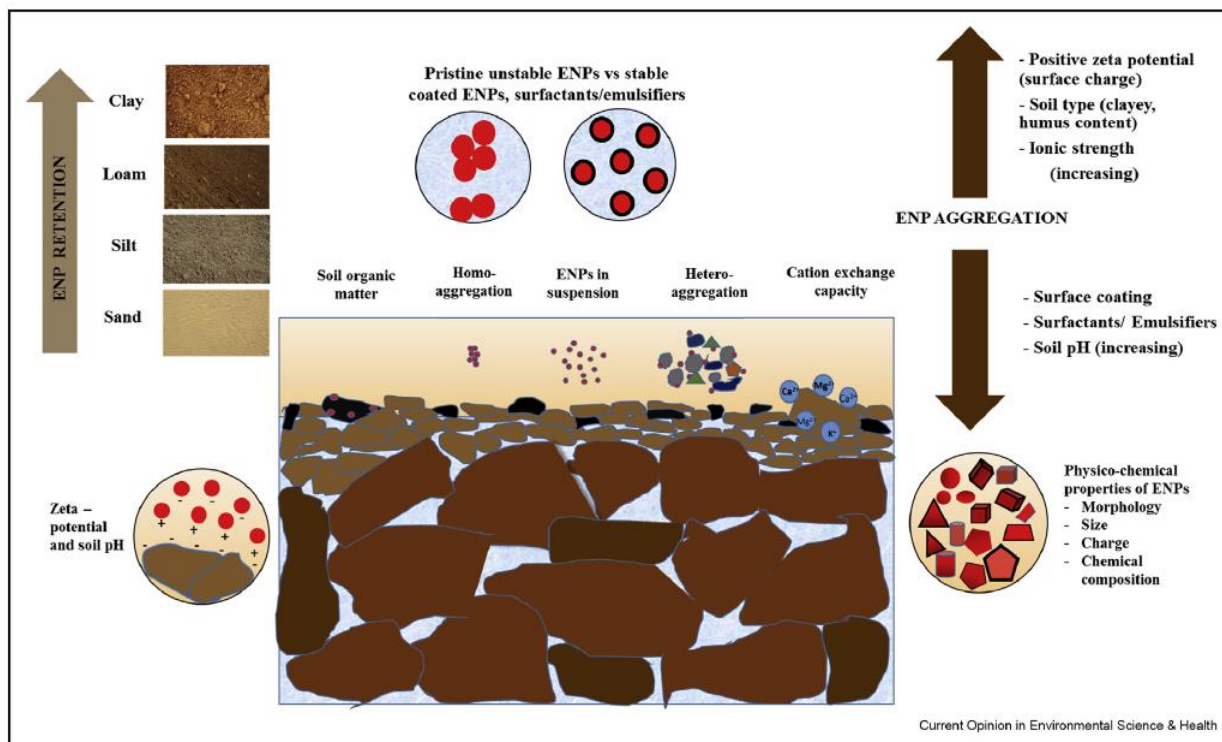


Fig. 1.1 Factors that affect the fate and transport of ENPs in soil. *Reproduced from* Rawat et al. (2018)

Previously, various studies have been done to investigate the effect of exposing nCuO and nTiO<sub>2</sub> to terrestrial plants. Servin et al. (2013) treated cucumber (*Cucumis sativus* L.) with 0 to 750 mg/kg nTiO<sub>2</sub> in sandy loam soil and cultivated for 150 days. The  $\mu$ -XRF and  $\mu$ -XANES analysis showed a root to fruit translocation without biotransformation of TiO<sub>2</sub>, which suggested a potential risk to human health through the food chain. Moreover, nTiO<sub>2</sub> at 750 mg/kg increased chlorophyll concentration in leaves compared with control. The FTIR spectra suggested an alteration of macromolecule contents (amide, lignin, and carbohydrates) in the fruit of cucumber treated with nTiO<sub>2</sub> ( $p \leq 0.05$ ). In addition, more K and P in fruit were found in plants treated with 500 mg/kg nTiO<sub>2</sub>, compared with control. In another study, the impact of released nTiO<sub>2</sub> on the nutritional quality of lettuce (*Lactuca sativa* L.) was investigated (Hu et al., 2020). After

hydroponically exposing plants to nTiO<sub>2</sub> suspensions at 0-400 mg/L for one week, the contents of Ca, Mg, Mn, Fe, Zn, and B in lettuce edible tissues were negatively affected. On the other hand, the root, shoot dry biomass, and pigment accumulations were significantly increased. Also, intense oxidative stress resulted in cell structure damage of root cells and thylakoids. The potential positive impact of applying nCuO in the agriculture field has been proposed. In a greenhouse experiment, 1-2 mL nCuO suspension at 500 mg/L was foliarly applied to 30-day-old tomato (*Solanum lycopersicum*) seedlings (Ma et al., 2019). The *Fusarium oxysporum* f. sp. *lycopersici* infection in plants was suppressed by this means, with increased plant growth. Three genes (Pathogenesis-related promoters, polyphenol oxidase, and plant resistance protein 1A1) related to plant defense were altered by nCuO treatments. A similar suppression effect was also found in watermelon (*Citrullus lanatus*). At 1000 mg/L, a foliar application of nCuO suspension to watermelon significantly repressed fungal disease induced by *Fusarium oxysporum* f. sp. *Niveum* (Borgatta et al., 2018). In addition, nCuO acted as potential agricultural fertilizer has been suggested by Wang et al. (2019) in the growth of lettuce (*var. ramosa Hort.*). Results showed that nCuO treatments increased lettuce shoot biomass (by 16.3–19.1%), while bulk CuO did not. It may be due to the enhanced plant photosynthesis system, with higher transpiration rate and stomatal conductance.

Scallion or green onion (*Allium fistulosum*), is used as an essential seasoning worldwide (Tabassum et al., 2016). They have a high concentration of allicin, flavonoids, vitamins, as well as other organosulfur compounds (Yin et al., 2003). Allicin, one of the most distinctive organosulfur compounds, is responsible for the pungency and flavor in *Allium* monocotyledonous flowering plants (Block et al., 1992). Additionally, scallions pose antioxidant and antibacterial properties and have shown the potential to benefit the cardiovascular system (Chan et al., 2013). In 2007, the top five producers countries (Japan, China, Republic of Korea, Nigeria, and New

Zealand) registered together more than three million metric tons of scallions (“The Top 5 Green Onion Producing Countries,” 2007). However, the scallion is not a very well-studied species in the *Allium* family. The effect of nCuO exposure on the growth of green onion is unknown.

On the other hand, carrot (*Daucus carota* L.) are economically relevant root crops that contain high nutritional value. Their 2018 annual total production was >2,450 million pounds in the U.S., representing a market price of >670 million dollars (Parr et al., 2019). Vegetables contribute to almost ~27% of the total consumed vitamin A in the U.S (Arscott and Tanumihardjo, 2010). The roots are the main consumed portion of many vegetables. Since they are in direct contact with soil, they will interact with the soil-incorporated ENPs. Thus, there is a need to investigate the effect of unaged/aged ENPs on the development of belowground crops through combination testing strategies (Grindal et al., 2004). Currently, the studies evaluating the effects of TiO<sub>2</sub> ENPs on root vegetables are very limited. Additionally, the weathering effects of different surface-coated nTiO<sub>2</sub> in soil and their effects on plant development are still undescribed.

The two-photon microscopy is gaining attention to study the fate of ENPs (Deng et al., 2020). Compared with other microscopy techniques such as scanning electron microscopy (SEM) or transmission electron microscopy (TEM), the two-photon microscopy has the advantage of penetrating the sample and view the internal structure via fluorescence. Additionally, samples are easily prepared, with no further damage during the detection while operated at room temperature. Since nCuO and nTiO<sub>2</sub> have self-fluorescence, no further dyeing process is needed, which makes nCuO and nTiO<sub>2</sub> good candidates for a two-photon microscopy study.

In this work, there were three study phases. In phase I, the physiological and biochemical effects of nCuO on green onion was studied. Green onions were harvested after growing for 80 days in soil treated with nano (nCuO), bulk (bCuO), and CuSO<sub>4</sub> at 75–600 mg/kg. In phase II, the

effects of different surface-coated nTiO<sub>2</sub> on carrot plant development were investigated. Carrots were grown in soils amended with nTiO<sub>2</sub> at 100, 200, and 400 mg/kg for 115 days until full-plant maturity. Three types of nTiO<sub>2</sub> in the form of pristine and hydrophilic and hydrophobic surface-coated were applied. In phase III, to investigate the effect of aging, differently surface-coated nTiO<sub>2</sub> were weathered in natural soil at 0, 100, 200, and 400 mg/kg for four months. Thereafter, seeds of carrot (*Daucus carota* L.) were sown in those soils and grown until full maturity. In all three phases, the agronomic parameters of plant growth and essential element accumulation were determined. The penetration and uptake of nCuO/nTiO<sub>2</sub> were obtained by inductively coupled plasma-optical emission spectroscopy (ICP-OES) and two-photon microscopy.

#### **GENERAL OBJECTIVES**

1. To evaluate the physiological and biochemical effect of nCuO on green onion plants (*Allium fistulosum*).
2. To investigate the surface coating effect (pristine, hydrophilic, and hydrophobic) of nanoTiO<sub>2</sub> on the physiological and biochemical responses of carrot (*D. carota* L.) grown in ENPs-amended soils.
3. To study the soil-weathering effect of different surface-coated nano TiO<sub>2</sub> on carrot plant development.

#### **RESEARCH QUESTIONS**

1. How will the allicin content in green onion be affected by nCuO exposure? What are the changes in antioxidant enzymes that green onion plants will present?

2. How deep could nTiO<sub>2</sub> penetrate into the main carrot root? Could they enter the inner section?
3. Will the different coated-nano TiO<sub>2</sub> undergo the same aging process? Will weathered coated-nano TiO<sub>2</sub> differently affect plants?
4. Is it necessary to regulate the use of nCuO/nTiO<sub>2</sub>? Do they have potential applications in agriculture?

### **HYPOTHESIS**

1. The exposure of nCuO will improve the development of green onion plants.
2. The nano TiO<sub>2</sub> with the diverse surface coating will be differently uptaken by carrot, and will affect plant development in particular forms.
3. The aging process will change the initial physiological and biochemical responses of plants exposed to unaged ENMs.

### **References:**

Abdussalam-Mohammed, W., 2019. Review of Therapeutic Applications of Nanotechnology in Medicine Field and its Side Effects. *J. Chem. Rev.* 1, 243–251.

<https://doi.org/10.33945/SAMI/JCR.2019.3.5>

Ahmadi, M.H., Ghazvini, M., Nazari, M.A., Ahmadi, M.A., Pourfayaz, F., Lorenzini, G., Ming, T., 2019. Renewable energy harvesting with the application of nanotechnology: A review. *Int. J. Energy Res.* <https://doi.org/10.1002/er.4282>

- Anjum, N.A., Adam, V., Kizek, R., Duarte, A.C., Pereira, E., Iqbal, M., Lukatkin, A.S., Ahmad, I., 2015. Nanoscale copper in the soil–plant system – toxicity and underlying potential mechanisms. *Environ. Res.* 138, 306–325. <https://doi.org/10.1016/J.ENVRES.2015.02.019>
- Arscott, S.A., Tanumihardjo, S.A., 2010. Carrots of Many Colors Provide Basic Nutrition and Bioavailable Phytochemicals Acting as a Functional Food. *Compr. Rev. Food Sci. Food Saf.* 9, 223–239. <https://doi.org/10.1111/j.1541-4337.2009.00103.x>
- Bergamonti, L., Alfieri, I., Lorenzi, A., Predieri, G., Barone, G., Gemelli, G., Mazzoleni, P., Raneri, S., Bersani, D., Lottici, P.P., 2015. Nanocrystalline TiO<sub>2</sub> coatings by sol–gel: photocatalytic activity on Pietra di Noto biocalcarene. *J. Sol-Gel Sci. Technol.* 75, 141–151. <https://doi.org/10.1007/s10971-015-3684-6>
- Block, E., Naganathan, S., Putman, D., Zhao, S.-H., 1992. Allium Chemistry: HPLC Analysis of Thiosulfinates from Onion. *J. Agric. Food Chem.* 40, 2418–2430.
- Borgatta, J., Ma, C., Hudson-Smith, N., Elmer, W., Plaza Pérez, C.D., De La Torre-Roche, R., Zuverza-Mena, N., Haynes, C.L., White, J.C., Hamers, R.J., 2018. Copper Based Nanomaterials Suppress Root Fungal Disease in Watermelon (*Citrullus lanatus*): Role of Particle Morphology, Composition and Dissolution Behavior. *ACS Sustain. Chem. Eng.* 6, 14847–14856. <https://doi.org/10.1021/acssuschemeng.8b03379>
- Calia, A., Lettieri, M., Masieri, M., Pal, S., Licciulli, A., Arima, V., 2017. Limestones coated with photocatalytic TiO<sub>2</sub> to enhance building surface with self-cleaning and depolluting abilities. *J. Clean. Prod.* 165, 1036–1047. <https://doi.org/10.1016/J.JCLEPRO.2017.07.193>
- Chan, J.Y.-Y., Yuen, A.C.-Y., Chan, R.Y.-K., Chan, S.-W., 2013. A Review of the Cardiovascular Benefits and Antioxidant Properties of Allicin. *Phyther. Res.* 27, 637–646.

<https://doi.org/10.1002/ptr.4796>

- Chen, P., Wei, B., Zhu, X., Gao, D., Gao, Y., Cheng, J., Liu, Y., 2019. Fabrication and characterization of highly hydrophobic rutile TiO<sub>2</sub>-based coatings for self-cleaning. *Ceram. Int.* 45, 6111–6118. <https://doi.org/10.1016/J.CERAMINT.2018.12.085>
- Chhipa, H., 2019. Applications of nanotechnology in agriculture, in: *Methods in Microbiology*. Academic Press Inc., pp. 115–142. <https://doi.org/10.1016/bs.mim.2019.01.002>
- Colangiuli, D., Lettieri, M., Masieri, M., Calia, A., 2019. Field study in an urban environment of simultaneous self-cleaning and hydrophobic nanosized TiO<sub>2</sub>-based coatings on stone for the protection of building surface. *Sci. Total Environ.* 650, 2919–2930. <https://doi.org/10.1016/J.SCITOTENV.2018.10.044>
- Cornelis, G., Hund-Rinke, K., Kuhlbusch, T., van den Brink, N., Nickel, C., 2014. Fate and Bioavailability of Engineered Nanoparticles in Soils: A Review. *Crit. Rev. Environ. Sci. Technol.* 44, 2720–2764. <https://doi.org/10.1080/10643389.2013.829767>
- Deng, C., Wang, Y., Cota-Ruiz, K., Reyes, A., Sun, Y., Peralta-Videa, J., Hernandez-Viezcas, J.A., Turley, R.S., Niu, G., Li, C., Gardea-Torresdey, J., 2020. Bok choy (*Brassica rapa*) grown in copper oxide nanoparticles-amended soils exhibits toxicity in a phenotype-dependent manner: Translocation, biodistribution and nutritional disturbance. *J. Hazard. Mater.* 398, 122978. <https://doi.org/10.1016/j.jhazmat.2020.122978>
- European Commission, 2018. *Science for Environment Police*.
- Grindal, M., Offutt, J., Andler, S.F., 2004. *Combination Testing Strategies: A Survey* \*.
- Hu, J., Wu, X., Wu, F., Chen, W., Zhang, X., White, J.C., Li, J., Wan, Y., Liu, J., Wang, X., 2020.



- TiO<sub>2</sub> nanoparticle exposure on lettuce (*Lactuca sativa* L.): Dose-dependent deterioration of nutritional quality. *Environ. Sci. Nano* 7, 501–513. <https://doi.org/10.1039/c9en01215j>
- Huang, S., Wang, L., Liu, L., Hou, Y., Li, L., 2015. Nanotechnology in agriculture, livestock, and aquaculture in China. A review. *Agron. Sustain. Dev.* 35, 369–400. <https://doi.org/10.1007/s13593-014-0274-x>
- Kah, M., 2015. Nanopesticides and Nanofertilizers: Emerging Contaminants or Opportunities for Risk Mitigation? *Front. Chem.* 3, 64. <https://doi.org/10.3389/fchem.2015.00064>
- Keller, A.A., Lazareva, A., 2014. Predicted Releases of Engineered Nanomaterials: From Global to Regional to Local. *Environ. Sci. Technol. Lett.* 1, 65–70. <https://doi.org/10.1021/ez400106t>
- Keller, A.A., McFerran, S., Lazareva, A., Suh, S., 2013. Global life cycle releases of engineered nanomaterials. *J. Nanoparticle Res.* 15, 1692. <https://doi.org/10.1007/s11051-013-1692-4>
- Liu, R., Lal, R., 2015. Potentials of engineered nanoparticles as fertilizers for increasing agronomic productions. *Sci. Total Environ.* 514, 131–139. <https://doi.org/10.1016/J.SCITOTENV.2015.01.104>
- Ma, C., Borgatta, J., De La Torre-Roche, R., Zuverza-Mena, N., White, J.C., Hamers, R.J., Elmer, W.H., 2019. Time-Dependent Transcriptional Response of Tomato (*Solanum lycopersicum* L.) to Cu Nanoparticle Exposure upon Infection with *Fusarium oxysporum* f. sp. *lycopersici*. *ACS Sustain. Chem. Eng.* 7, 10064–10074. <https://doi.org/10.1021/acssuschemeng.9b01433>
- Mitrano, D.M., Motellier, S., Clavaguera, S., Nowack, B., 2015. Review of nanomaterial aging

- and transformations through the life cycle of nano-enhanced products. *Environ. Int.* 77, 132–147. <https://doi.org/10.1016/J.ENVINT.2015.01.013>
- Pancrecius, J.K., Ulaeto, S.B., Ramya, R., Rajan, T.P.D., Pai, B.C., 2018. Metallic composite coatings by electroless technique – a critical review. *Int. Mater. Rev.* 63, 488–512. <https://doi.org/10.1080/09506608.2018.1506692>
- Parr, B., Bond, J.K., Minor, T., 2019. *Vegetables and Pulses Outlook*.
- Piccinno, F., Gottschalk, F., Seeger, S., Nowack, B., 2012. Industrial production quantities and uses of ten engineered nanomaterials in Europe and the world. *J. Nanoparticle Res.* 14, 1109. <https://doi.org/10.1007/s11051-012-1109-9>
- Rawat, S., Pullagurala, V.L.R., Adisa, I.O., Wang, Y., Gardea-Torresdey, J.L., 2018. Factors affecting fate and transport of engineered nanomaterials in terrestrial environments. *Curr. Opin. Environ. Sci. Heal.* 6, 47–53. <https://doi.org/10.1016/J.COESH.2018.07.014>
- Robichaud, C.O., Uyar, A.E., Darby, M.R., Zucker, L.G., Wiesner, M.R., 2009. Estimates of Upper Bounds and Trends in Nano-TiO<sub>2</sub> Production As a Basis for Exposure Assessment. *Environ. Sci. Technol.* 43, 4227–4233. <https://doi.org/10.1021/es8032549>
- Servin, A.D., Morales, M.I., Castillo-Michel, H., Hernandez-Viezcas, J.A., Munoz, B., Zhao, L., Nunez, J.E., Peralta-Videa, J.R., Gardea-Torresdey, J.L., 2013. Synchrotron Verification of TiO<sub>2</sub> Accumulation in Cucumber Fruit: A Possible Pathway of TiO<sub>2</sub> Nanoparticle Transfer from Soil into the Food Chain. *Environ. Sci. Technol.* 47, 11592–11598. <https://doi.org/10.1021/es403368j>
- Tabassum, A., Reitz, S., Rogers, P., Pappu, H.R., 2016. First Report of Iris yellow spot virus

- Infesting Green Onion (*Allium fistulosum*) in the United States. *Plant Dis.* 100, 2539–2539.  
<https://doi.org/10.1094/PDIS-05-16-0599-PDN>
- Tan, W., Peralta-Videa, J.R., Gardea-Torresdey, J.L., 2018. Interaction of titanium dioxide nanoparticles with soil components and plants: current knowledge and future research needs – a critical review. *Environ. Sci. Nano* 5, 257–278. <https://doi.org/10.1039/C7EN00985B>
- Tewari, D., Baul, S., 2019. Nanotechnology Market Size, Share and Trend | Industry Forecast - 2025 [WWW Document]. *Allied Mark. Res.* URL  
<https://www.alliedmarketresearch.com/nanotechnology-market> (accessed 3.11.20).
- The Top 5 Green Onion Producing Countries [WWW Document], 2007. . FAOSTAT data. URL  
<https://top5ofanything.com/list/0b9685cc/Green-Onion-Producing-Countries> (accessed 4.5.19).
- Wang, Y., Lin, Y., Xu, Y., Yin, Y., Guo, H., Du, W., 2019. Divergence in response of lettuce (*var. ramosa Hort.*) to copper oxide nanoparticles/microparticles as potential agricultural fertilizer. *Environ. Pollut. Bioavailab.* 31, 80–84.  
<https://doi.org/10.1080/26395940.2019.1578187>
- White, J.C., Gardea-Torresdey, J., 2018. Achieving food security through the very small. *Nat. Nanotechnol.* 13, 627–629. <https://doi.org/10.1038/s41565-018-0223-y>
- Yin, M.-C., Hsu, P.-C., Chang, H.-H., 2003. In Vitro Antioxidant and Antibacterial Activities of Shallot and Scallion. *J. Food Sci.* 68, 281–284. <https://doi.org/10.1111/j.1365-2621.2003.tb14153.x>
- Zuverza-Mena, N., Martínez-Fernández, D., Du, W., Hernandez-Viezcas, J.A., Bonilla-Bird, N.,

López-Moreno, M.L., Komárek, M., Peralta-Videa, J.R., Gardea-Torresdey, J.L., 2017.  
Exposure of engineered nanomaterials to plants: Insights into the physiological and  
biochemical responses-A review. *Plant Physiol. Biochem.* 110, 236–264.  
<https://doi.org/10.1016/j.plaphy.2016.05.037>

## **Chapter 2: Spectroscopic and Microscopic Studies Demonstrate Nutrient Improvement in Green Onion (*Allium fistulosum*) Plants Exposed to CuO Nanoparticles: Its Role as a Potential Nanofertilizer**

### **2.1 INTRODUCTION**

Metallic engineered nanoparticles (ENPs), such as nano silver (nAg), nano copper (Cu) oxide (nCuO), nano copper hydroxide (nCu(OH)<sub>2</sub>), and nano cerium oxide (nCeO<sub>2</sub>), have promising use in the agriculture (Iavicoli et al., 2017; Prasad et al., 2017; Servin and White, 2016; White and Gardea-Torresdey, 2018). They can benefit agricultural productivity through controlling pests, supplying nutrients, and suppressing plant diseases (White and Gardea-Torresdey, 2018). It is estimated that from total nanoproducts production, nearly 9% may be used in agriculture in the form of nanopesticides, nanoherbicides, and nanofertilizers, among others (Iavicoli et al., 2017; Rai and Ingle, 2012; White and Gardea-Torresdey, 2018).

Nanoscale Cu materials reached a total global production of 200 tons in 2010 (Keller et al., 2013b). The global market of nCuO was \$24.66 million in 2015, and expected to reach \$120.67 million by 2022 (“Nano Copper Oxide Market Size and Industry Forecast - 2022,” 2016). Recently, nCuO was reported to be a potential pesticide to deal with fungi and bacteria (Adisa et al., 2019; Huang et al., 2019; Zhang et al., 2018). As a result, the amount of nCuO in the environment may increase. Previous studies on the interaction of nCuO with plants showed species-dependent results (Du et al., 2019; Fatima et al., 2020; Shang et al., 2019). For instance, the growth of duckweed (*Lemna minor*) was restrained after seven days of hydroponic exposure to nCuO at 150 µg/L (Yue et al., 2018). Chloroplast and starch grain shrinkage were also found.

However, a full life cycle study on soil-grown bell pepper (*Capsicum annuum* L.) revealed that nCuO and bulk CuO particles (bCuO), at 125 to 500 mg/kg, did not change dry plant biomass, foliar area, leaf pigments, and fruit yield (Rawat et al., 2018b).

Two-photon microscopy has shown many advantages in detecting ENPs in biological samples (Bonilla-Bird et al., 2018). Compared with the scanning electron microscope or confocal microscopy, it is capable of penetrating the sample and obtaining images deep from the surface up to 1 mm. As previously shown, nCuO exhibited autofluorescence by two-photon laser excitation (Bonilla-Bird et al., 2018), thus, this nanoparticles (NPs) is a good candidate to explore its uptake mechanism by plant cells.

Scallion or green onion (*Allium fistulosum*), is used as an important seasoning worldwide (Tabassum et al., 2016). They have a high concentration of allicin, flavonoids, vitamins, as well as other organosulfur compounds (Yin et al., 2003). Allicin, one of the most distinctive organosulfur compounds, is responsible for the pungency and flavor in *Allium* monocotyledonous flowering plants (Block et al., 1992). Additionally, scallions pose antioxidant and antibacterial properties and have shown potential to benefit the cardiovascular system (Chan et al., 2013). In 2007, the top five producers countries (Japan, China, Republic of Korea, Nigeria, and New Zealand) registered more than three million metric tons of scallions (“The Top 5 Green Onion Producing Countries,” 2007).

However, the scallion is not a very well-studied species in the *Allium* family. To the authors’ best knowledge, only one study has been focused to evaluate the effects of ENPs on scallion plants. This mentioned study reported an antimycotic effect of nAg against the fungus *Sclerotium cepivorum* that impairs green onion plants (Jung et al., 2010). However, the uptake of ENPs by scallion plants, the effects of ENPs on the nutrient elements, allicin, and antioxidant

species are still unknown. Thus, the aim of this study was to perform a full-lifecycle study to examine the effect of Cu-based compounds on the nutrient element behavior, allicin content, and enzyme antioxidant responses in scallion plants. The Cu uptake and nutrient element accumulation on different parts of scallion were determined by inductively coupled plasma-optical emission spectroscopy (ICP-OES). The root samples were screened by two-photon microscopy to observe the penetration and retention of nCuO and bCuO. To the authors' knowledge, this is the first report that describes the effects of ENPs on allicin accumulation in plants.

## **2.2 MATERIALS AND METHODS**

### **2.2.1 Preparation of nCuO<sub>2</sub> amended Soil**

The nCuO were obtained from the University of California Center for Environmental Implications of Nanotechnology (UC-CEIN). Copper sulfate (CuSO<sub>4</sub>) and bCuO were purchased from Sigma Aldrich (St. Louis, MO). Hong et al. previously reported the characterization data of nCuO and bCuO, which can be found in Table S1 (Hong et al., 2015).

A mixing ratio of 2:1 by weight between nature soil and potting soil was used to ensure optimum plant growth. Commercial Miracle-Gro® organic potting soil was purchased from a local supermarket. Natural soil was collected at Socorro TX, USA, an agricultural land at latitude: 31°67' N, longitude: 106°28' W, and elevation: 1115 m asl. The soil was characterized previously as medium loam (19% clay, 44% silt, and 36% sand; 2.8% organic matter, pH = 7.8 ± 0.02, EC = 1705 ± 47.6 μS cm<sup>-1</sup>, and TDS = 847.5 ± 23.8 mg/L) (Majumdar et al., 2015a). To remove plant-based residues and gravel, the soil collected was sieved through an 8 mm sieve, and air-dried for two days.

Before the soil amendment, suspensions/solutions of each of the three Cu-based compounds (nCuO, bCuO, and CuSO<sub>4</sub>·5H<sub>2</sub>O) were made to obtain 75, 150, 300, and 600 mg Cu content/kg soil. Environmentally relevant concentrations of Cu compounds were selected for the current study. For example, the lowest concentration was selected according to the highest Cu content reported in agricultural soil amended with sewage sludge (75 mg/kg) (McGrath et al., 1994). Briefly, nCuO, bCuO, and CuSO<sub>4</sub> were weighted, suspended in 50 mL Milli-Q 18 MΩ deionized water (DI), and sonicated in a water bath at 25 °C for 30 min and 180 watts. The 1.5 kg soil was then amended with suspensions and mixed manually for 20 min until homogenous. The control soil was prepared with 50 mL of DI. The treatments were then filled with DI to 60% of the maximal field capacity and prepared in triplicate. All the pots were allowed to equilibrate for three days before use.

### **2.2.2 Seed germination and plant growth**

Scallion seeds (evergreen bunching) were purchased from the Ferry-Morse Seeds Company and stored at 4 °C. Seeds were rinsed with 2% NaClO for 15 min and washed three times with DI. For hydration, seeds were soaked with DI for 12 h and sowed in germination soil. Two weeks after sowing, seedlings were transplanted into pots containing the Cu-treatments or control and placed in the greenhouse with temperature setpoint at 30/20 °C day/night temperature 50-75% relative humidity, and daily light integral of 10 mol m<sup>-2</sup> d<sup>-1</sup> on average. All pots were fertilized with 100 mL per day of water-soluble fertilizer 15N–2.2P–12.5K (Peters 15-5-15 Cal-Mag Special; Scotts, Marysville, OH) at 1.0 g·L<sup>-1</sup>. Plants were harvested 80 days after transplanting, washed with 0.01% HNO<sub>3</sub> and DI for three times and prepared for different analyses.



### **2.2.3 Chlorophyll measurement**

Fresh leaf samples (~0.5 g) were ground and the chlorophyll was extracted with 80% acetone. A UV-Vis Spectrometer (Perkin Elmer Lamda, Uberlinger, Germany) was used to measure the absorbance as described by Porra (Porra, 2002).

### **2.2.4 Quantification of allicin**

Allicin content was determined using a UV-Vis Spectrometer (Perkin Elmer Lamda) according to Han et al. (Han et al., 1995). Briefly, ~0.3 g of dry green onion leaf tissues were ground and dissolved in 150 mL of DI. After centrifugation, only the supernatants remained. A mixture of 0.1 mL of the extract and 0.24 mL of 2mM L-cysteine was kept at room temperature for 10 minutes. After adding 0.6 mL of 50 mM HEPES buffer (pH 7.6) and 0.2 mL DTNB, the mixture was shaken for 2 min and read at 412 nm using UV-Vis Spectrophotometer.

### **2.2.5 Antioxidant enzymatic activities**

A UV-Vis Spectrometer (Perkinelmer lamda) was used to determine the enzyme activities. Antioxidant enzymatic activities of catalase (CAT), ascorbate peroxidase (APOX), guaiacol peroxidase (GPOX), and superoxide dismutase (SOD) were analyzed to understand scallion antioxidant defense system under the interaction of Cu based compounds. All the analyses were done at 25 °C. The crude extraction for CAT and SOD was prepared following Lee et al. (Lee and Lee, 2000). The CAT and SOD activity was determined according to Aebi (Aebi, 1974), and Beyer and Fridovich (Beyer and Fridovich, 1987), respectively. APOX and GPOX extractions were prepared according to Xu et al. (Xu and Chen, 2011). The APOX and GPOX activity was

determined following Nakano and Asada (Nakano and Asada, 1981), and Egley (Egley et al., 1983), respectively.

### **2.2.6 Essential Element Quantification by ICP-OES and Two-photon microscopy sample preparation**

Macronutrients (Ca, Mg, P, S, and K) and micronutrients (Cl, Zn, Fe, B, Mn, Cu, Mo, and Ni) were measured by inductively coupled plasma – optical emission spectrometry (ICP-OES, Perkin-Elmer Optima 4300 DV; Shelton, CT). Plants were severed into roots, bulbs, and leaves. Each sample was oven-dried at 70 °C for 72 h. A coffee grinder (Hamilton Beach) was used to homogenize dry samples. Around 0.2 g of dry tissues were acid-digested after adding 2 mL of pure trace HNO<sub>3</sub> (SPC Science, Champlain, NY), at 115°C for 45 min in a Digiprep hot block (SCP Science). To digest completely, another 20 min incubation was applied with an additional 1 mL of 30% hydrogen peroxide. The digested solutions were adjusted to 45 mL with DI. To validate the measurements, blanks (no plant tissues), standard reference material (peach leaf, 1547, National Institute of Standards and Technology, Gaithersburg, MD) and spiked samples of 10 and 50 mg/kg were also treated by the same procedure. For QC, the multi-elemental standard solution was evaluated every 20 samples. The recovery rate was 99%.

For two-photon microscope imaging, fresh root samples of 80-day-old scallion control and treatment exposed to nCuO at 600 mg/kg soil was collected and cut to thin slices using Microtome. Then, the samples were analyzed by a mode-locked Ti: Sapphire laser (Spectra-Physics, Mai-Tai HP) at 710 nm light and 200 W. A 665 nm long-pass dichroic mirror was used to deflect the fluorescence signal from the sample. In the end, two-dimensional images were acquired using a custom software program (Acosta et al., 2014).

### **2.2.7 Statistical analysis of the data**

All the data were analyzed by the Statistical Package for the Social Sciences 25 (SPSS, Chicago, IL, USA). Statistical significance was accepted at a p-value of 0.05. Data are mean  $\pm$  standard error (SE) of three replicates as stated in tables/figures. One-way ANOVA followed by the Tukey–Kramer multiple comparison tests were used to determine the differences among treatment means.

## **2.3. RESULT AND DISCUSSION**

### **2.3.1 Uptake of nCuO and bCuO particles**

The Cu uptake in the roots of plants treated with nCuO and bCuO was detected using two-photon microscopy (Fig. 2.1). This was also quantitatively corroborated by the ICP-OES. Figs. 2.1d and 1f show fluorescent points from root tissue exposed to bCuO and nCuO, respectively, at 600 mg/kg. Representative spots are pointed out by yellow arrows and squares as examples. These glittering points are similar to those of the pure compounds suspended in DI (Figs. 2.1e and g); thus, they are suggested to belong to bCuO (Fig. 2.1d) and nCuO (Fig. 2.1f). Both bCuO and nCuO were mainly distributed in or near the vascular tissues and in the intercellular spaces of roots, indicating an apoplastic uptake. Accordingly, Bonilla et al. previously showed that bCuO and nCuO compounds were accumulated in intercellular spaces of sweet potato roots (Bonilla-Bird et al., 2018).

Conversely, Figs. 2.1a and 2.1b are representative images of root samples of plants exposed to H<sub>2</sub>O (control) and CuSO<sub>4</sub> at 600 mg/kg, respectively. In these micrographs, parameters were set

to detect fluorescence from nCuO/bCuO, but no flashing or bright signal was found. Barely, structures of root cells and vascular tissue with typical autofluorescence were only encountered. Besides, the image of CuSO<sub>4</sub> dissolved in DI water at 600 mg Cu/L is shown in Fig. 2.1c. No visible fluorescence of ion Cu<sup>2+</sup> is seen due to the dissolution.

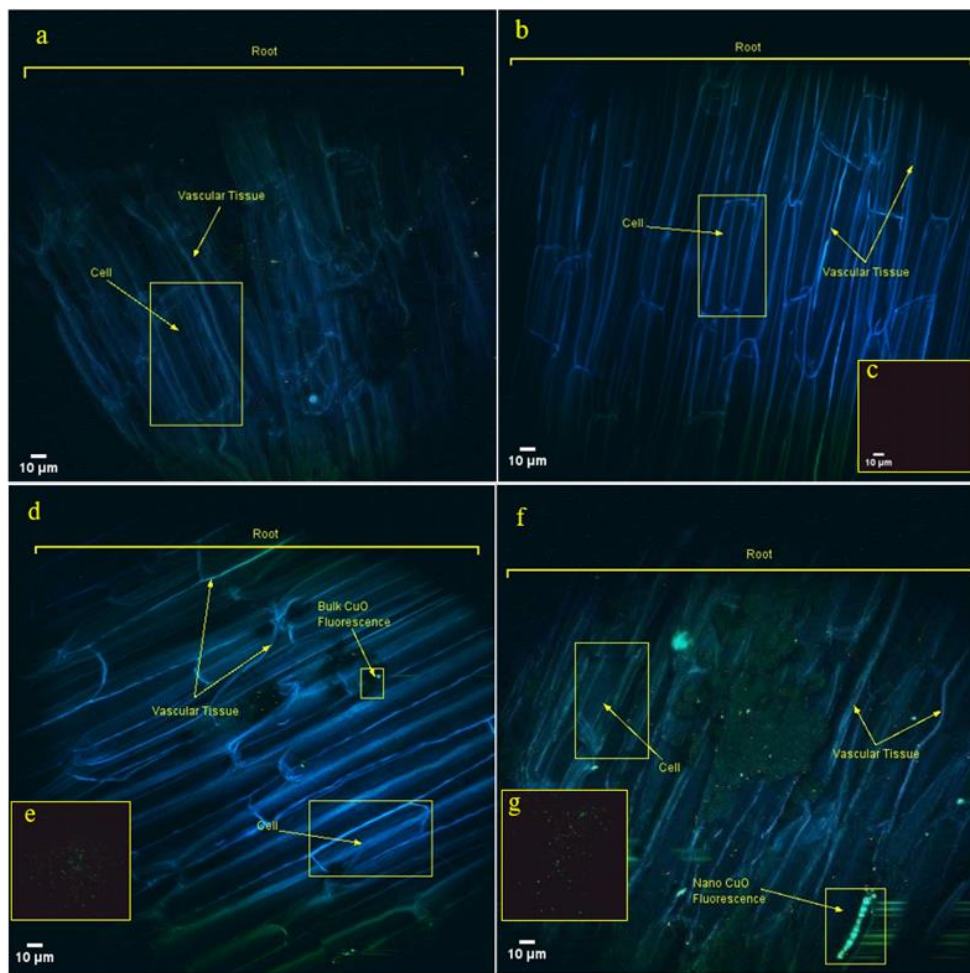


**Fig. 2.1.** Two-photon microscopy images of root samples of control plants (a) and plants treated with (b) CuSO<sub>4</sub>, (d) bCuO and (f) nCuO at 600 mg/kg. The inserted pictures correspond to (c) CuSO<sub>4</sub> in DI water, (e) pure bCuO suspension in DI and (g) pure nCuO suspension in DI. The fluorescence of root cell walls and vascular tissue is shown. Arrows inside the square indicate fluorescence from bCuO (d) or nCuO (f) particles.

### 2.3.2 Copper Content in Roots, Bulbs, and Leaves

In roots, all Cu-based treatments at  $\geq 300$  mg/kg significantly increased Cu compared with

control (Fig. 2.2a) ( $p \leq 0.05$ ). Both bCuO and CuSO<sub>4</sub> at 75 and 150 mg/kg, did not affect root Cu accumulation, compared with control. Meanwhile, nCuO at 150 mg/kg increased root Cu by 9.5-fold compared with control ( $p \leq 0.05$ ). It is worth noting that at 150 mg/kg, nCuO treatment significantly increased root Cu concentration compared with bCuO and CuSO<sub>4</sub> (90.0 vs. 33.8 and 43.7 mg/kg dry weight (DW), respectively) ( $p \leq 0.05$ ).

Figure 2.2b shows that at  $\geq 300$  mg/kg, all Cu-based compounds significantly increased bulb Cu (11-17 mg/kg DW), compared with control (4.5 mg/kg DW) ( $p \leq 0.05$ ). Moreover, when plants were treated with  $\leq 150$  mg/kg Cu compounds, the nCuO treatment did not significantly increase Cu content in the bulb compared with control, as was predominantly exhibited by bCuO and CuSO<sub>4</sub> (Fig. 2.2b).

Fig. 2.2c shows that Cu accumulation in leaves was significantly increased in plants treated with nCuO at  $\leq 150$  mg/kg and with CuSO<sub>4</sub> at  $\geq 150$  mg/kg. When comparing the effect of different compounds at 75 mg/kg, the results showed that nCuO induced a greater Cu accumulation in leaves than bCuO and CuSO<sub>4</sub> (31 vs. 15 and 12 mg/kg DW, respectively) ( $p \leq 0.05$ ). In contrast to CuSO<sub>4</sub>, which dissolves easily, and its ions can actively move through ion transporters, nCuO and bCuO exhibit slow Cu release. However, nCuO and bCuO may be taken by roots in particulate forms, as confirmed by the two-photon images (Figs. 2.1 d and f). Interestingly, at 75 mg/kg, a possible combination of less aggregation, smaller particle size, and a higher dissolution rate of the nCuO treatment enabled the higher accumulation of Cu in leaves, compared with bCuO and CuSO<sub>4</sub> (Fig. 2.2c). With the increasing concentration of nCuO, the characteristics mentioned above were no longer obvious due to the apparent aggregation of nCuO. Similar results were reported before in nCuO or bCuO treated bell pepper (*Capsicum annum* L.) and sugarcane (*Saccharum officinarum*) plants (Rawat et al., 2018b; Tamez et al., 2019). Additionally, released ions from particulate

compounds might be involved in the Cu uptake.

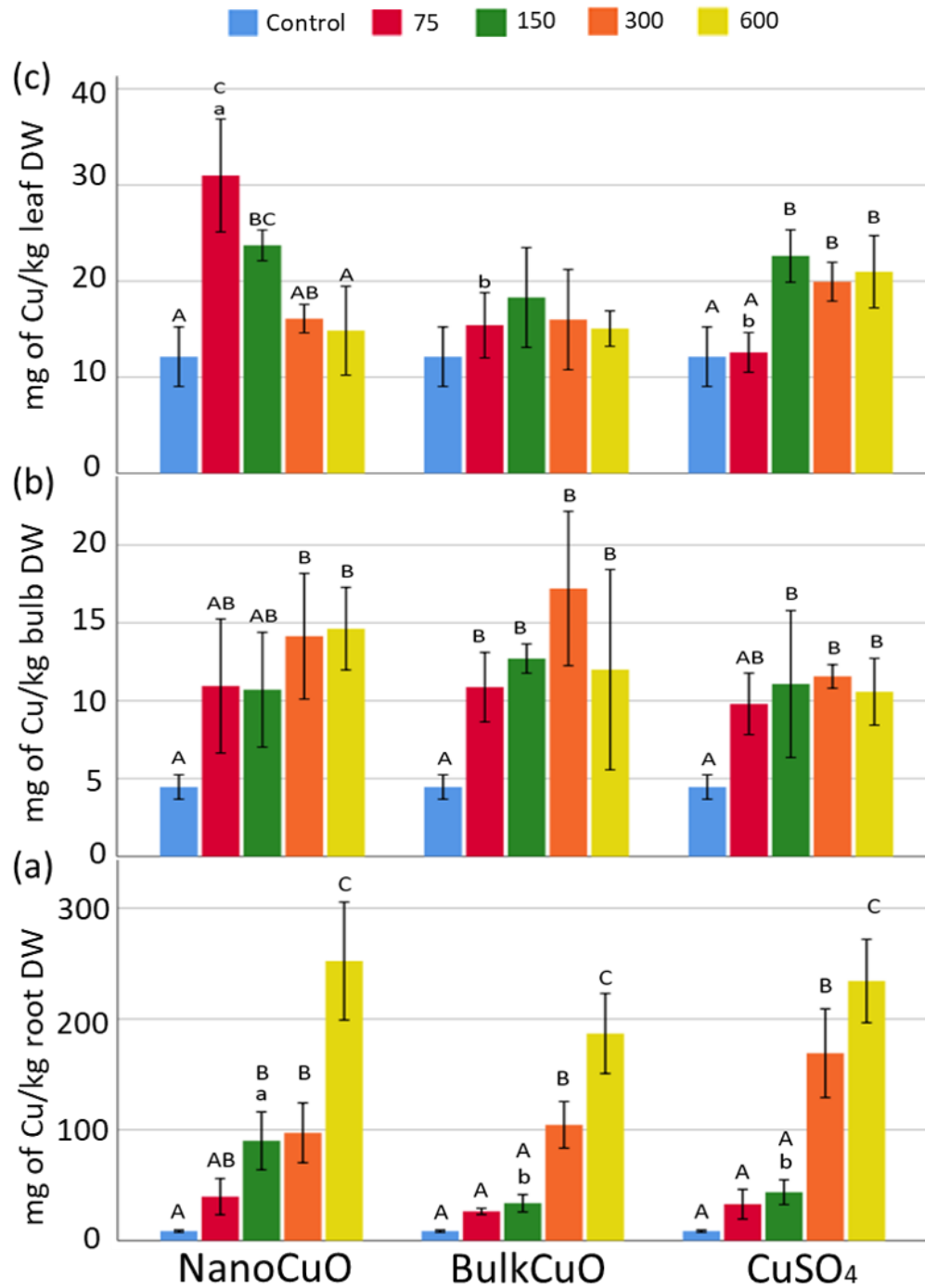


**Fig. 2.2.** Copper concentration (mg/kg DW) in scallion roots (a), bulbs (b) and leaves (c) exposed to nCuO, bCuO, and CuSO<sub>4</sub> at 0, 75, 150, 300 and 600 mg/L. Data are the average of three replicates ± standard error (SE). Lowercase letters stand for statistical differences among

different compounds at the same concentration. Uppercase letters represent significant differences among different concentrations of the same compound ( $p \leq 0.05$ ,  $n = 3$ ).

In this study, the maximum Cu concentration in aerial parts of plants exposed to 75 mg/kg soil was lower than 32 mg/kg DW (Fig. 2.2b and 2.2c). Scallion is consumed in small amounts as a seasoning; thus, this Cu concentration appears to be safe for human consumption (Bost et al., 2016). Similar results were reported by Soudek et al., who exposed *Allium* plants to 46.9 mg/L  $\text{Cu}(\text{NO}_3)_2$  (Rastilantie et al., 2009). These authors found that Cu was mainly accumulated in roots (~5,500 mg/kg DW) with small translocation to bulbs (~120 mg/kg DW) and leaves (~10 mg/kg DW).

### 2.3.3 Elements accumulation in tissues

Data on macro and microelements uptake showed that nCuO, bCuO, and  $\text{CuSO}_4$ , differentially affected the accumulation of essential elements (Ca, K, Mg, P, Fe, Mn, Ni) and Al (a non-essential element) in scallion tissues. Undisturbed essential elements have not been discussed in this work.

#### 2.3.3.1 Macronutrient elements in roots

Fig. 2.3 shows the concentration of macroelements that were affected by Cu treatments. At the root level, there were significant changes in the accumulation of Ca, K, Mg, and P (Figs. 2.3a-d).

*Calcium*- Compared with control (16,607 mg/kg DW), only nCuO at 150 mg/kg (30,971 mg/kg DW) and at 300 mg/kg (32,621 mg/kg DW) induced a significant increment on root Ca content (Fig. 2.3a) ( $p \leq 0.05$ ). Conversely, bCuO and  $\text{CuSO}_4$  at 150 mg/kg, with values of ~5,500

and ~6,600 mg/kg, respectively, showed a significant reduction in root Ca when compared with control ( $p \leq 0.05$ ). Excess Cu induces the overproduction of reactive oxygen species (ROS), which alter the permeability of Ca channels, interfering with Ca uptake by root cells (Demidchik et al., 2007). Additionally, bCuO particles are more negatively charged compared with nCuO (Table S1), which may result in a higher attraction for positive  $\text{Ca}^{2+}$  ions at the root-soil interface. Consequently, a reduction in  $\text{Ca}^{2+}$  mobility should be expected and would explain, at least in part, the lower Ca uptake by root cells in plants treated with bCuO compounds. Regarding the lessening of Ca content caused by the ionic treatment, it has also been reported that ionic  $\text{Cu}^{2+}$  reduced  $\text{Ca}^{2+}$  concentration in Norway spruce (*Picea abies*) (Trujillo-Reyes et al., 2014). This species was treated with elevated concentrations of ionic Cu (1.5  $\mu\text{M}$ ), which resulted in a decreasing of Ca content in roots and wood. Moreover, Ca addition diminished the accumulation of Cu, indicating a competing relationship between Cu and Ca elements (Österås and Greger, 2006).

*Potassium* – None of the treatments altered K concentration, compared with control. However, K uptake was differentially affected by the diverse Cu compounds evaluated at the same concentration (Fig. 2.3b). For instance, at 75 and 150 mg/kg treatments, bCuO significantly enhanced root K (57,663 and 61,969 mg/kg DW, respectively) compared with nCuO (39,602 and 45,668 mg/kg DW, respectively) ( $p \leq 0.05$ ). Interestingly, this was contrary to root Cu uptake, where nCuO at 150 mg/kg increased Cu content respecting to bCuO (Fig. 2.2a) ( $p \leq 0.05$ ). Thus, higher root Cu acquisition generated by nCuO treatment reduced K content in scallion plants. Concurring with these findings, an increase in  $\text{Cu}^{2+}$  led to a decrease of  $\text{K}^+$  in *Arabidopsis* root cells (Demidchik et al., 1999). Regarding  $\text{CuSO}_4$ -exposed plants in the present study, no significant changes were registered, thus, the observed responses suggest this effect is driven by the Cu particles. In previous literature, Wang et al. reported that nCuO increased  $\text{K}^+$  leakage in maize (*Zea*



*mays*) plants due to damages in the lipid bilayer (Wang et al., 2012).

*Magnesium* – Compared with control, bCuO, at all concentrations, except 300 mg/kg, significantly decreased root Mg up to 33% ( $p \leq 0.05$ ) (Fig. 2.3c). The reduction in bCuO treatments were significantly more compared with nCuO. The pattern on Mg and Ca accumulation in plants exposed to nCuO and bCuO treatments was similar (Fig. 2.3a and 2.3c). This behavior may be explained since both Ca and Mg share the same transporter, namely AtCNGC10 (Guo et al., 2010a), which suggests that nCuO may induce AtCNGC10 expression, facilitating  $Mg^{2+}$  transport inside cells. However, the latter needs a further experimental demonstration.

*Phosphorus* –  $CuSO_4$  at 600 mg/kg significantly augmented P in roots, compared with nCuO (45.7%), bCuO (47.1%), and control (24.2%) (Fig. 2.3d) ( $p \leq 0.05$ ). A possible explanation about the increment in P at higher  $CuSO_4$  doses may be related to an up-regulation of the Pht1 transporter.<sup>47</sup> Nevertheless, there exists the possibility that particles of nCuO or bCuO physically blocked the P transporters, reducing its uptake (Zuverza-Mena et al., 2015). Rawat et al. reported that bCuO at 500 mg/kg, reduced P absorption in bell pepper roots by 36%, compared with control (Rawat et al., 2018b). Hong et al. found a reduction of root P in lettuce and alfalfa plants exposed to bCuO and nCuO at 5, 10, 20 mg/L (Hong et al., 2015). Hong et al. found a reduction of root P in lettuce and alfalfa plants exposed to bCuO and nCuO at 5, 10, 20 mg/L (Hong et al., 2015). This later work also reported that 10 and 20 mg/L of  $CuCl_2$  resulted in the highest P accumulation in alfalfa shoot ( $p \leq 0.05$ ). None of the remaining treatments affected root P, compared with control.

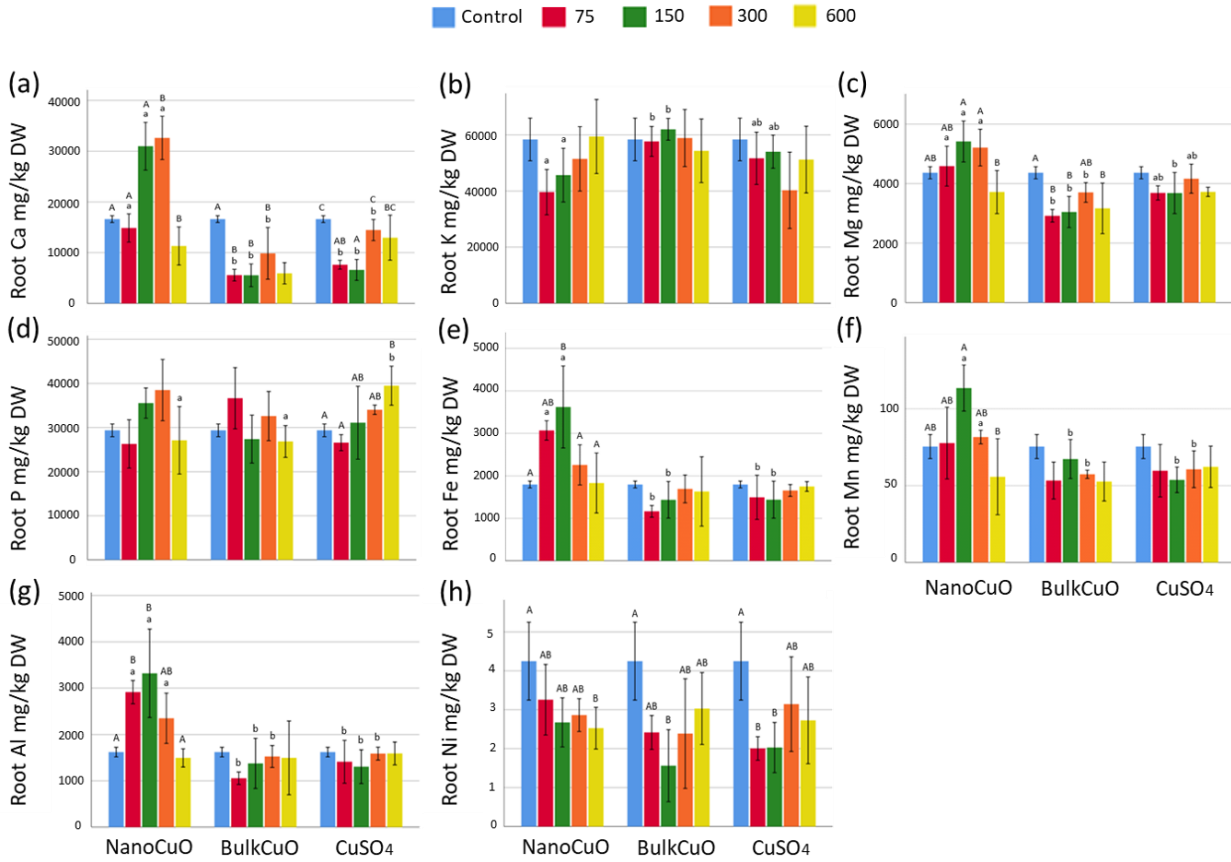


**Fig. 2.3.** Concentration (mg/kg DW) of the elements (a) Ca, (b) K, (c) Mg, (d) P, (e) Fe, (f) Mn, (g) Al, and (h) Ni, in scallion roots. Plants were cultivated for 80 days in soil amended with nCuO, bCuO, and CuSO<sub>4</sub> at 0 (control), 75, 150, 300 and 600 mg of Cu/kg of soil. Data are averages of three replicates  $\pm$  standard error (SE). Lowercase letters stand for statistical differences among different compounds at the same concentration. Uppercase letters represent significant differences among different concentrations of the same compound ( $p \leq 0.05$ ).

### 3.3.2 Micronutrients and aluminum in roots

Fig. 2.3 also shows the concentration of the microelements that were affected by the Cu treatments in roots. There were changes in the accumulation of Fe, Mn, Al and Ni, this latter a non-essential element (Fig. 2.3e-h).

*Iron* – Fe in roots (Fig. 2.3e) was significantly increased by nCuO at 75 and 150 mg/kg (3,070 and 3,622 mg/kg), compared with bCuO (1,165 and 1,437 mg/kg), CuSO<sub>4</sub> (1,496 and 1,439

mg/kg), and control (1,797 mg/kg) ( $p \leq 0.05$ ). The observed differences between nCuO and CuSO<sub>4</sub> at  $\leq 150$  mg/kg suggest that Fe uptake was due to an effect of particle size and/or surface properties and ion release. Hence, Cu ions released from CuSO<sub>4</sub> may compete with Fe for transporters active sites, inhibiting its uptake (Apodaca et al., 2017; Hong et al., 2015). Additionally, Deák et al. suggested that the stress caused by nanoparticles increased the production of ferritin, an intracellular protein with a high affinity to bind Fe (Deák et al., 1999).

*Manganese and aluminum* – Fig. 2.3f shows that Cu treatments did not affect root Mn content, compared with control. However, there were differences among Cu forms evaluated at the same concentration. When the plants were exposed to 150 and 300 mg/kg of nCuO, bCuO, and CuSO<sub>4</sub>, the roots treated with nCuO significantly showed higher Mn than bCuO and CuSO<sub>4</sub> ( $p \leq 0.05$ ). Similarly, nCuO at 75-300 mg/kg, increased root Al content compared with bCuO and CuSO<sub>4</sub> (Fig. 2.3g) ( $p \leq 0.5$ ). It is possible that the uptake of Mn and Fe is affected by similar mechanism; thus, the negativity of bCuO and the high amount of Cu ions released by CuSO<sub>4</sub> might be affecting Mn uptake in a similar manner than Fe uptake. An increase in Al uptake was previously reported in lettuce hydroponically exposed to Cu/CuO NPs (Trujillo-Reyes et al., 2014). The uptake of Al may follow a comparable trend than similar cations. However, because Al is not an essential element, not much discussion on its uptake is presented herein.

*Nickel* – Differences in Ni concentrations at the root level are presented in Fig. 2.3h. A significant reduction in Ni content was found when plants were exposed to 600 mg/kg of nCuO, 150 mg/kg of bCuO, and  $\leq 150$  mg/kg of CuSO<sub>4</sub>, compared with control ( $p \leq 0.05$ ). However, the Ni content did not exhibit a particular trend with increasing doses of the Cu compounds. The literature has shown that Ni<sup>2+</sup>, Cu<sup>2+</sup>, and Zn<sup>2+</sup> are taken up by the same carrier (Cataldo et al., 1978a, 1978b); thus, excess of Cu<sup>2+</sup> may compete with Ni<sup>2+</sup> uptake.

### 3.3.3 Essential elements in bulbs and leaves

Fig 2.4 shows the concentration of macro and microelements that were affected by the Cu treatments in bulbs. Basically, lower Cu copper acquisition and lesser alteration were observed in bulbs than in roots, which suggested a “phytostabilization effect” of the underground tissues of scallion.<sup>34</sup>

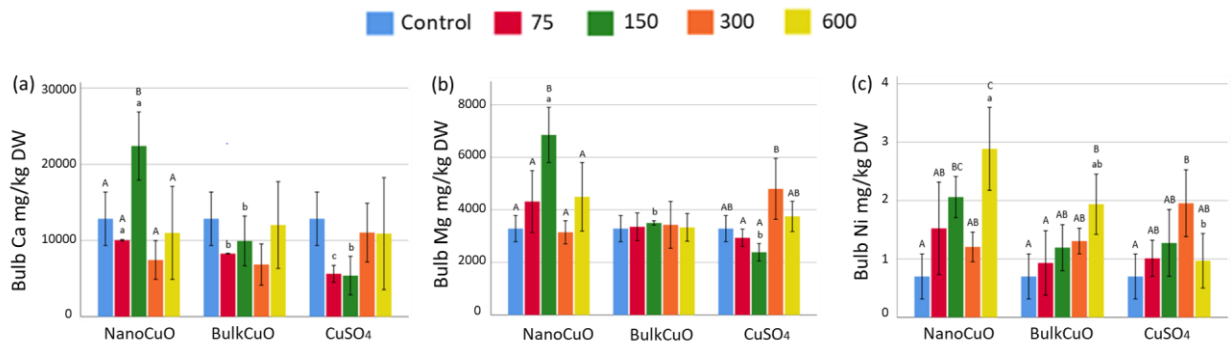


**Fig. 2.4.** Concentration (mg/kg DW) of the essential elements (a) Ca, (b) Mg, and (c) Ni in dry bulbs of scallion plants. Green onions were cultivated for 80 days in soil amended with nCuO, bCuO, and CuSO<sub>4</sub> at 0 (control), 75, 150, 300 and 600 mg of Cu/kg of soil. Data are averages of three replicates  $\pm$  standard error (SE). Lowercase letters represent statistical differences among different compounds at the same concentration. Uppercase letters represent significant differences among different concentrations of the same Cu-based compounds ( $p \leq 0.05$ ).

Plants exposed to nCuO at 150 mg/kg had significantly more Ca and Mg in bulbs, compared with control (74% and 108%) (Figs. 4a and 4b). Bulk CuO and CuSO<sub>4</sub> did not alter Ca and Mg accumulation in bulbs. The delivery of Mg to edible tissues is determined by the MRS2, MHX, and the MRS2-11 transporters (Li et al., 2017), which suggests that only nCuO, at 150 mg/kg, could have had an effect on their transport activity. The average Ca and Mg contents in scallion bulbs reported by the U.S. Department of Agriculture are 720 and 200 mg/kg fresh weight

(~ 7,200 and 2,000 mg/kg DW) (*Food Composition Databases Show Foods -- Onions, spring or scallions (includes tops and bulb), raw*, 2018), which are lower than the average values of control (12,846 and 3,286 mg/kg). This may be due to the variety or the experimental conditions. The adequate intake of Mg and Ca for adult are ~300 mg/d and 1000 mg/d (Moore-Schiltz et al., 2015), respectively. The results of the current study revealed that nCuO improves the nutritional values of scallion bulbs by increasing Mg and Ca concentrations. In bulbs, Nickel showed an increase with rising doses of Cu compounds (Fig. 4c). Cataldo et al. stated that in soybean plants  $Ni^{2+}$  tends to form organic complexes within tissues, which are carried out through the xylem and deposited in the leaf and in the seeds of the soybean plants (Cataldo et al., 1978a). In bell pepper, Ni was found in fruit (Rawat et al., 2018b). This suggests the distribution of Ni in plants is species dependent.

#### **2.3.4 Plant growth and chlorophyll content**

In this study, none of the Cu-based compounds caused significant changes in fresh weight, plant height, water content, and chlorophyll, compared with control (data are shown in Figs. S2.1 and S2.2,  $p \leq 0.05$ ). No obvious signs of toxicity were found through the growth period. However, a comparison between treatments showed that nCuO treatments, except at 75 mg/kg, had significantly higher plant height, compared with bCuO and  $CuSO_4$ . This was probably due to the increase in nutrient elements given by nCuO, which benefits plant growth.

#### **2.3.5 Allicin content**

The effect of Cu-based treatments on leaf allicin content is depicted in Fig. 2.5. As shown

in the figure, nCuO and CuSO<sub>4</sub> at all concentrations, significantly increased allicin content in the range 56-187% and ~ 34-90%, respectively, compared with control ( $p \leq 0.05$ ). Meanwhile, bCuO treatments did not affect allicin content. This outcome was somehow in agreement with leaf Cu contents at the same treatments (Fig. 2.2c). Allicin has a beneficial effect in preventing alterations of lipid profile induced by Cu (Metwally and Metwally, 2009). In addition, allicin scavenges ·OH, which reduces lipid peroxidation (Prasad et al., 1995). Thus, it is possible that the increase in allicin concentration was due to counteracting the oxidative stress caused by the Cu-based treatments.

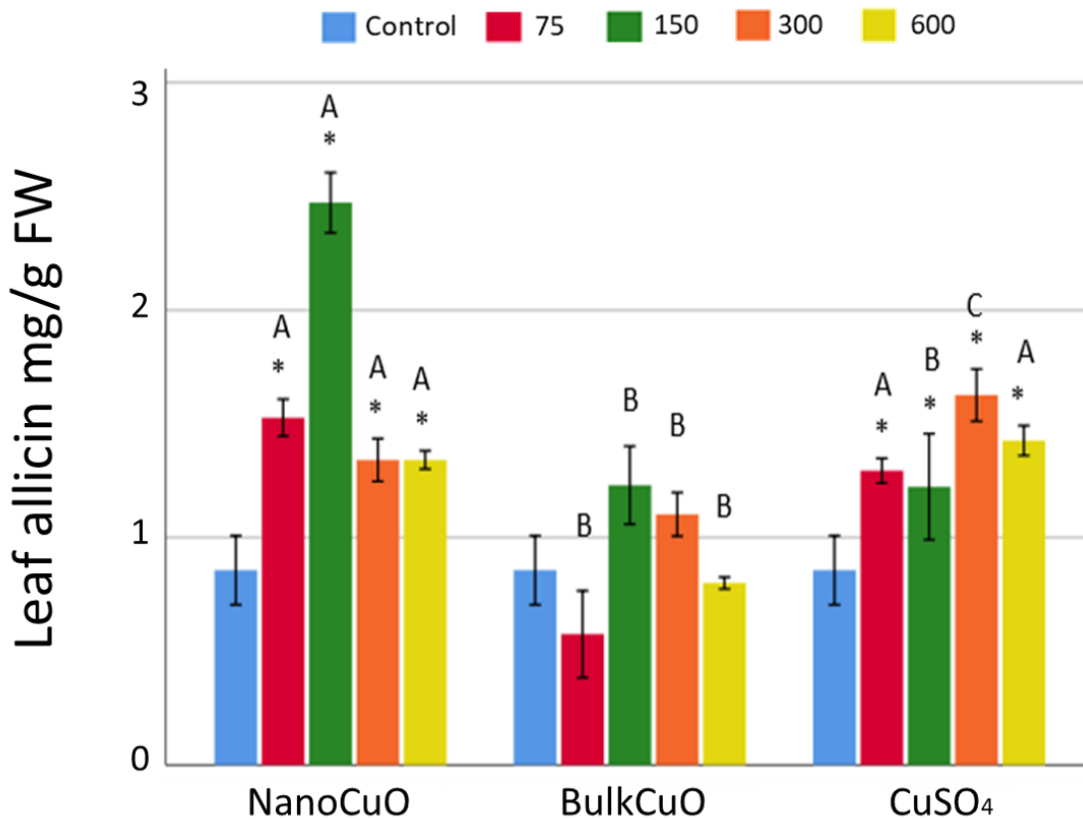


**Fig. 2.5.** Allicin content (w%) in leaves of plants cultivated for 80 days in soil amended with nCuO, bCuO, and CuSO<sub>4</sub> at 0, 75, 150, 300 and 600 mg/L. Data are averages of three replicates  $\pm$  standard error (SE). Uppercase letters stand for significant differences among different compounds evaluated at the same concentration. Asterisks (\*) represent statistical differences in treatments compared to control ( $n=3, p \leq 0.05$ ).

### 2.3.6 Antioxidant defense system in roots and leaves

Figure 2.6 shows the activity of APOX, CAT, GPOX, and SOD in different scallion tissues. In root tissue, the nCuO at 75-300 mg/kg increased GPOX by 121.5- 245.7% (Fig. 2.6a), while at  $\geq 150$  mg/kg reduced CAT activity by 44.6-58.2% (Fig. 2.6c), respect to control ( $p \leq 0.05$ ). Contrarily, none of the treatments affected APOX (Fig. 2.6b) and SOD (Fig. 2.6d) activities in the root. At leaf levels, no changes were observed in GPOX and SOD. However, APOX and CAT activities in leaves presented some alterations, as shown in figure 2.6e and 2.6f, respectively. Plants exposed to bCuO at all concentrations, and nCuO and CuSO<sub>4</sub> at concentrations  $\geq 150$  mg/kg, showed a significant APOX activity increment in leaves (Fig. 2.6e) ( $p \leq 0.05$ ). Finally, nCuO at all concentrations significantly reduced leaf CAT activity (Fig. 2.6f), compared with control ( $p \leq 0.05$ ). In this study, the activity of stress-related enzymes from roots and leaves were differentially affected by Cu compounds. For instance, the nCuO significantly induced GPOX (Fig. 2.6a) activity and reduced CAT (Fig. 2.6c) in roots, while the three Cu-based treatments augmented APOX activity in leaves (Fig. 2.6e). These results suggest a specific size effect of nCuO, compared with the other two compounds. It can be speculated that the nCuO interacts with the binding sites of CAT reducing its activity, while APOX-increased activity in leaves may be a direct response to reduce the stress imposed by the three compounds (Rico et al., 2013; Stark, 2011).

The forthcoming formation of peroxy radicals in roots induced by nCuO enhanced root GPOX (Fig. 2.6a), while in leaves the increased APOX activity (Fig. 2.6e) may be caused by high H<sub>2</sub>O<sub>2</sub> formation. Since the APOX-H<sub>2</sub>O<sub>2</sub> affinity is higher than CAT-H<sub>2</sub>O<sub>2</sub> (Lin et al., 2009). the increased activity of APOX in leaves was possibly enough to reduce the oxidative stress; then, no further increase of CAT was needed in the leaves. Additionally, to support the enzymatic

antioxidant defenses, the data suggest that the plants produced a higher alliin content to combat an excess of  $\cdot\text{OH}$  in leaves.

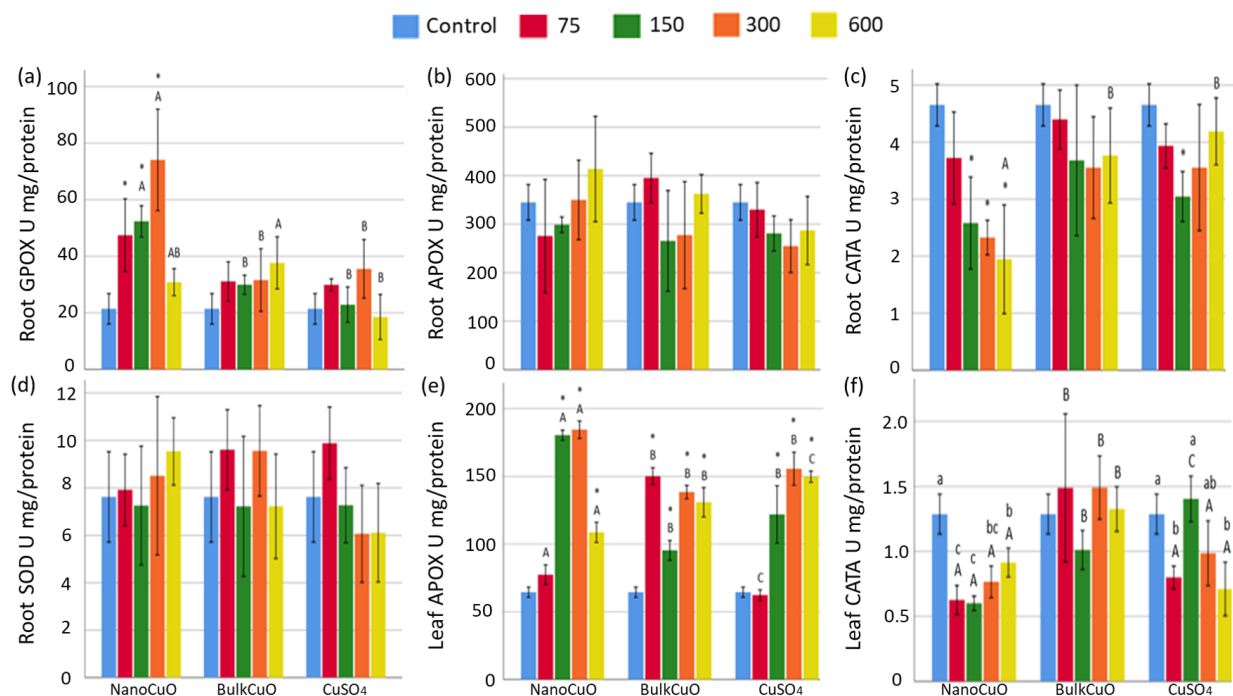


**Fig. 2.6.** Enzyme activities of CAT, GPOX, SOD, and APOX in the roots and leaves of soil-grown green onion plants. Chinese scallions were exposed to nCuO, bCuO, and CuSO<sub>4</sub> at 0, 75, 150, 300 and 600 mg/L. Data are the average of three replicates ± standard error (SE). Uppercase letters represent statistical differences among different compounds tested at the same concentration. Asterisks (\*) represent statistical differences in treatments compared to control (n=3,  $p \leq 0.05$ ).

## 2.4. CONCLUSIONS

This study describes the physiological responses of scallion plants exposed to nano, bulk, and ionic Cu-based compounds. Two-photon microscopy showed that both nano and bulk CuO compounds were taken up by the roots, and none of the Cu-based tested concentrations produced visible signs of toxicity. Though, significant physiological and biochemical changes were observed



in mature plants. Scallion plants exposed to nCuO at 75-300 mg/kg, improved their nutrient quality by increasing the allicin and essential element (Ca, Fe, Mg, Mn, and Ni) contents. This was, in most of the cases, contrary to the results observed with bCuO. Although nCuO significantly increased root GPOX and leaf APOX, it reduced CAT in both roots and leaves. Overall, the data suggest that nCuO at concentrations lower than 600 mg/kg may be used as nanofertilizer for green onion production.

## **Chapter 3: Effects of Different Surface-coated nTiO<sub>2</sub> on Full-life Grown Carrot Plants: Impacts on Root Splitting, Essential Elements Accumulation, and Ti Uptake**

### **3.1 INTRODUCTION**

Nanotechnology is proliferating and has become one of the most promising technologies. The engineered nanoparticles (ENPs) are its building blocks. Titanium dioxide nanoparticles (nTiO<sub>2</sub>) are among the most produced ENPs worldwide (Mitrano et al., 2015; Piccinno et al., 2012). It has been estimated that the annual production of nTiO<sub>2</sub> would reach nearly 2.5 million metric tons in 2050, which convert nearly 100% of the total TiO<sub>2</sub> market to nano (Robichaud et al., 2009). The TiO<sub>2</sub> production mainly comprises cosmetics (sunscreens), plastics, and coatings (Piccinno et al., 2012). An increase of nTiO<sub>2</sub> in the environment is expected as a result of its direct or indirect release (Keller and Lazareva, 2013). By 2014, the estimated emissions into soil and water were up to 23,130 and 36,664 metric tons/year, respectively (Keller and Lazareva, 2013). Since part of wastewater and sewage sludges would also flow into soil, an increasingly large amount of nTiO<sub>2</sub> will end up in agricultural soils that, due to its extreme chemical stability, will potentially impact crops (Cornelis et al., 2014).

To achieve superior performance and meet the demands from various consumers, modifications of nTiO<sub>2</sub> surfaces have been widely used (Pancrecius et al., 2018). Better appearance, enhanced properties, or advanced functionalities such as corrosion resistance, less catalytic degradation, self-cleaning, and depolluting abilities are achieved in hydrophilic or hydrophobic coated nTiO<sub>2</sub> (Bergamonti et al., 2015; Calia et al., 2017; Chen et al., 2019; Colangiuli et al., 2019). The effect of different surface coated nTiO<sub>2</sub> on plant development is still not well studied. The physiological responses of plants to ENPs depend on their surface coating

properties such as surface area, charge, hydrophilicity, and suspension stability, soil type, plant species, exposure method, and also the plant growth stage. Currently, no full-lifecycle studies have investigated the impact of nTiO<sub>2</sub> on the fruit quality of taproot crops. Tan et al. investigated the impacts of different surface-coated nTiO<sub>2</sub> on soil-grown basil (*Ocimum basilicum*) plants (Tan et al., 2017a). Shoot biomass was significantly decreased (by 37%) by hydrophobically coated nTiO<sub>2</sub>; root elongation (53%), total sugar (38%) and starch (35%) concentration were also declined, as compared with controls (Tan et al., 2017a). Foltête et al. (Foltête et al., 2011) reported that Ti internalization and high metal concentrations were detected in *Vicia faba* roots exposed to hydrophobically coated nTiO<sub>2</sub>.

Carrot (*Daucus carota* L.) is an economical and nutritionally important vegetable crop that is popular worldwide. It had a total annual production of 38.84 million metric tons in 2014 (Sharma, 2018). Mainly, the taproot is the consumed portion of the plant. It is expected that it will directly interact with ENPs from soils; hence, it is of great importance to investigate the effect of ENPs on the belowground crop development, especially those grown in natural soil. However, studies on this topic are limited. To the best of our knowledge, the only study of carrot and ENP interactions was published by Ebbs et al. (Ebbs et al., 2016). In the latter study, ZnO, CuO, or CeO<sub>2</sub> NPs were added into the soil at 0.5, 5, 50, or 500 mg/kg dry weight (DW). Root and total biomass were decreased in a concentration-dependent manner after being exposed to ZnO NPs. However, the effects of different surface coatings of nTiO<sub>2</sub> on the growth of carrot are still unknown.

The two-photon microscopy technique was applied in this study to analyze the uptake of nTiO<sub>2</sub> particles. This approach has the advantage of penetrating the sample and showing the internal structure via fluorescence, which is deeper than the traditional confocal microscopy. Additionally, samples are easily prepared at room temperature, which minimizes further damage

during the detection. Since nTiO<sub>2</sub> has self-fluorescence, no further dyeing process is needed, which makes nTiO<sub>2</sub> a feasible candidate for the two-photon microscopy study.

Thus, in this work, the impact of different surface coatings nTiO<sub>2</sub> on the carrot plant taproot development was studied. The agronomic parameters of the carrot plant, Ti uptake, and the nutrient elements disturbance were analyzed. Moreover, the penetration and uptake of Ti in carrot roots treated with pristine and two different coated nTiO<sub>2</sub> were assessed to compare the potential uptake pathways.

## **3.2. MATERIALS AND METHODS**

### **3.2.1 Preparation of nTiO<sub>2</sub> and soil treatments**

Pristine, hydrophilic, and hydrophobic surface-coated nTiO<sub>2</sub> were obtained from US research Nanomaterials and Sachtleben Chemie, Germany, respectively. The characterization is shown in Table S1, previously reported by Tan et al. (Tan et al., 2017a). All the three nTiO<sub>2</sub> have a rutile phase, with the same size of 50 ± 25 nm. The surface-modified nTiO<sub>2</sub> were both first capped with 6 wt% Al<sub>2</sub>O<sub>3</sub>. Then 1 wt% of glycerol or 2 wt% of dimethicone were further encapsulated in order to obtain the hydrophilic or hydrophobic properties. The release of Al<sup>3+</sup> from the surface coated nTiO<sub>2</sub> was previously tested (Tan et al., 2017a).

Nature soil and potting soil were mixed at the ratio of 5:1. Potting soil providing additional organic matters was purchased from a local supermarket (Miracle-Gro® organic). Natural soil was collected from a local agricultural area (Socorro TX, USA, an agricultural land at latitude: 31°67' N, longitude: 106°28' W, and elevation: 1115 m asl) and was previously characterized as medium loam: 19% clay, 44% silt, and 36% sand; 2.8% organic matter, pH =

$7.825 \pm 0.021$ ,  $EC = 1705 \pm 47.6 \mu\text{S cm}^{-1}$ , and  $TDS = 847.5 \pm 23.8 \text{ mg/L}$  (Majumdar et al., 2015b). Before use, natural soil was sieved through an 8 mm sieve and air-dried for three days.

The  $\text{nTiO}_2$  suspensions were made to reach the final concentration of 100, 200, and 400 mg Ti/kg soil. The highest concentration was chosen based on the predicted environmental  $\text{nTiO}_2$  concentrations, especially in the U.S. (Gottschalk et al., 2009). Pristine, hydrophilic, and hydrophobic  $\text{nTiO}_2$  were weighed and sonicated in 50 ml Millipore water (MW) suspensions using a water-based sonicator (Crest Ultrasonics, Trenton, NJ) for 30 min. Pure 50 mL MW was applied as a control. They were then added to soil and manually homogeneously mixed for 20 min. All the pots were then filled with MW until reaching 60% of the maximal field capacity and left for three days for equilibrium. Three replicates were applied for each treatment.

### **3.2.2 Seed germination and plant cultivation**

Carrot seeds (Royal Chantenay variety) were purchased from AGWAY® and stored at 4 °C for one week. Then, they were sterilized and disinfected with 2% NaClO MW solution for 20 min. After washing, seeds were then soaked in MW and stirred for 24 h for awakening and planted into soil. Fourteen days after germination in soil, seedlings were transplanted into pots containing the  $\text{TiO}_2$ -treated soils and placed into a growth chamber (Environmental Growth Chamber, Chagrin Falls, OH) in a randomized factorial design. The conditions set to benefit the plant growth were: 65% relative humidity, 25/20 °C day/night with  $340 \mu\text{mol m}^{-2} \text{ s}^{-1}$  light intensity, and 14 h photoperiod. No additional fertilizer or nutrient solution was added. After 115 days of growth, all the plants reached full maturity and were harvested.

### **3.2.3 Plant harvest and agronomic parameters**

At harvesting, plants were carefully separated from the soil and divided by lateral roots, taproots (peel and flesh), stems, and leaves. Each of the tissue sample was washed three times, with 0.01 M HNO<sub>3</sub> and MW to remove surface adhered soil and nanoparticles. Agronomic parameters of plant height, aboveground tissue weight, taproot length, taproot weight, and taproot water content were measured and recorded.

### **3.2.4 Ti uptake and nutrient element concentration**

Titanium uptake as well as macronutrients (Ca, Mg, P, S, and K) and micronutrients (Cl, Zn, Fe, B, Mn, Cu, Mo, and Ni) were measured by inductively coupled plasma – optical emission spectrometry (ICP-OES) (Perkin-Elmer Optima 4300 DV), according to previous literature (Larue et al., 2014a). Tissues were oven-dried at 70 °C in paper envelopes for 72 h. Dry samples were ground, and ~0.2 g were weighed for further acid-digestion according to a previous protocol (Tan et al., 2017b). To validate the measurements, blank (no plant tissues), pure nTiO<sub>2</sub> powder, standard reference material (NIST-SRF 1570a and 1547, Metuchen, NJ), and spiked samples were also treated by the same procedure and analyzed at every 20 samples interval. The recovery rate was 83%.

### **3.2.5 Two-photon microscopy**

Root fresh samples of carrots exposed to nTiO<sub>2</sub> at 400 mg/kg were mounted in the water-immersion objective lens (Olympus LUM Plan FLN) (Wang et al., 2020a). The light source used in the microscope was a mode-locked Ti: Sapphire laser (Spectra-Physics, Mai-Tai HP). 710 nm

light and 200 W was selected to achieve two-photon excitation. The fluorescence signal from the sample was deflected with a 665 nm long-pass dichroic mirror. The pulse duration was ~100 fs width, and the repetition rate was 80 MHz. Long-pass dichroic beam splitters (LDBS) were used to split the blue and green/red fluorescence signal. The blue, green, and red signals were transmitted through band-pass filters of 417-477 nm, 500-550 nm, and 570-616 nm, respectively, and finally, detected by a photomultiplier tube (PMT) at 2.10V, 2.20V, and 0.9V, respectively. The outputs of these three PMTs were fed into red/green/blue channels of a frame grabber installed on a computer. Two-dimensional images in the x-y plane are acquired through a custom software program. The imaging speed was 30 frames/sec, and each final static image was an average of 50 frames. Furthermore, some images exhibited red artifacts, such as streaks across the image, when processed by the frame grabber; but the artifacts were removed through minimal image processing (Acosta et al., 2014).

### **3.2.6 Statistical analysis**

All the data were analyzed using the Statistical Package for the Social Sciences 25 (SPSS, Chicago, IL, USA). Differences between treatments were determined by one-way ANOVA followed by a Post-Tukey test with a level of confidence of  $p \leq 0.05$ . Reported data are means  $\pm$  standard errors (SE) of triplicates.

## **3.3. RESULTS AND DISCUSSIONS**

### **3.3.1 Ti uptake**

Figure 3.1 shows that plants treated with hydrophilic and hydrophobic nTiO<sub>2</sub> at 400 mg/kg,

accumulated  $100.5 \pm 9.8$  mg/kg DW and  $140.1 \pm 19.0$  mg/kg DW of Ti in their secondary roots, respectively. These were the only treatments in which significant increased Ti uptake was found, compared to control plants, which had  $46.8 \pm 5.0$  mg Ti/kg DW (Fig. 3.1) ( $p \leq 0.05$ ). The Ti accumulation in plant roots have also been reported in different plant systems such as basil (Tan et al., 2017a), lettuce (Zahra et al., 2015) and soybean (Burke et al., 2015), after long-term exposure. Meanwhile, in this study, no detectable Ti was found in leaves, neither in flash nor core of carrot taproot.

The overall penetration of Ti into plant systems was relatively low. It has been reported that nTiO<sub>2</sub> NPs with sizes of less than 30 nm have the potential to penetrate cell membranes (Tan et al., 2018). In the current study, the three nTiO<sub>2</sub> particles exhibited the same ~50 nm average size as specified by the manufacturer and previously confirmed by TEM microscopy (Tan et al., 2017a), which is larger than the suggested limit for Ti cell uptake. However, since the latter parameter was evaluated by TEM microscopy, it is possible that a particular portion of unmeasured particles with smaller sizes eventually entered into carrot roots. Moreover, the Ti ions released from particulate compounds, although at a limited expected amount, could also be a possible source for Ti acquisition by cells. Another uptake pathway by which NPs might enter root cells is through the wound and breakage of the surface of lateral roots. Most of the treatments in this work did not result in changes in Ti uptake, suggesting the nTiO<sub>2</sub> application did not cause any morphologic injury or damage on the carrot root surface.

The significant higher uptake of Ti in root plants treated with coated nTiO<sub>2</sub> over the pristine-treated plants (Fig. 3.1), might occur due to the interaction of surface-coated materials with root surface external molecules. The root surface of cell membranes is negatively charged (Cooper GM., 2000; Kinraide and Wang, 2010), which may benefit the adsorption of the



positively charged coated nTiO<sub>2</sub> (Table S3.1). Moreover, according to the distribution of hydrodynamic particle size suspended in DI, the hydrophobic coated nanoTiO<sub>2</sub> exhibited a more substantial proportion of smaller-sizes (~ 250 nm) NPs (Fig. S3.1 A), compared with the other two TiO<sub>2</sub>-based compounds (Fig. S3.1 B and C). In addition, ions in soil with positive charge can adsorb a portion of the negatively charged pristine nTiO<sub>2</sub> (Table S3.1), reducing their bioavailability. Hence, our study illustrated a nanoparticle surface-component dependent effect on the element uptake.

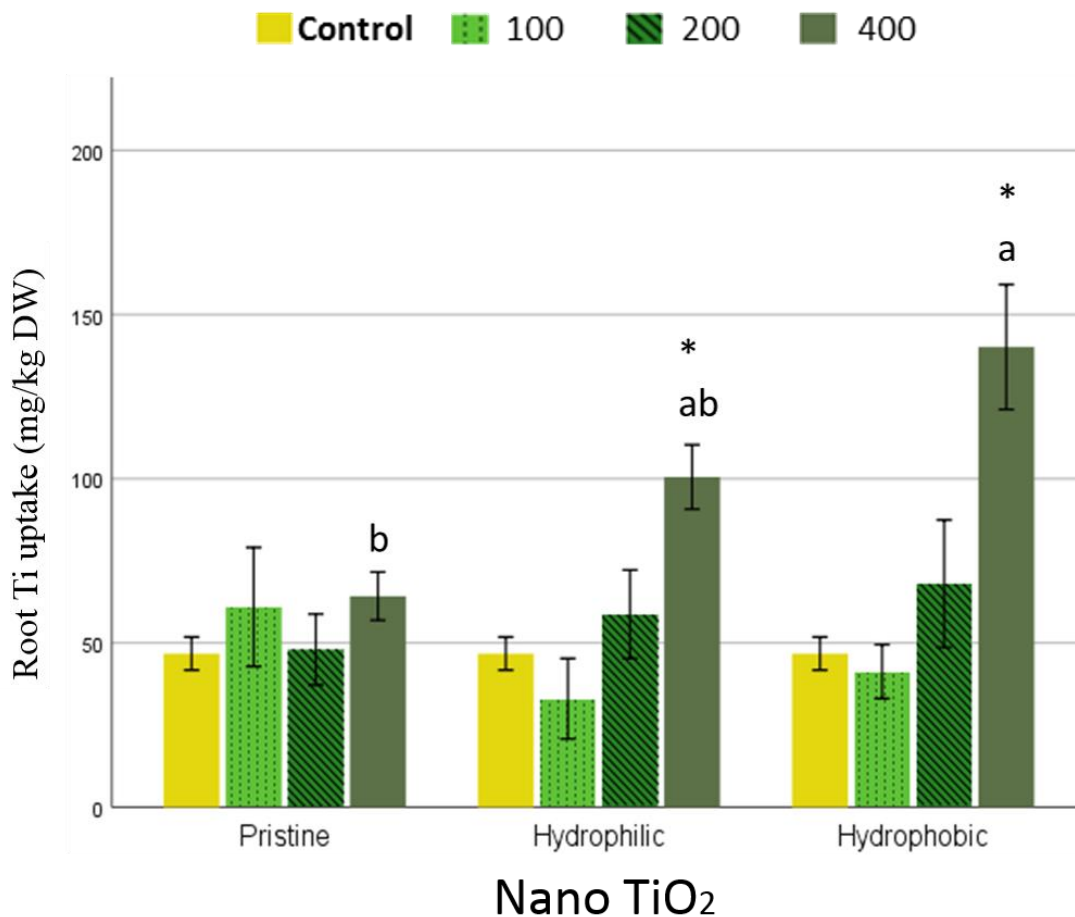


**Fig. 3.1.** Titanium concentration (mg/kg DW) in carrot roots exposed to pristine, hydrophilic, and hydrophobic coated nTiO<sub>2</sub> at 0, 100, 200 and 400 mg/kg. Data are the average of three replicates ± SE. Lowercase letters stand for statistical differences between different compounds

at the same concentration. Asterisk represent significant differences with respect to control ( $p \leq 0.05$ ,  $n = 3$ ).

Since the Ti uptake by root was low, it was expected to see a very reduced or no translocation of Ti to the aboveground tissues of the plant. The lack of mobility of Ti in plant roots has also been reported in previous literature (Tan et al., 2018). This output may be due to the aggregation, chemical inactivity, and nearly no dissolution properties of nTiO<sub>2</sub>. For example, nTiO<sub>2</sub> only with diameters lower than 36 nm succeeded to cross the Casparian band and were translocated from root to shoot in wheat (Larue et al., 2012).

### **3.3.2 Agronomical parameters**

#### **3.3.2.1 Leaf fresh weight and plant height**

As shown in Fig. 3.2A, fresh leaf weight remained unchanged in most treatments with respect to control. Only pristine nTiO<sub>2</sub> at 100 mg/kg increased leaf biomass by 51% compared with control, with values of  $44.6 \pm 4.0$  and  $29.6 \pm 3.0$  g/kg DW, respectively ( $p \leq 0.01$ ). At this concentration, fresh leaf biomass in plants exposed to pristine nanoTiO<sub>2</sub> was significantly higher than hydrophilic nTiO<sub>2</sub> and hydrophobic nTiO<sub>2</sub> treated plants by 31% and 84%, respectively ( $p \leq 0.01$ ). Since the tender foliage is also consumed as a stir-fried herb and in salads by many countries, the observed increment in leaf biomass may benefit the agriculture industry (Rubatzky et al., 1999).

A possible explanation of the increment of leaf biomass by pristine nanoTiO<sub>2</sub> may be linked to the root nitrogen assimilation improvement, as it has previously been reported in spinach (Yang et al., 2007, 2006). Also, highly enhanced mRNA expressions, arabinogalactan

proteins, and increase in protein levels, have been detected in response to nanoTiO<sub>2</sub> treatments (Gao et al., 2006; Tumburu et al., 2015). These biomolecules, along with hormone signaling pathways, play important roles in plant growth and development. Moreover, nTiO<sub>2</sub> are well-known as effective bactericides attributed to their photocatalytic activities, which may eliminate bacterial pathogen contamination in soil and increase plant resistance to stress (Ge et al., 2011; Mandeh et al., 2012a). Moreover, the improvement of plant photosynthetic activity caused by nTiO<sub>2</sub> photocatalytic properties has been mentioned before (Tumburu et al., 2015). Nano TiO<sub>2</sub> may induce oxidation-reduction reactions and benefit electron transfer, thus increasing light absorption efficiency, improving the photochemical reaction of chloroplasts (Hong et al., 2005a), and facilitating chloroplast protection against free radicals production (Hong et al., 2005b). For instance, a genomic study of thale cress (*Arabidopsis thaliana*) seedlings watered by non-coated nTiO<sub>2</sub> suspension at 500 mg/L induced photosynthesis-related genes (Tumburu et al., 2017). However, it has been suggested that plant growth and development are nTiO<sub>2</sub> concentration and species-dependent (Tan et al., 2018)(Song et al., 2012)(Raliya et al., 2015). In the present study, an enhancement of leaf nutrient elements accumulation (Ca, Mg, Fe, Se, and Zn) was also found (Fig. 3.5), which also benefits carrot leaves' growth.

The plant height was significantly increased by ~18% when plants were treated with pristine nTiO<sub>2</sub> at all concentrations, and hydrophobic nTiO<sub>2</sub> at 100 mg/kg, compared to control (Fig. 3.2B). Similar results were reported with rice (Zahra et al., 2017), tomato (Raliya et al., 2015), and wheat (Rafique et al., 2015) in long-term soil exposure studies.

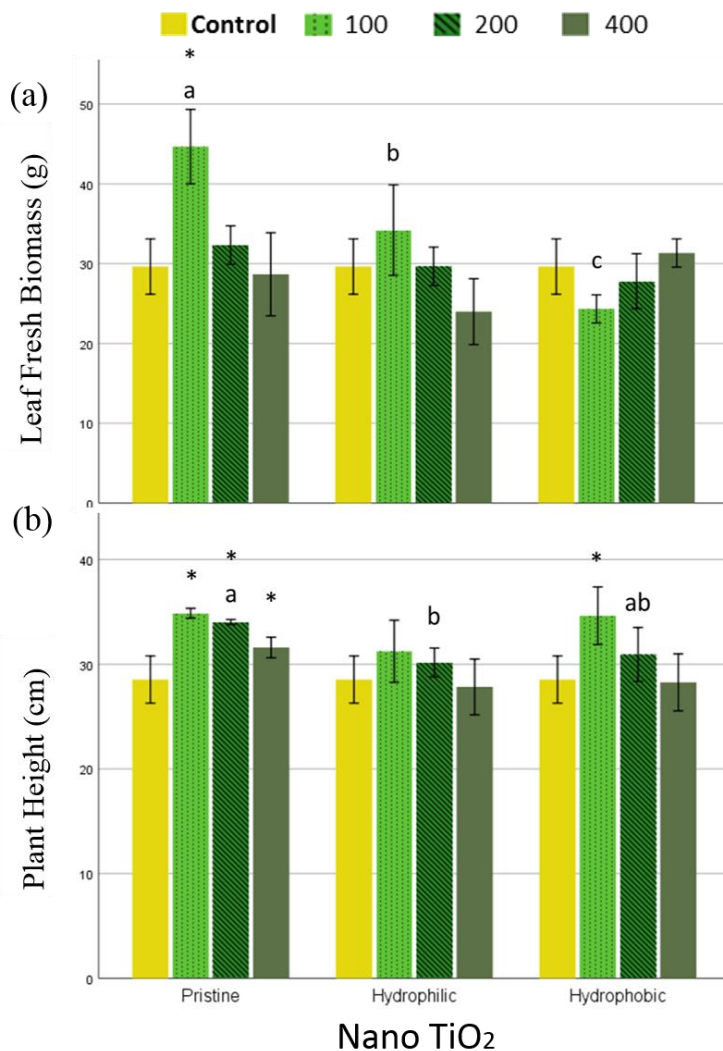


**Fig. 3.2.** (A) Leaf fresh biomass (g) and (B) plant height (cm) of carrots exposed to pristine, hydrophilic, and hydrophobic coated nTiO<sub>2</sub> at 0, 100, 200 and 400 mg/kg. Data are the average of three replicates  $\pm$  SE. Lowercase letters stand for statistical differences between different compounds at the same concentration. Asterisk represent significant differences with respect to control ( $p \leq 0.05$ ,  $n = 3$ ).

### 3.3.2.2 Taproot morphology, splitting, and fresh weight

During the days of growth, no adverse health signs such as wilting, or necrosis were observed in treated plants. However, at harvesting, taproots splitting increased as a result of TiO<sub>2</sub> exposure (Fig. 3.3). This phenomenon was also previously reported with other plants such as

tobacco and wheat. In the experiment related to tobacco species, the seedlings that grew in 1% nTiO<sub>2</sub> Petri dish-suspension produced two roots, instead of one root (Frazier et al., 2014). In the other study, wheat seedlings grown for 14-days in hydroponic conditions, showed an increment in lateral roots after nTiO<sub>2</sub> exposure at 10~1000 mg/L, compared to control (Jiang et al., 2017). Concerning the latter result, the authors refereed that the splitting of the taproots was a strategy of carrot plants to overcome the stress caused by the adherence of nTiO<sub>2</sub> onto the root surface, facilitating the obtention of enough water and nutrients for plant development. In the same study, a dose-dependent increase of abscisic acid content was detected, which would also explain the lateral root development, since abscisic acid triggers the growth of root (Jiang et al., 2017). Besides, it has been proved that nTiO<sub>2</sub> could induce cell division in the root tip, attributed to its photocatalytic and antimicrobial activity (Mandeh et al., 2012a). It could pass through the apoplast and induce the production of hydroxyl radicals, which are reported as potential cell wall-loosening agents and cell enlargement stimulators (Larue et al., 2012). The rapid emergence may eventually induce taproot splitting, change soil pH, moisture, and soil compaction property.

The fresh taproot weight of plants was reduced by almost all nano-TiO<sub>2</sub> treatments compared to control (Fig. 3.4). Hydrophilic and hydrophobic surface coated nTiO<sub>2</sub> significantly decreased taproot biomass at all concentrations in a range of 29-46% and 39-56%, respectively, compared with control. However, pristine nTiO<sub>2</sub> only affected the fresh weight at the highest concentration ( $p \leq 0.01$ ). This result was different compared with leaf biomass (Fig. 3.2A). In a previous short-term exposure experiment, the biomass of basil was significantly decreased by ~16% after being exposed to pristine and hydrophobic nTiO<sub>2</sub> (Tan et al., 2017a). Similar results were found in other long-time exposure studies. The biomass of wheat (Du et al., 2011; Rafique et al., 2015), tomato (Vittori Antisari et al., 2015), and rice (including grain yield) (Wu et al.,

2017) were reduced after the nTiO<sub>2</sub> application. Asli and Neumann explained that the aggregated nTiO<sub>2</sub> cluster would block the absorption of water by root cell, thus, reducing root hydraulic conductivity. These may cut down the water supply and induce moisture stress, thus ultimately affecting root elongation (ASLI and NEUMANN, 2009).

On the other hand, contrasting results have been reported. Nano TiO<sub>2</sub> was reported to enhance the growth of plant roots in cucumber and wheat by Servin et al. (2012) and Larue et al. (2012) reported positive effects of rutile nTiO<sub>2</sub> at the concentration of 0.025–0.4% on germination and seedling growth of naturally aged spinach (*Spinacia oleracea* L.) seeds. The root length of duckweed increased along with the increased nTiO<sub>2</sub> concentrations below 500 mg/L (Song et al., 2012). In another study, nTiO<sub>2</sub> exposure caused reduced root elongation in cabbage, corn, lettuce, and oat, while improved cucumber and onion roots, indicating that the effect was species-dependent (Andersen et al., 2016).

Additionally, the data of the taproot core diameter is shown in Fig. S3.2. They were decreased in pristine and hydrophilic-coated nTiO<sub>2</sub> treated plants at 400 mg/kg, and hydrophobic-coated nTiO<sub>2</sub> at all concentrations. The overall average reduction caused by nTiO<sub>2</sub> treatments was  $1.2 \pm 0.1$  cm, compared with control (3.8 cm). The core is mainly xylem, tasting woody and slightly bitter. Thus, carrots considered to have high quality should have a smaller core proportion. In this study, the shape of the carrot taproot was defined by the values of total length, top, and mid perimeters. Although the total biomass of taproots was reduced, total taproot length, taproot top, and mid perimeter remained unchanged in most treatments. Only at 400 mg/kg, the total taproot length and taproot mid perimeter treated by pristine nTiO<sub>2</sub> was significantly less than control ( $p \leq 0.05$ ).



**Fig. 3.3.** Taproot of control (a), un-coated nTiO<sub>2</sub> treated plants at 100 (b), 200 (c) and 400 (d) mg/kg, hydrophilic coated nTiO<sub>2</sub> treated plants at 100 (e), 200 (f) and 400 (g) mg/kg, and hydrophobic coated nTiO<sub>2</sub> treated plants at 100 (h), 200 (i) and 400 (j) mg/kg.

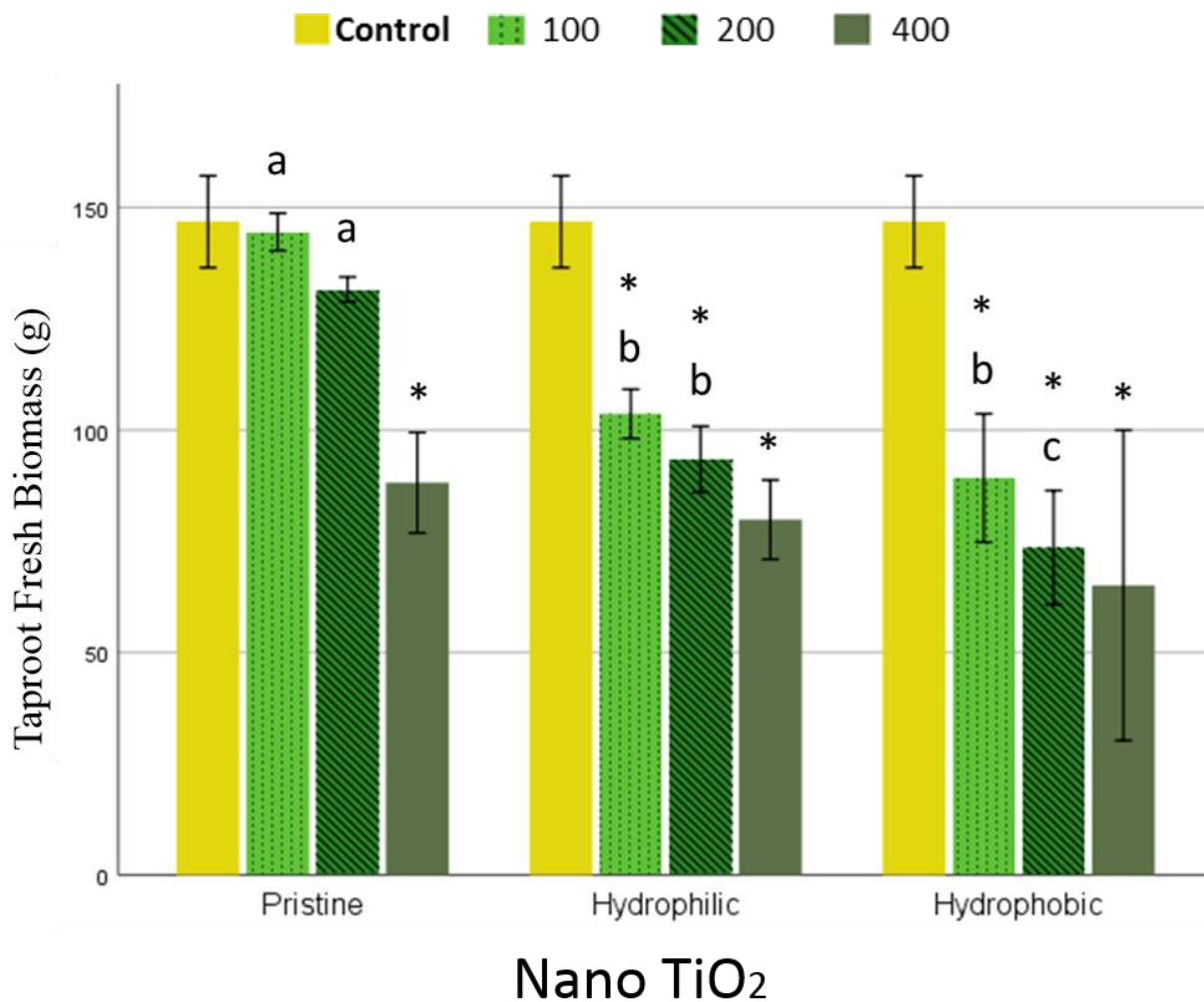


**Fig. 3.4.** Taproot fresh biomass (g) of carrots exposed to pristine, hydrophilic, and hydrophobic coated nTiO<sub>2</sub> at 0, 100, 200 and 400 mg/kg. Data are the average of three replicates ± SE. Lowercase letters stand for statistical differences between different compounds at the same concentration. Asterisk represent significant differences with respect to control ( $p \leq 0.05$ ,  $n = 3$ ).

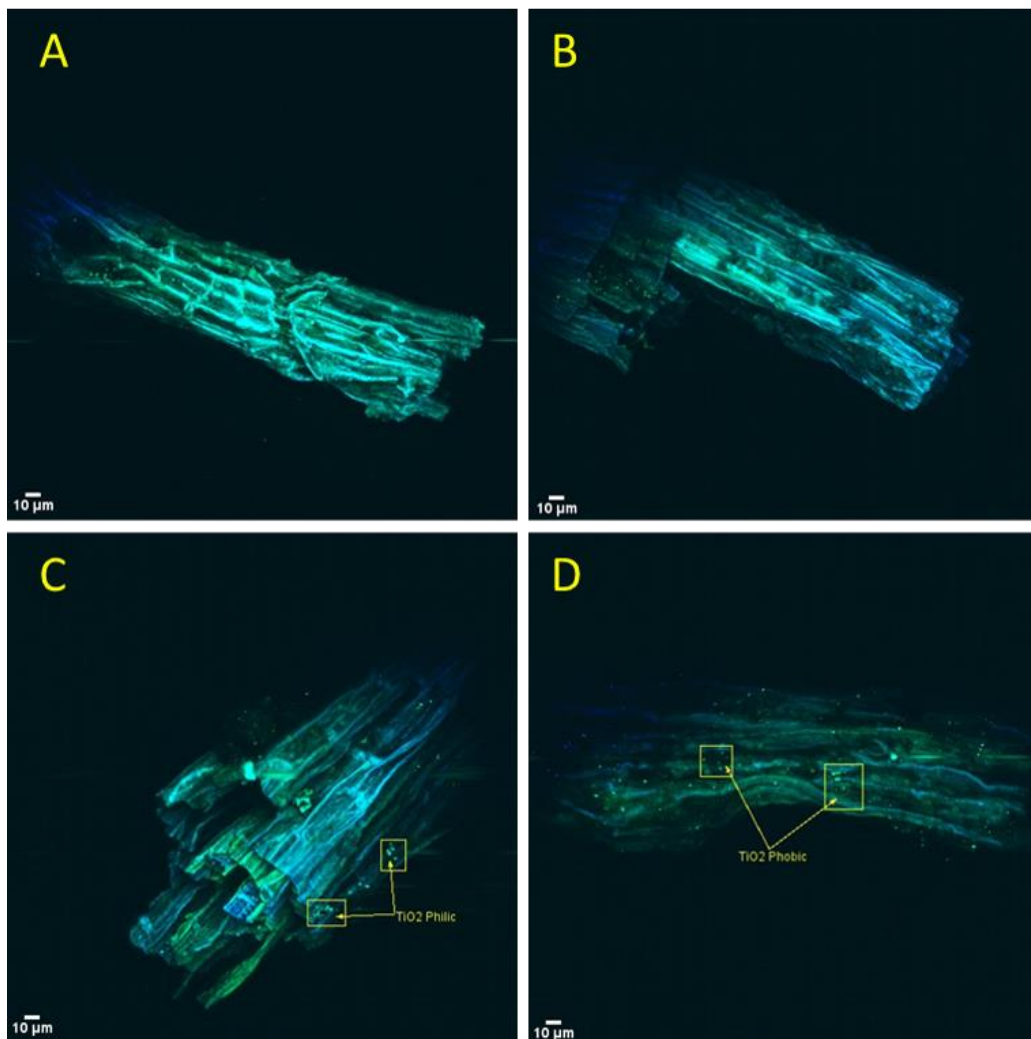
### 3.3.3 Two-photon microscopy image of root Ti uptake

Fig. 3.5 shows representative images of control plant roots (Fig. 3.5A) and roots exposed to pristine (Fig. 3.5B), hydrophobic (Fig. 3.5C) and hydrophilic (Fig. 3.5D) nTiO<sub>2</sub>. The fluorescence emission characterization of pristine, hydrophilic, and hydrophobic nTiO<sub>2</sub> in DI



water is presented in Supplementary Fig. S3.3. The images (Fig. 3.5C-D) suggest that roots were able to acquire Ti from soils treated with different types of surface-coated nTiO<sub>2</sub>; while no detectable signal of uptake was found in control and pristine nTiO<sub>2</sub> treated roots. Slight differences in the fluorescence patterns (hydrophilic with linear rainbow and hydrophobic as bright points) of each nTiO<sub>2</sub> were observed, due to possibly the different chemistry of surface coatings. These differences were also detected when characterizing the surface coated nTiO<sub>2</sub> suspensions (Fig. S3.3). These distinctive fluorescence patterns may suggest that even after uptaken by root tissue, a certain portion of the surface coatings may remain unchanged. This may also provide a potential method to distinguish nano TiO<sub>2</sub> with different surface coatings inside plant tissues. To confirm the potential chemical transformation, more microscope studies are needed in the future.

When comparing the fluorescence spots in Fig. 3.5C and 3.5D, the NPs distribution patterns looked similar to each other. These patterns indicated that the penetration and uptake mechanism of two surface-coated nTiO<sub>2</sub> were likely the same. Possibly, the hydrophilic or hydrophobic surface coating did not affect the NP uptake pathway. In a previous study of nCuO treated green onion, an apoplastic pathway of Cu uptake was suggested using the two-photon microscopy (Wang et al., 2020a). The fluorescence distribution patterns are also depending on the plant varieties. Previously, the different biodistribution of Cu in bok choy leaves of two phenotypes exposed with nCuO was observed (Deng et al., 2020).



**Fig. 3.5.** Two-photon microscopy images of carrot (A) control root and roots treated with (B) pristine, (C) hydrophilic, (D) hydrophobic coated nTiO<sub>2</sub> at 400 mg/kg soil, and. The fluorescence of root cell walls and vascular tissue is shown. Fluorescence from (C) hydrophilic, (D) hydrophobic coated nTiO<sub>2</sub> are pointed out by arrows inside the square.

### 3.3.4 Micro and macro elements in leaf

Leaf macro (Ca, K, Mg, N, P, and S) and micro (B, Cl, Cu, Fe, Mn, Mo, Ni, Se, and Zn) element concentrations were determined by ICP-OES. Table 3.1 displays the elements with significant changes in comparison to control plants (Ca, Mg, Fe, Se, and Zn).

**Calcium**-Leaf Ca concentration in plants treated with hydrophilic and hydrophobic coated nTiO<sub>2</sub> at 400 mg/kg (32,184 and 30,607 mg/kg, respectively), were significantly higher than the pristine one and control (22,824 and 20,706 mg/kg) ( $p \leq 0.05$ ). Interestingly, this was in line with the root Ti uptake pattern results. The average Ca content in control is similar to a previously reported value, which is 2% of dry leaf weight (Septian, 2017). Calcium plays a messenger role between environmental changes and plant responses, which involves hormone production, enzymatic activity, and nodulation. A higher Ca content benefits leaf growth and development.

Calcium can be translocated to the xylem as Ca<sup>2+</sup> solely or complexed with organic acids through the root apoplast (Hepler, 2005). The improvement of Ca uptake by nTiO<sub>2</sub> application to plants has previously been reported. High level of roots, shoots, and kernels Ca was found in nTiO<sub>2</sub> treated barley at 500 and 1000 mg/kg of soil (Pošćić et al., 2016). In another study, the higher accumulation of Ca in lettuce root epidermis was presented by nTiO<sub>2</sub> suspension at the highest concentration of 1000 mg/L, which was not observed at lower concentrations, indicating a dose-dependent mechanism (Larue et al., 2016a). However, this phenomenon was not nTiO<sub>2</sub>-specific since a similar profile with the exposure to nano-Ag was found in the same study. Another possible explanation laid within the different surface charges of three nTiO<sub>2</sub>. The negatively charged pristine nTiO<sub>2</sub> is likely to attract and complex with positive Ca<sup>2+</sup> ions at the root-soil interface, reducing its mobility and uptake. On the other hand, unlike the pristine one, hydrophilic and hydrophobic coated nTiO<sub>2</sub> with a positively charged surface (Table S1) could be associated with the fusaric acid, which could bind divalent metals forming chelating complexes in soil, thus, increase the bioavailable positively charged Ca<sup>2+</sup> and accelerate the absorption to

the negatively charged root surface (Cooper GM., 2000; Kinraide and Wang, 2010). Similar results were found in tomato treated with positively charged nano CeO<sub>2</sub> (Adisa et al., 2018a).

**Magnesium**-No significant impacts were found at 100 and 200 mg/kg. However, at 400 mg/kg, hydrophilic and hydrophobic nTiO<sub>2</sub> induced significantly more Mg in leaves (4,372 and 4,136 mg/kg) than the pristine one (2,688 mg/kg), as well as than control (3,022 mg/kg). This trend was in consist with leaf Ca. Mg has a role in maintaining the permeability of cell membranes and plays an important role in the formation of chromosomes, energy production, protein synthesis, and is the core of the chlorophyll molecule (“Magnesium | Linus Pauling Institute | Oregon State University,” n.d.).

This result was expected since it is known that both Ca and Mg share the same transporter, AtCNGC10 (Guo et al., 2010b). This suggests that the surface coated nTiO<sub>2</sub> might induce the activation of the AtCNGC10 protein in root, improving the translocation of Mg<sup>2+</sup> to leaves. Similarly, Hrubý et al. (2002) reported that oat (*Avena sativa* L.) showed an increase in Mg content with increased Ti(IV) concentrations in nutrient solutions.

**Iron**-The Fe concentrations in carrot leaf were only significantly increased by hydrophilic and hydrophobic nTiO<sub>2</sub> treatments (61.0 and 51.1 mg/kg, respectively) at the highest concentration compared with control (26.2 mg/kg,  $p \leq 0.05$ ). In addition, the increment at 200 mg/kg induced by hydrophobic nTiO<sub>2</sub> (60.9 mg/kg) was significantly higher than the pristine one (29.3 mg/kg). Again, this trend is very similar to the changes in leaf Ca and Mg.

As reported in previous literature, a significantly positive correlation (coefficients > 0.79) between concentrations of Fe and Ti was found after the exposure of nTiO<sub>2</sub> (Jacob et al., 2013), same as detected in this present study. In another study with lettuce, higher accumulation of root Fe was found at the highest applied concentration of nTiO<sub>2</sub> (1000 mg/L), while not at the lower

ones (10 and 100 mg/L) (Larue et al., 2016a). This last result is also in line with our findings, indicating a dose-dependent impact. To explain this phenomenon, other than the surface charge effect of NPs pointed out above, it is also possible that the stress caused by nTiO<sub>2</sub> treatments increased the production of ferritin, a protein that binds iron (Deák et al., 1999).

**Selenium**-Significant responses were observed only at the highest concentration in the hydrophobic nTiO<sub>2</sub> treatment, where the leaf Se concentration was higher by 211% and 203%, with respect to control and pristine equivalent ( $p \leq 0.05$ ).

No corresponding data was found in the literature; thus, it was impossible to compare our results to the previous one. Usually, Se is uptaken by plants as SeO<sub>4</sub><sup>2-</sup>. Since Se is chemically similar to S, they share the same metabolic pathway and transporters (Sors et al., 2005). Among the three nTiO<sub>2</sub> treatments, a significant increase was only detected in leaves from plants treated with hydrophobic compounds. Since no differences were caused by pristine nTiO<sub>2</sub>, and no similar result was found in literature in other plants treated by pristine nTiO<sub>2</sub>, we could infer that the specific increment of Se was due to the hydrophobic surface coating.

**Zinc**-Compared with control (33.5 mg/kg), both two surface-coated nTiO<sub>2</sub> increased leaf Zn accumulation significantly at all exposed concentrations by the range of 71-138% and 158-344%, respectively ( $p \leq 0.05$ ). At each concentration, the lowest value was in pristine treatment, while the highest one laid with hydrophobic one. At all concentrations, hydrophobic coated nTiO<sub>2</sub> caused significantly higher leaf Zn concentration than the pristine one by the range of 86-375%.

Zn plays a critical role as a cofactor of numerous plant enzymes and transcription regulation (Lindsay, 1972). Previously, Zn concentration improved by 500 mg/kg TiO<sub>2</sub> in barley kernels was reported (Pošćić et al., 2016). However, the enhance mechanism is still not clear.

Since Zn and Fe share the same transporters of the ZIP family, it is possible that the increase of Zn is related to the up regulation of Zn transporter, the same as the increase of Fe. However, this does not explain why only hydrophobic coated nTiO<sub>2</sub> showed the most significant changes. Thus, the following reason should be applied. Several types of superoxide dismutases (SODs), an efficient antioxidant against ROS, uses Zn as their cofactors (R. G. Alscher et al., 2002). Thus, it is also highly possible that the over-accumulation of Zn was a strategy by plants against the excess of ROS induced by the nTiO<sub>2</sub> treatments. It could be deduced that the hydrophobic-coated nTiO<sub>2</sub> induced more ROS stress to carrot plants, compared with the pristine.

### **3.3.5 Micro and macro elements in secondary roots**

*Zinc*-Interestingly, although all the nTiO<sub>2</sub> were applied to the soil, and interacted only and directly with plant roots, most of the nutrient element concentration changed to a lesser extent, compared with the leaf. The only significant difference was found in Zn accumulation. Significantly higher Zn concentration were observed in secondary roots of plants treated with hydrophobic nTiO<sub>2</sub> at all concentrations compared with control, by the range of 139-270% ( $p \leq 0.05$ ) (Table 1). Hydrophobic coated nTiO<sub>2</sub> induced significantly higher root Zn accumulation at 200 and 400 mg/kg (263.0 and 202.2 mg/kg) than pristine (89.6 and 64.7 mg/kg), and at 200 mg/kg than hydrophilic coated one (94.9 mg/kg). No significant changes were found in all the pristine and hydrophilic nTiO<sub>2</sub> treatments. Similar with the increment of Zn in leaves, it is likely that the hydrophobic nTiO<sub>2</sub> induced relatively higher ROS formation in carrot roots than the other two treatments; thus, more uptake of Zn was required as cofactors of SODs, to protect plants against the exogenous stress.

**Table 3.1.** Concentration (mg/kg DW) of micro- and macro-elements in carrot leaves (Ca, Mg, Fe, Se and Zn), secondary roots (Zn) and taproots (K, Mg, Mn and Zn). Plants were cultivated for 115 days in soil amended with pristine, hydrophilic and hydrophobic coated nTiO<sub>2</sub> at 0 (control), 100, 200 and 400 mg of Ti/kg of soil. Data are averages of 3 replicates ± Standard Error (SE).

Plant part	Element	Treatment	Concentration	Mean	Std. Error
Leaf	Ca	Control		20,705.501	1,064.91
		Pristine	400	22,824.25	1,249.43
		Hydrophilic	400	32,184.25	1,980.39
		Hydrophobic	400	30,607.24	2,227.91
	Mg	Control		3021.94	110.35
		Pristine	400	2,688.36	171.51
		Hydrophilic	400	4,372.12	65.65
		Hydrophobic	400	4,135.79	252.13
	Fe	Control		26.18	1.64
		Pristine	200	29.34	4.33
		Pristine	400	41.97	4.29
		Hydrophilic	200	45.28	9.06
		Hydrophilic	400	60.98	4.31
		Hydrophobic	200	60.87	4.44
		Hydrophobic	400	51.10	7.09
		Se	Control	0	5.99
	Pristine		400	6.16	.67
	Hydrophilic		400	12.79	.83
	Hydrophobic		400	18.65	2.48
	Zn	Control	0	33.51	4.03

		Pristine	100	48.60	16.10
		Pristine	200	31.34	1.89
		Pristine	400	46.50	3.84
		Hydrophilic	100	57.36	7.84
		Hydrophilic	200	67.99	1.30
		Hydrophilic	400	79.85	4.69
		Hydrophobic	100	112.58	15.53
		Hydrophobic	200	148.86	6.98
		Hydrophobic	400	86.55	3.62
<b>Root</b>	Zn	Control	0	71.08	8.36
		Pristine	100	100.82	8.14
		Pristine	200	89.55	11.17
		Pristine	400	64.71	7.96
		Hydrophilic	100	88.75	17.71
		Hydrophilic	200	94.94	39.55
		Hydrophilic	400	172.07	26.22
		Hydrophobic	100	169.77	26.05
		Hydrophobic	200	262.96	19.96
		Hydrophobic	400	202.16	18.07
<b>Taproot flesh</b>	K	Control	0	19992.43	2395.34
		Pristine	100	22108.44	315.67
		Pristine	200	24980.34	1795.36
		Pristine	400	31672.96	2340.89
		Hydrophilic	100	32156.96	2581.50
		Hydrophilic	200	34564.44	3932.10
		Hydrophilic	400	39800.94	1427.25
		Hydrophobic	100	32430.41	765.29
		Hydrophobic	200	40070.22	5782.00



	Hydrophobic	400	42658.82	5896.70
Mg	Control	0	814.67	35.70
	Pristine	100	633.81	13.36
	Pristine	200	513.31	39.77
	Pristine	400	542.20	47.24
	Hydrophilic	100	481.98	61.47
	Hydrophilic	200	532.54	73.91
	Hydrophilic	400	414.72	20.59
	Hydrophobic	100	534.48	43.51
	Hydrophobic	200	511.70	38.59
	Hydrophobic	400	626.64	38.55
Mn	Control	0	8.14	.54
	Pristine	100	9.13	.03
	Pristine	200	6.70	.63
	Pristine	400	2.47	.28
	Hydrophilic	100	2.57	.58
	Hydrophilic	200	4.40	.78
	Hydrophilic	400	4.49	.53
	Hydrophobic	100	4.44	.72
	Hydrophobic	200	3.55	1.06
	Hydrophobic	400	4.39	.12
Zn	Control	0	8.77	.35
	Pristine	100	9.82	.68
	Pristine	200	2.96	1.13
	Pristine	400	1.81	.78
	Hydrophilic	100	3.74	.65
	Hydrophilic	200	4.27	1.48
	Hydrophilic	400	2.83	.24
	Hydrophobic	100	5.05	.85

Hydrophobic	200	4.25	.98
Hydrophobic	400	5.12	.96

### 3.3.6 Micro and macro elements in the taproot

**Potassium**-As shown in Table 3.1, all the three types of nTiO<sub>2</sub> increased taproot flesh K concentrations. The enhancement was more significant with hydrophilic and hydrophobic coated treatments. At 100 mg/kg, they caused significantly higher K accumulation than the pristine (22,108 mg/kg DW) by 45.5 and 46.7%, respectively. Compared with control (19,992 mg/kg DW), significant increments were found in plants treated with two surface coated nTiO<sub>2</sub> at 200 and 400 mg/kg (by 72.9-113.4%), and the pristine one at 400 mg/kg (by 58.4%) ( $p \leq 0.05$ ). In addition, dose-dependent responses were found. On average, taproot K accumulation was significantly increased by nTiO<sub>2</sub> treatments at 100 (28,899 mg/kg) and 400 mg/kg (38,044 mg/kg), with respect to control (19,992 mg/kg).

**Magnesium, Manganese, and Zinc**-As seen in Table 3.1, taproot flesh Mg accumulation was significantly decreased in all the treatments by up to 49.1%, compared with control (814 mg/kg) ( $p \leq 0.05$ ). However, no dose-dependent trend was found. In addition, at 400 mg/kg, the reduction in hydrophobic coated nTiO<sub>2</sub> treatments (626.6 mg/kg) was less than the hydrophilic coated one (414.7 mg/kg). A very similar pattern was found of Mn and Zn concentrations in taproots (Table 1), where their value in most treatments was significantly lower than control. Again, at 400 mg/kg, less reduction effect was detected by hydrophobic coated nTiO<sub>2</sub> on Mn and Zn accumulations (4.39 and 5.12 mg/kg), with respect to pristine (2.47 and 1.81 mg/kg). The different particle surface charges could be one of the reasons. The positively charged

hydrophobic nTiO<sub>2</sub> may repel those cations of Mg<sup>2+</sup>, Mn<sup>2+</sup>, and Zn<sup>2+</sup> in soil, increasing their bioavailable amount, different from the negatively charged pristine nTiO<sub>2</sub>.

Similar results of the reduction of Mg and Mn concentrations were reported by Jacob et al. using beans, wheat, and curly dock exposed to pristine nTiO<sub>2</sub>. In their experiment, seedlings grown in Petri dishes were transplanted to hydroponics and exposed for 4-weeks to the NPs (Jacob et al., 2013). With the addition of nTiO<sub>2</sub>, the concentration of Mg and Mn decreased from 2479 and 5219 mg/kg to 2041 and 4340 mg/kg, respectively (Jacob et al., 2013). A potential explanation could be the nutrient-nutrient interactions summarized previously by other researchers. They found the divalent cation transporter, which involved in Mn uptake by plants interacted with Mg and Zn (Bindraban et al., 2015). The excess of other elements may also cause the deficiency of Mg, Mn, and Zn (Chen et al., 2009). In addition, Mn and Zn act as a cofactor for the antioxidant enzymes of Mn/Zn superoxide dismutase (Mn/ZnSOD) and MnSOD, which protects plants against ROS damage.

### **3.4 CONCLUSION**

This study describes the surface coating chemistry-dependent responses of carrot plants treated with nTiO<sub>2</sub>. Ti accumulation in roots exposed to coated nTiO<sub>2</sub> was higher than pristine nTiO<sub>2</sub> and control, as proved by the ICP data. A similar distribution pattern of hydrophilic and hydrophobic-nTiO<sub>2</sub> treatments secondary roots may suggest an uptake pathway independent of the surface coating chemistry of nTiO<sub>2</sub>. No detectable Ti translocation was found in taproots or the up-ground parts. Although no visible signs of toxicity were observed in carrot up-green parts and secondary roots, abnormal taproot splitting decreased taproot biomass and essential element

(Mg, Mn and Zn) accumulations. The contents of Ca, Mg, Fe, and Zn in leaves was increased after treated with pristine and hydrophilic nTiO<sub>2</sub> but not after hydrophobic nTiO<sub>2</sub> application, suggesting a surface coating effect. Due to the impacts mentioned above, more sustainable, and biocompatible surface coatings developments are needed. The effect of NPs and their surface coatings need to be considered when making regulations, since they differently affected plant Ti uptake, root splitting biomass, and elements accumulation. More studies on the long-term effect of surface-coated NPs in the ecosystem are required.

## **Chapter 4: Aging Process as A Sustainable Strategy to Alleviate Phytotoxicity of Nanoparticles: Soil-Aged Surface-Coated nano TiO<sub>2</sub> Improve Full-grown Carrot Physiological Performance**

### **4.1 INTRODUCTION**

Agricultural crops are the main source used to feed the rapidly growing world population, which is estimated to be 9 billion in 2050. Agriculture production will constantly face adverse conditions such as climate change and shrinking farmlands. Engineered nanoparticles (ENPs) are being studied and applied as potential nanopesticides or nanofertilizers (White and Gardea-Torresdey, 2018). The possibility of direct and indirect contact of ENPs with farmlands has increased, along with other pathways via ENPs-treated wastewater irrigation, unregulated industrial waste discharge, landfill leaching, and accidental spills (Rawat et al., 2018a). Thus, the potential effects of the released ENPs to the ecological environment, especially agriculture crops, need to be thoroughly investigated.

Nano TiO<sub>2</sub> (nTiO<sub>2</sub>), used mainly as cosmetics (sunscreens), plastics, and coatings (Piccinno et al., 2012), is considered as the most produced ENPs worldwide (Mitrano et al., 2015; Piccinno et al., 2012). In 2010, the estimated annual emissions into soil and water were up to 23,130 and 36,664 metric tons, respectively (Keller and Lazareva, 2013). It is estimated that the TiO<sub>2</sub> world annual production will be around 2.5 million metric tons by 2050, which will occupy nearly 100% of the total TiO<sub>2</sub> material market (Robichaud et al., 2009). Remarkably, nTiO<sub>2</sub> with hydrophilic or hydrophobic surface coatings have been developed and widely used nowadays to achieve advanced functionalities and meet unique demands, such as corrosion resistance, less catalytic degradation, self-cleaning and depolluting abilities (Bergamonti et al., 2015; Calia et al., 2017; Chen et al., 2019; Colangiuli et al., 2019).

As one of the leading sinks, soils could preserve ENPs for a longer time compared to the aquatic media (Peijnenburg et al., 2016). The interaction between ENPs and soil is relatively complex, since a soil-water-air interface is included in the vadose zone (Yechezkel et al., 2016). Factors involved in ENPs fate and transformation in soil include soil porosity, texture, structure, matrix surface charge, pH, organic matter content, salinity, and microbial activity. Besides, environmental conditions such as moisture, temperature, and the properties of ENPs such as chemical composition and surface coatings, should also be considered (Rawat et al., 2018a). Among all of them, the surface chemistry of ENPs plays a significant role since they affect solubility and chemical reactivities due to the presence of differently coated functional groups. However, the function that those surface coatings have on the development of plants is still not well understood.

Moreover, the effect of soil-aged nTiO<sub>2</sub> with different surface coatings on plant development is still unknown. Soil plays a unique role in the physical or chemical transformations of environmental pollutants over time (Alexander†, 2000; Coutris et al., 2012). Since the chemical properties of nTiO<sub>2</sub> are largely stable, they could be retained in the surface region of soil for a relatively long time (Chen et al., 2012; Godinez and Darnault, 2011). During the weathering process, nTiO<sub>2</sub> interact with the soil and affect soil microorganism's function. In addition, the nTiO<sub>2</sub> coatings can be removed or react with the organic matter during the weathering in soil (Lapied et al., 2011). Previously, nano and micro TiO<sub>2</sub> mixtures from aged paint were foliarly-exposed to lettuce for 7 days (Larue et al., 2014b). The results of this study showed that both TiO<sub>2</sub> particles were internalized and found in all types of tissues. Since time is a significant factor that affects ENPs aging process (Labille et al., 2010), long term aging of TiO<sub>2</sub> in soil and its effects on plant performance in a full life cycle are needed.

Carrots (*Daucus carota* L.), with a total annual production of 38.84 million metric tons in 2014, is a widely consumed and nutritionally important root crop (Sharma, 2018). Compared to other vegetables and in spite of the fact that its main edible part is laid in soil under potentially direct interaction with the ENPs, few studies on carrot plants after ENPs exposure exist. To the authors' knowledge, the effect of aged ENPs on the development of carrot plants is unknown.

Here, we present a follow-up study from our previous work on carrot plants. The mentioned research demonstrated the phytotoxic effects of surface-coated nTiO<sub>2</sub> on carrot development (Wang et al., 2020b). Hence, we were interested in evaluating the TiO<sub>2</sub> weathering effect on carrot physiological performance. This study aimed to determine the effects of aged nTiO<sub>2</sub> modified with different surface coatings on carrot plant development, grown in natural soil. After interacting with the chemical/biochemical components in natural soil over 4 months, we expected that the surface properties of the nTiO<sub>2</sub> would change and induce different responses of carrot plants, respect to control and the corresponding phytotoxic results found in our previous unaged study (Wang et al., 2020b). The specific effect on plant Ti uptake, taproot biomass and morphology, leaf growth, nutrient element and biomacromolecule accumulations was investigated.

## **4.2 MATERIALS AND METHODS**

### **4.2.1 Preparation of nTiO<sub>2</sub> aging in soil**

Three types of nTiO<sub>2</sub> (pristine, hydrophilic, and hydrophobic surface-coated) were obtained from US research Nanomaterials and Sachtleben Chemie, Germany. Their particle sizes have been characterized using SEM, with the same size of  $50 \pm 25$  nm; all the three nTiO<sub>2</sub> belonged to a rutile phase (Table S3.1), as previously reported (Tan et al., 2017a). To obtain the hydrophilic or hydrophobic surface properties, pristine nTiO<sub>2</sub> particles were first capped with 6 wt% Al<sub>2</sub>O<sub>3</sub>,

then 1 wt% of glycerol or 2 wt% of dimethicone, respectively (Tan et al., 2017a). Suspensions of each nTiO<sub>2</sub> were made with 50 mL Millipore water (MW) using a water-based sonicator (Crest Ultrasonics, Trenton, NJ).

Natural soil was selected locally in an agricultural field (Socorro TX, USA, latitude: 31°67' N, longitude: 106°28' W, and elevation: 1115 m asl) and sieved through an 8 mm sieve. They were previously characterized as medium loam: 19% clay, 44% silt, and 36% sand; 2.8% organic matter, pH = 7.8 ± 0.021, EC = 1705 ± 47.6 μS/cm, and TDS = 847.5 ± 23.8 mg/L (Majumdar et al., 2015c). Potting mix (Miracle-Gro® organic) was purchased from the supermarket. Both natural soil and potting mix (providing additional organic matters) were used at the ratio of 5:1 by weight. Then the NPs suspensions prepared above were added into these soils to reach a final concentration of 100, 200, and 400 mg Ti/kg soil. Pure 50 mL MW was applied as a control. They were manually mixed for 20 min until homogeneous. The highest concentration was chosen based on the predicted environmental nTiO<sub>2</sub> concentrations, especially in the U.S. (Gottschalk et al., 2009). All the pots were filled with MW until reaching 60% of the maximal field capacity and left for 4 months in a growth chamber (the conditions are listed below). During the aging process, pots were checked every day and MW was added when necessary to keep soil moisture. Three replicates were applied for each treatment.

#### **4.2.2 Seed germination and plant cultivation**

Carrot seeds of Royal Chantenay variety were bought from AGWAY®. They were stored at 4 °C before use. After sterilized with 2% NaClO for 20 min, seeds were washed and stirred in MW for 24 h for awakening. After germination for fourteen days, seedlings were planted into pots filled with soil amended with nTiO<sub>2</sub> prepared above. All pots were placed in a growth chamber



(Environmental Growth Chamber, Chagrin Falls, OH) in a randomized factorial design for 115 days until full maturity. The conditions were remained at: 65% relative humidity, 25/20 °C day/night with  $340 \mu\text{mol m}^{-2} \text{s}^{-1}$  light intensity, and 14 h photoperiod. No additional fertilizer or nutrient solution was added.

#### **4.2.3 Plant harvest and agronomic parameters**

At harvesting, secondary roots, taproots (peer and flesh), stems, and leaves were carefully separated and collected. All the tissue samples were washed three times with 0.01 M HNO<sub>3</sub> and MW to remove surface-adhered soil and nanoparticles. Agronomic parameters such as plant height, aboveground tissue weight, taproot length, taproot weight, and taproot water content were measured and recorded.

#### **4.2.4 Ti uptake and nutrient element concentration**

Titanium uptake, macronutrients (Ca, Mg, P, S, and K) and micronutrients (Cl, Zn, Fe, B, Mn, Cu, Mo, and Ni) were measured using inductively coupled plasma – optical emission spectrometry (ICP-OES) (Perkin-Elmer Optima 4300 DV) (Larue et al., 2014a). Tissues were stored in paper envelopes and dried at 70 °C for 72 h in oven. About 0.2 g ground sample were weighed and acid-digested (Tan et al., 2017b). Briefly, Teflon reaction vessels (Anton Paar GmbH, Austria) were used to hold tissue samples which were treated with 1 mL H<sub>2</sub>O<sub>2</sub> and 2 mL plasma pure HNO<sub>3</sub>. After 30 min, another 5 mL plasma pure H<sub>2</sub>SO<sub>4</sub> were added. After 10 min, all the samples were further digested in a multiwave 3000 Anton Paar microwave system (Perkin-Elmer, Austria) at 800 W ( $170 \pm 10$  °C,  $1,100 \pm 300$  kPa) for 15 min. A cool-down procedure was added

in the end (from 800 to 0 W for 30 min). To validate the measurements, blank (no plant tissues), pure nTiO<sub>2</sub> powder, standard reference material (NIST-SRF 1570a and 1547, Metuchen, NJ), and spiked samples were also treated by the same procedure and analyzed at every 20 samples interval. The recovery rate was 83%.

#### **4.2.5 Sugar and Starch**

Dry tissue samples of ~100 mg were homogenized in 10 mL 80% ethanol, boiled in water bath at 80 °C for 30 min and then centrifuged at 22,000 × *g* for 20 min (DuBois et al., 1956). The supernatant was kept. This extraction steps were repeated for three times and all the extracts were added together. They were evaporated to 3 mL by evaporation and then diluted to 25 mL with MW for the total sugar content analysis according to DuBois et al. (1956). To measure the starch content, briefly, 2 mL MW was added to dry residues. After heated in water bath (100 °C) for 15 min, they were cooled to room temperature and 2 mL of concentrated H<sub>2</sub>SO<sub>4</sub> were added. After 15 min incubation, tubes were brought to 10 mL with MW. The solutions were centrifuged at 3000 × *g* for 20 min and the supernatant was recovered. The extraction was repeated using 50% of H<sub>2</sub>SO<sub>4</sub>. Then, all the supernatants were mixed and brought to 50 mL with MPW. The starch content was quantified according to the method of DuBois et al. (1956).

#### **4.2.6 Statistical analysis**

To analyze the statistical differences between each treatments, Statistical Package for the Social Sciences 25 (SPSS, Chicago, IL, USA) was applied using one-way ANOVA followed by a Post-Tukey test ( $p \leq 0.05$ ). Data were reported as means ± standard errors (SE) of triplicates.

### 4.3. RESULTS AND DISCUSSION

#### 4.3.1 Ti uptake by roots changed along with the zeta potential of aged nTiO<sub>2</sub>

Soil-grown carrots were exposed to 4-month-aged nTiO<sub>2</sub> (with different surface coatings) for 115 days until full maturity. Significant 79% higher Ti concentration was only found in pristine and hydrophobic-coated nTiO<sub>2</sub> treated secondary roots at 400 mg/kg, compared with control (Fig. 4.1) ( $p \leq 0.05$ ). No significant Ti translocation was detected in the other parts of the carrot plant, including taproots flesh, taproots core, shoots, and leaves. Compared with our previous study without aging (Wang et al., 2020b), the Ti uptake in secondary carrot roots was ceased after the aging process in the hydrophilic-coated nTiO<sub>2</sub> treatments, from  $140.1 \pm 19.0$  mg/kg at 400 mg/kg DW to undetectable amounts. Meanwhile, Ti increased from undetectable amounts in the unweathered pristine to  $76.5 \pm 3.7$  mg/kg DW in the aged pristine nTiO<sub>2</sub> at 400 mg/kg (Fig. 4.1).

The observed change in nTiO<sub>2</sub> surface charge may be an important factor that affected Ti uptake results after the aging process. The data of zeta potential obtained from aged-nTiO<sub>2</sub> in DI suspensions is shown in Fig. 4.2. After the aging process, the zeta potential value of hydrophilic-coated nTiO<sub>2</sub> changed from +26.9 to 1.97 (at pH 7.0). This decrement suggested less charge on the particle surface to repel each other, which made the hydrophilic easier to aggregate into big clusters. Thus, although significantly higher root Ti uptake than control was previously found in unaged hydrophilically-treated plants at 400 mg/kg (Wang et al., 2020b), it no longer remained after aging.

For the hydrophobic coated nTiO<sub>2</sub>-treated plants, significant Ti uptake at 400 mg/kg by root was detected both in the present study and the previous reported non-aged work (Wang et al., 2020b). However, the increased Ti amount was lower after aging (by 40%), as normalized with

the corresponding controls. This may also be due to the change of surface charge from +27.0 to -7.56 after aging. Same as the above, this can result in more aggregation and less attachment to roots, since the membrane of root cells is negatively charged on the surface (Cooper GM., 2000). During the weathering process, some of the hydrophobic surface coatings may be unstable and release into the soil (Auffan et al., 2010). According to the previous studies of surface coated nAu, the positively surface-charged nAu were uptaken by plants with more preference than the negative nAu (Judy et al., 2012; Koelmel et al., 2013). The preferent uptake of positively charged nTiO<sub>2</sub> over negatively charged ones was also suggested by our previous study of un-aged nTiO<sub>2</sub> with carrot plants (Wang et al., 2020b). In addition, the interaction between the surface coating and soil may also play an ineluctable role. After aging, the zeta potential of the pristine nTiO<sub>2</sub> changed from -14.5 to -31.6, at pH 7.0. It was likely that during the aging process, pristine nTiO<sub>2</sub> interacted with the soil organic matter or microorganisms, and were consequently attached or coated (Auffan et al., 2010) (Lapied et al., 2011). Specifically, citric acid in soil could make NPs electronegative and stimulate the metal ion uptake (Mudunkotuwa et al., 2012). In a column study with polyacrylamide beads, the positively charged stationary Ag NPs were transformed into a negative charge and became mobile after aging (Naftaly et al., 2016). Thus, with improved stability and biocompatibility, pristine nTiO<sub>2</sub> penetrated the carrot root more easily after a 4-month interaction with soil, concerning our previous unaged study.

Concentration was another parameter that played a role during the aging process. The impact of the aging process on Ti uptake was shown only at 400 mg/kg. Since nTiO<sub>2</sub> is likely to aggregate in soil, the amount of bioavailable Ti might consequently be decreased. The 100 and 200 mg/kg nTiO<sub>2</sub> treatments may be too low to show a significant difference in Ti uptake. Thus,

only at the highest concentration, a significant Ti uptake and changes due to the aging process were observed.

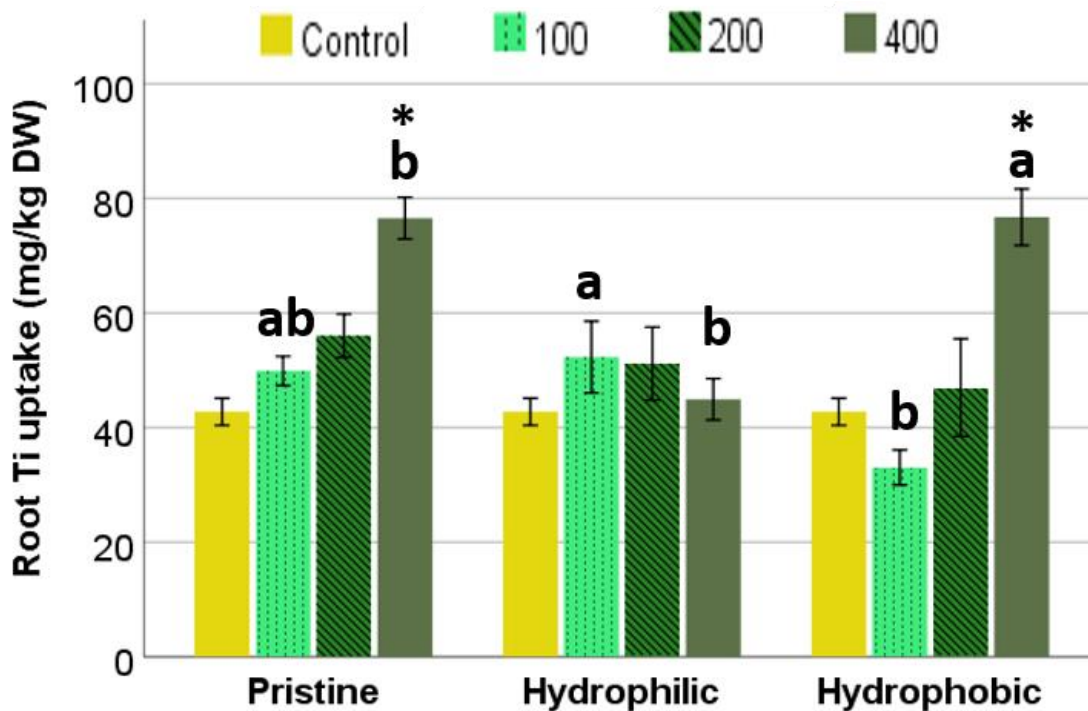


**Fig. 4.1.** Titanium concentration (mg/kg DW) in carrot roots exposed to 4-month-aged pristine, hydrophilic, and hydrophobic coated nTiO<sub>2</sub> at 0, 100, 200 and 400 mg/kg. Data are the average of three replicates ± SE. Lowercase letters stand for statistical differences between different compounds at the same concentration. Asterisks represent significant differences between treatments and control ( $p \leq 0.05$ ,  $n = 3$ ).

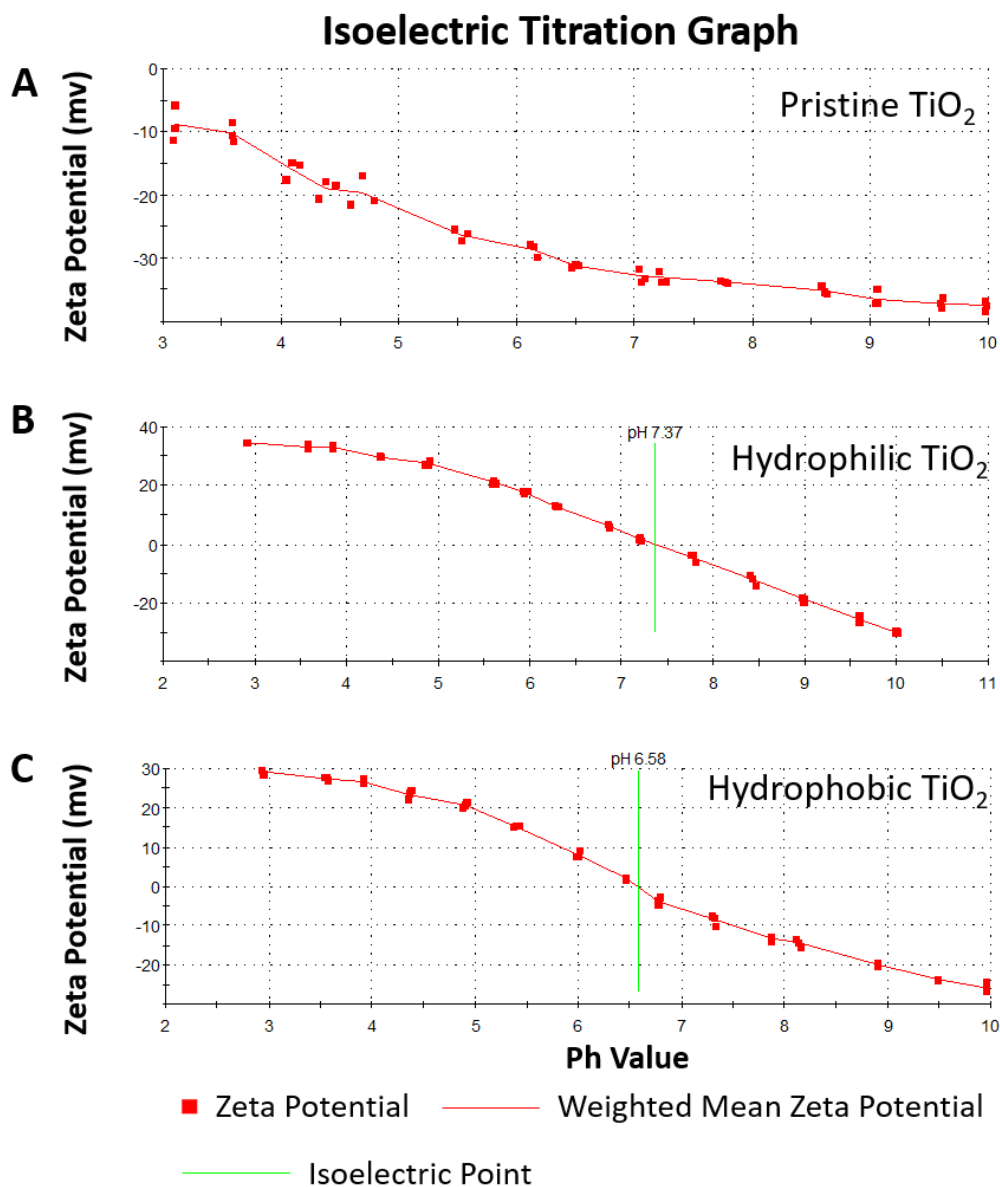


**Fig. 4.2.** Effect of pH (ranged from 3-10) on the  $\zeta$ -potential of 4-month-aged (A) pristine, (B) hydrophilic coated and (C) hydrophobic coated nTiO<sub>2</sub> at 400 mg/kg suspended in MW.

#### 4.3.2 Taproots fresh biomass were improved by the two aged nTiO<sub>2</sub> with surface coatings

The biomass data of fresh carrot taproot grown in soil amended with aged nTiO<sub>2</sub> for 115 days is shown in Fig. 4.3A. Interestingly, when comparing these results with our previous study

(Wang et al., 2020b), where freshly amended soil with nTiO<sub>2</sub> were used instead, the aging process alleviated the inhibition effect of pristine nTiO<sub>2</sub> application on taproot growth overall. Moreover, the aging process enhanced taproot fresh biomass of plants treated by surface-coated nTiO<sub>2</sub>, which depended on both concentration and coating type.

Specifically, taproot fresh biomass of carrots treated with 400 mg/kg of hydrophilic nTiO<sub>2</sub> and 100 mg/kg of hydrophobic nTiO<sub>2</sub> were increased by 43% and 64%, compared with control; while without the 4-month-aging, it was significantly decreased at all concentrations ( $p \leq 0.05$ ) (Wang et al., 2020b). In our previous study, the 400 mg/kg pristine nTiO<sub>2</sub>-treated carrot taproot showed significantly lighter taproot biomass than control by 40%. However, after 4-month-aging in soil, the 400 mg/kg pristine nTiO<sub>2</sub> treatment, did no longer cause any harmful effect (Fig. 4.3A). With the increased concentrations, different trends of responses were shown by the plants treated with surface-coated nTiO<sub>2</sub>. Hydrophobic coated nTiO<sub>2</sub>-treated carrot developed the heaviest taproot at 100 and 200 mg/kg, while at 400 mg/kg, the highest taproot biomass was found in hydrophilic coated nTiO<sub>2</sub>-treated plants. This surface coating and concentration-dependent interaction effect was also confirmed by a two-way ANOVA test ( $p \leq 0.001$ , partial eta squared = 0.761). Soil or foliar applied Ti/nTiO<sub>2</sub> has been reported to enhance crop performance by stimulating enzyme or photosynthesis activities, promoting nutrient contents and strengthening stress tolerance, thus improving crop yield (Lyu et al., 2017). Commercial fertilizers such as Tytanit and Mg-Titanit containing Ti as biostimulants, could enhance the production of agriculture crops. To our best knowledge, our results showed, for the first time, that the aged nTiO<sub>2</sub> with different surface coatings increased carrot taproot fresh biomass. These results would give constructive suggestions in future regulations and applications of surface coated nTiO<sub>2</sub>.

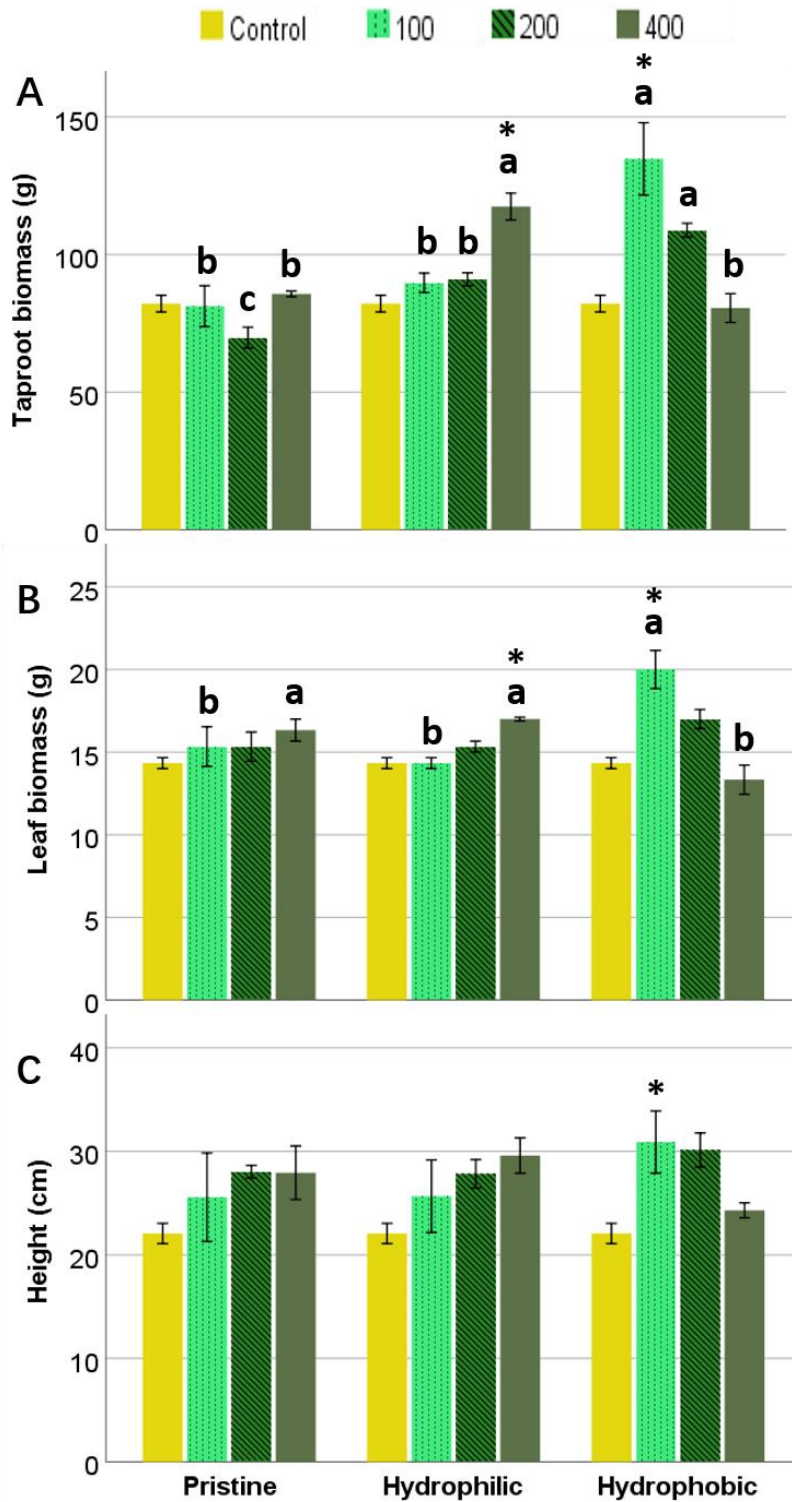


**Fig. 4.3.** (A) Taproot fresh biomass, (B) Leaf fresh biomass (g) and (C) plant height (cm) of carrot exposed to 4-month-aged pristine, hydrophilic, and hydrophobic coated nano TiO<sub>2</sub> at 0, 100, 200 and 400 mg/kg soil. Data are the average of three replicates  $\pm$  SE. Lowercase letters



stand for statistical differences between different compounds at same concentration. Asterisks represent significant differences between treatments and control ( $p \leq 0.05$ ,  $n = 3$ ).

### **4.3.3 Leaves fresh biomass and height were improved by aged surface-coated nTiO<sub>2</sub>**

The changes trend in leaves fresh weight (Fig. 4.3B) was similar to taproot biomass. Carrots treated with 400 mg/kg hydrophilic nTiO<sub>2</sub> and 100 mg/kg hydrophobic nTiO<sub>2</sub> had higher leaves fresh weight by 19% and 40%, respectively, than control ( $p \leq 0.05$ ). A corresponding increment of plant height (by 40%) was found in the 100 mg/kg hydrophobic nTiO<sub>2</sub> treatment, compared to control (Fig. 4.3C) ( $p \leq 0.05$ ). These improvements in top green may benefit the biomass accumulation in taproots (Fig. 4.3A).

The enhancements in leaves fresh weight and taproot biomass caused by two surface coated nTiO<sub>2</sub> mentioned above was not observed in the plants treated with corresponding unaged nTiO<sub>2</sub>. On the other hand, after the aging process, all the enhancement in leaves fresh biomass and plant height by unaged pristine nTiO<sub>2</sub> exposure observed in the previous study disappeared (Fig. 4.3B and 4.3C). The increment of plant height after plants were exposed to 100 mg/kg hydrophobic coated nTiO<sub>2</sub> was remained, before and after aging (Fig. 4.3C). After aging in the soil and interacting with certain chemical components, the biocompatibility and surface charge of these nTiO<sub>2</sub> changed. Particularly, the hydrophilic nTiO<sub>2</sub> showed positive effects only after the aging process.

### **4.3.4 Taproot morphology**

We previously reported a major impairment in carrot when they grew in soils amended with surface-coated nTiO<sub>2</sub>. The main roots were abnormally split (Wang et al., 2020b).

Interestingly, here we found that the splitting of taproots disappeared after the weathering process. No wilting or necrosis was observed in any treatments. To better describe the shape of each taproot, the value of total length, top, mid perimeters, and core diameter were measured. Significant changes compared with control were only found in taproot total length and top perimeter (Fig. 4.4) ( $p \leq 0.05$ ).

As shown in Fig. 4.4A, taproot total length was significantly increased by the application of 400 mg/kg aged hydrophilic nTiO<sub>2</sub> (12.1 cm) and 100 mg/kg aged hydrophobic nTiO<sub>2</sub> (11.4 cm), respectively, compared with control (7.9 cm) ( $p \leq 0.05$ ). This increment was in line with taproot fresh biomass (Fig. 4.3A), leaves fresh biomass (Fig. 4.3B) and taproot top perimeter data (Fig. 4.4B) in the corresponding treatment conditions. In our previous study without aging, no such enhancement of taproot total length and top perimeter was found (Wang et al., 2020b). On the other hand, at the highest concentration, the positive effect of pristine nTiO<sub>2</sub> reported in the unaged study did no longer exist. According to the results mentioned above, the aging process played a substantial role, and exerted different influences on carrot taproots development. In addition, since root splitting was considered as an anti-stress strategy adopted by plants, much less abiotic stress due to nTiO<sub>2</sub> exposure such as root surface adherence, were imposed to carrots after the aging process (Jiang et al., 2017).

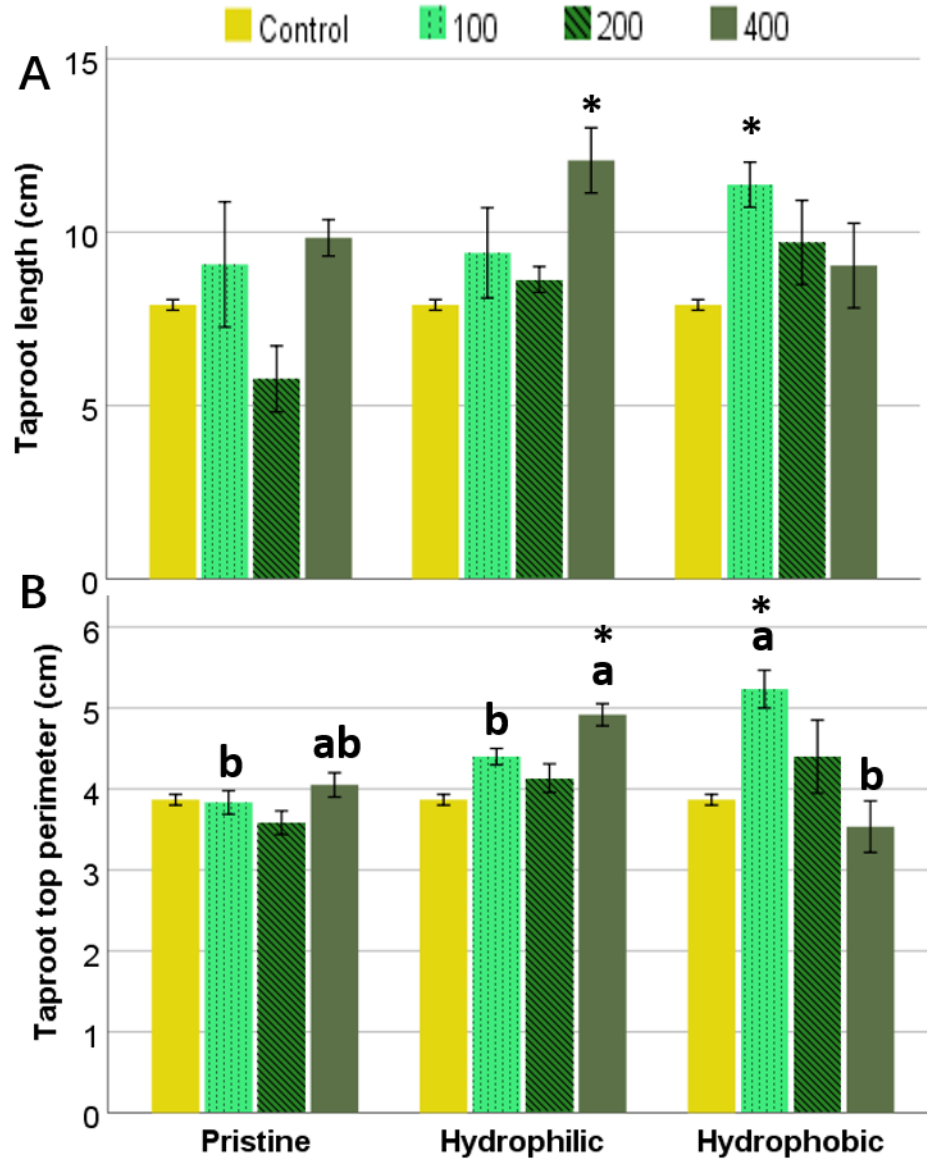


**Fig. 4.4.** (A) Taproot total length (cm) and (B) taproot top perimeter (cm) of carrots exposed to 4-month-aged pristine, hydrophilic, and hydrophobic coated nTiO<sub>2</sub> at 0, 100, 200 and 400 mg/kg. Data are the average of three replicates  $\pm$  SE. Lowercase letters stand for statistical differences between different compounds at the same concentration. Asterisks stand for significant differences between treatments and control ( $p \leq 0.05$ ,  $n = 3$ ).

#### 4.3.5 Nutrient element accumulations in roots and leaves

Macro (Ca, K, Mg, N, P and S) and micro (B, Cl, Cu, Fe, Mn, Mo, Ni, Se and Zn) element concentrations in carrot roots and leaves were determined. Only data that is significantly different with respect to control plants is shown in Table 4.1 (Ca, K, Fe and Zn). Compared with control, Ca, Zn, K in roots and Fe accumulation in leaves increased in hydrophobic nTiO<sub>2</sub>- treated plants; root Zn, K and leaf Fe concentration augmented in hydrophilic nTiO<sub>2</sub> treatments; in the pristine nTiO<sub>2</sub>-treated roots, only Ca content was enhanced ( $p \leq 0.05$ ).

**Calcium**—At 400 mg/kg, roots treated with pristine and hydrophobic coated nTiO<sub>2</sub> accumulated significantly higher Ca than control by 32% and 35%, respectively ( $p \leq 0.05$ ). This agreed with the root Ti uptake data shown above. Similar results of the increased Ca accumulation by nTiO<sub>2</sub> exposure have been reported in shoots and kernels of barley (*Hordeum vulgare*), and lettuce (*Lactuca sativa*) roots at 500 or 1000 mg/kg, but not at lower concentrations. (Pošćić et al., 2016) (Larue et al., 2016b) In nCuO-treated green onion (*Allium fistulosum*) (Wang et al., 2020a) and nCeO<sub>2</sub> treated tomato (*Solanum lycopersicum*) (Adisa et al., 2018b), enhanced Ca contents were also found due to the potential alteration of the permeability of Ca channels. In our previous study, Ti caused Ca concentration increment in leaves. Since the Ti root uptake results changed after the aging process, the Ca increment was also different from the previous one. After the aging process of nTiO<sub>2</sub> in soil, more beneficial effects of pristine nTiO<sub>2</sub> exposure were observed. The comparison between this present study and our previous work without aging (Wang et al., 2020b), indicated that the Ca content was not only affected by the positive correlation effect with Ti accumulation in roots, but also by different aging mechanisms that the three differently coated nTiO<sub>2</sub> underwent. Calcium play the role known as messengers between environmental changes

and plant responses involving hormone production, enzymatic activity, and nodulation. The higher Ca could benefit leaf growth and development.

**Zinc**—As seen in Table 4.1, significantly Zn accumulations were found in carrot roots treated by the two coated nTiO<sub>2</sub> at higher concentrations, with respect to control. The increment was up to 143% and 86% corresponding to the hydrophilic and hydrophobic treatments, respectively. Very similar results were found in our previous study (Wang et al., 2020b). Without aging, the two coated nTiO<sub>2</sub> significantly increased Zn accumulation in carrot roots as well as leaves, at different concentrations. The impact of nTiO<sub>2</sub> on Zn uptake was independent of the aging process, and only related to particle surface coatings. Zn plays a critical role as a cofactor of plant enzymes and transcription regulation, such as superoxide dismutases (SODs), an efficient antioxidant against ROS (Ruth Grene Alscher et al., 2002). The increased Zn concentration in roots may improve the anti-stress ability of plants against the formation of ROS species. In a previous study of barley, the increased Zn accumulation in kernels was also reported after the soil exposure of nTiO<sub>2</sub> at 500 mg/kg (Pošćić et al., 2016).

**Potassium**—Significant increase of K concentration was found in carrot roots treated with 400 mg/kg of hydrophilic coated nTiO<sub>2</sub> and 100 mg/kg of hydrophobic coated nTiO<sub>2</sub> ( $p \leq 0.05$ ). This result agreed with the data found in this study regarding taproot biomass, leaf biomass, taproot length and top perimeter. In our previous study, a higher accumulation of K in taproots treated by the three nTiO<sub>2</sub> was also reported (Wang et al., 2020b). The positive effect of pristine nTiO<sub>2</sub> at 400 mg/kg previously shown did not remain after the aging process. Potassium is an essential element for plant biochemical and physiological function. It plays a vital role in stabilizing pH for optimum enzyme activities, water and nutrient transport, and stomata on-off. In the present study, increased K may contribute to the development and nutritional value of carrot, and aid in regulating

enzyme activities. Servin et al. (2013) reported a significant K increase in cucumber fruit grown in soil amended with 500 mg/kg pristine anatase-rutile nano TiO<sub>2</sub>. Wu et al. (2003) demonstrated by electrophysiological and genetic studies that the uptake of K was affected by plant hormones like cytokinins. Moreover, channel mediates K<sup>+</sup> release into the root xylem was controlled by abscisic acid, the stress hormone (de Boer, 1999). In a wheat seedling study treated with nano TiO<sub>2</sub>, a dose-dependent increase of abscisic acid was detected (Jiang et al., 2017). In another study, the author claimed that nano TiO<sub>2</sub> may have a similar function as cytokinin in plant (Mandeh et al., 2012b). Thus, it was likely that nano TiO<sub>2</sub> based treatment, acted as cytokinin hormone, also increased the concentration of abscisic acid in carrot plant, up-regulated the K<sup>+</sup> release.

**Iron**—Concentration of Fe in leaves was significantly enhanced by hydrophilic and hydrophobic-coated nTiO<sub>2</sub> by up to 39% at ≥200 mg/kg and by up to 66% at all concentrations, respectively, compared to control ( $p \leq 0.05$ ). In our previous study, a similar increment of leaf Fe content by 400 mg/kg of hydrophilic and hydrophobic coated nTiO<sub>2</sub> exposure was reported (Wang et al., 2020b). After the aging process, this positive effect remained. It has been reported that Ti could benefit plants by increasing Fe absorption (Abadía, 2012). It has also been suggested that Ti and Fe have synergistic relationships. Titanium could activate the gene expressions related to Fe acquisition when needed, thus improve Fe uptake and plant growth (Lyu et al., 2017). In another study with the exposure of nTiO<sub>2</sub> to lettuce, this positive correlation between Ti and Fe was reported (Larue et al., 2016b). In addition, since Zn and Fe share the same transporters of ZIP family, it is also possible that the increment of Fe is related to the up-regulation of Fe transporter, same as the increase of Zn.

#### 4.3.6 Nutrient element accumulations in taproot flesh and core

Macro (Ca, K, Mg, N, P and S) and micro (B, Cl, Cu, Fe, Mn, Mo, Ni, Se and Zn) element concentrations in carrot taproot flesh and core were determined. Only data that is significantly different with respect to control plants is shown in Table 4.1 (Ca, K, Fe and Zn). Compared with control, lower Mn and Ca in flesh and core, lower Fe and Zn in core, and higher flesh and core Mg accumulation were detected in hydrophobic nTiO<sub>2</sub> treatments; Mn concentration in flesh and core were reduced, while core Mg was improved in hydrophilic nTiO<sub>2</sub> treatments ( $p \leq 0.05$ ).

*Manganese*—As seen in Table 4.1, Mn concentration in both taproot flesh and core were decreased by the two surface-coated nTiO<sub>2</sub>. Specifically, at 400 mg/kg, the significant decrement in the flesh by hydrophilic and hydrophobic coated nTiO<sub>2</sub> was by 35% and 33%, compared with control; while in the core, similarly, 25% and 50% lower Mn accumulation was found, respectively ( $p \leq 0.05$ ).

Referring to our previous study, the inhibition effect of surface-coated nTiO<sub>2</sub> at 100 and 200 mg/kg on taproot Mn uptake was alleviated by the aging process. Without weathering in soil, significant decreases were found in taproot flesh and core at nearly all the concentrations in surface coated nTiO<sub>2</sub> treatments (Wang et al., 2020b). Besides, there is only one study that reported the change of Mn accumulation by plant after nTiO<sub>2</sub> exposure. At 500 mg/kg, Mn concentration of soil-grown barley kernels was improved by pristine nTiO<sub>2</sub> (Pošćić et al., 2016). Compared with our present results, it indicated that the surface coating and the aging process changed the initial impact of nTiO<sub>2</sub> on plant Mn accumulation. However, to clearly understand this phenomenon, further studies are needed.

*Magnesium*—In taproot flesh, Mg concentrations were significantly increased by hydrophobic-coated nTiO<sub>2</sub> at 100 and 200 mg/kg. In core, an improvement was found in 400

mg/kg hydrophilic-coated nTiO<sub>2</sub>-treated plants and at 100 mg/kg hydrophobic-coated nTiO<sub>2</sub> treatment. This was different from the results reported in our previous study (Wang et al., 2020b). Without aging, all the treatments had lower flesh Mg accumulation than control. More future works at molecular levels are needed to investigate the potential alteration of Mg transporter activities and the bioavailability of Mg in soil that were affected by the aged nTiO<sub>2</sub>.

*Calcium, Iron and Zinc*—In 400 mg/kg hydrophobic-coated nTiO<sub>2</sub> treatment, Ca concentrations in flesh and core, and Fe and Zn concentrations in core, were all significantly lower than control ( $p \leq 0.05$ ). On the contrary, all these nutrient elements were increased in roots or leaves as discussed above. In our previous study, Zn concentrations in flesh were previously reported to be decreased by all the nTiO<sub>2</sub> treatments (Wang et al., 2020b). However, after aging, this inhibition effect remained only with 400 mg/kg hydrophobic coated nTiO<sub>2</sub>, indicating its long-term impact compared with the others.

**Table 4.1.** Concentration (mg/kg DW) of micro- and macro-elements in carrot leaves (Ca, Mg, Fe, Se and Zn), secondary roots (Zn) and taproots (K, Mg, Mn and Zn). Plants were cultivated for 115 days in soil amended with 4-month-aged pristine, hydrophilic and hydrophobic coated nTiO<sub>2</sub> at 0 (control), 100, 200 and 400 mg of Ti/kg of soil. Data are averages of 3 replicates  $\pm$  Standard Error (SE).

Plant part	Element	Treatment	Concentration	Mean (mg/kg)	Std. Error
Root	Ca	Control		3604.01	316.32
		Pristine	400	4747.65	237.49
		Hydrophobic	200	5072.11	233.24
		Hydrophobic	400	4856.72	344.8
	Zn	Control		17.9	3.8
		Hydrophilic	100	32.2	3.82



		Hydrophilic	200	43.06	1.25
		Hydrophilic	400	43.55	1.54
		Hydrophobic	200	33.28	5.94
		Hydrophobic	400	31.68	2.81
		Control		30412.62	3724.91
	K	Hydrophilic	400	44482.48	3954.62
		Hydrophobic	100	37781.34	1720.64
		Control		11.43	0.85
		Hydrophilic	200	15.67	1.17
		Hydrophilic	400	15.85	2.14
<b>Leaf</b>	Fe	Hydrophobic	100	19.02	0.73
		Hydrophobic	200	17.81	1.5
		Hydrophobic	400	16.19	2.37
		Control		2757.03	153.97
	Ca	Hydrophobic	400	1891.23	235.84
		Control		16.41	0.71
	Mn	Hydrophilic	400	10.63	1.86
<b>Taproot flesh</b>		Hydrophobic	400	10.89	1.21
		Control		924.36	145.78
	Mg	Hydrophobic	100	1325.1	83.84
		Hydrophobic	200	1575.33	186.58
		Control		2609.4	171.32
<b>Taproot core</b>	Ca	Hydrophobic	400	1464.48	351.17

Fe	Control		60.54	10.37
	Hydrophobic	400	21.47	8.68
Zn	Control		19.22	3.8
	Hydrophobic	400	11.36	0.72
Mn	Control		11.72	0.74
	Hydrophilic	400	8.75	0.94
	Hydrophobic	400	5.9	0.81
Mg	Control		1094.66	161.5
	Hydrophilic	400	1554.13	220.01
	Hydrophobic	100	1795.59	332.07

#### 4.3.7 Biomacromolecule contents

*Sugar and starch*—Taproot sugar and starch concentrations (Fig. 4.5) were negatively affected by the exposure of aged surface-coated nTiO<sub>2</sub>. At 400 mg/kg, the reduction of starch by hydrophilic and hydrophobic coated nTiO<sub>2</sub> were by 36% and 60%, respectively; meanwhile, hydrophobic-coated nTiO<sub>2</sub> decreased sugar content by 31% compared with control ( $p \leq 0.05$ ). This inhibition effect was only shown after the long-term aging process, compared with the results in our previous study (Wang et al., 2020b). One reason could be the decreased nutrient element accumulation of Ca, Fe, Zn and Mn in taproots. In previous studies of plants exposed to nano TiO<sub>2</sub>, sugar and starch accumulation in basil leaves were significantly decreased (Tan et al., 2017b). In wheat (Jaberzadeh et al., 2013) and chick pea (Hajra and Mondal, 2017), increased sugar and starch contents were detected even at a relatively high dose of 1000 ppm. This also suggested an

unneglected role that the aging process played on the effect of surface coated nTiO<sub>2</sub> on plant sugar and starch developments.

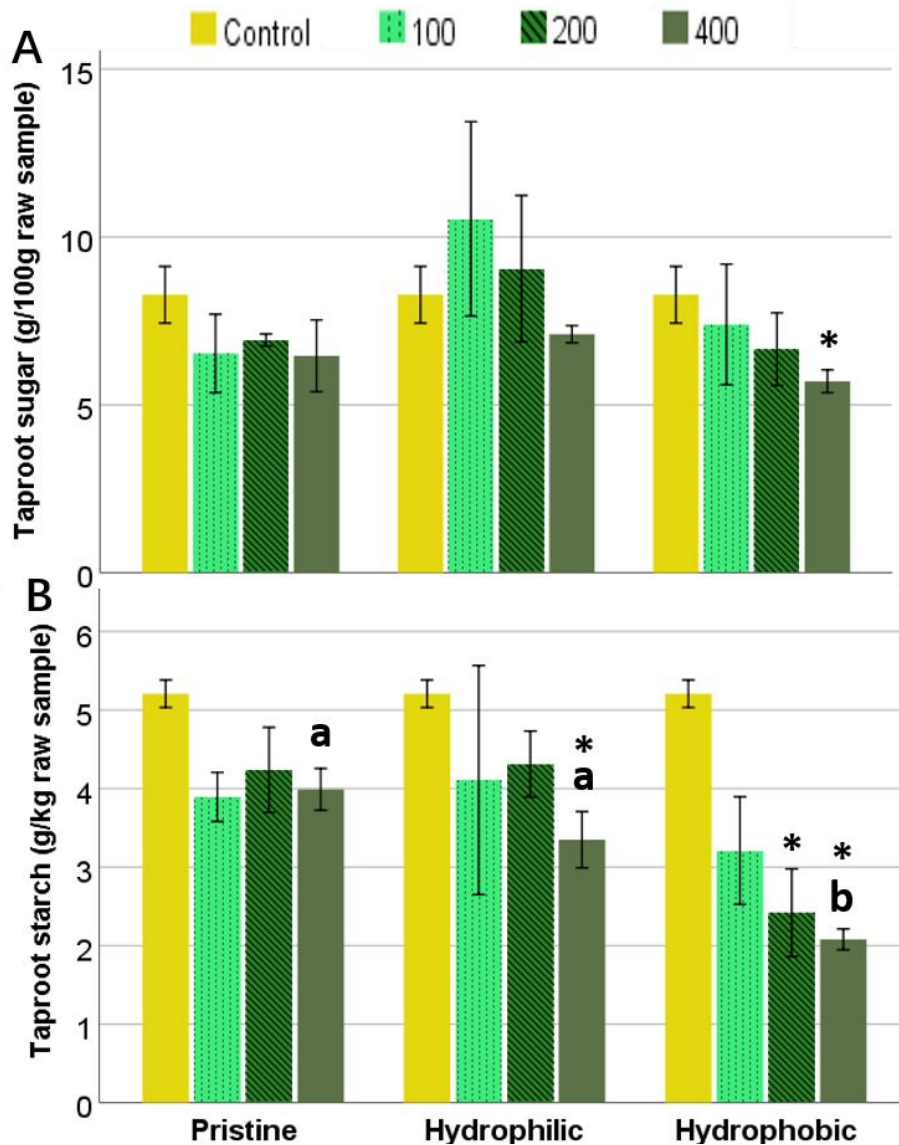


**Fig. 4.5.** Taproot (A) sugar and (B) starch contents of carrots exposed to 4-month-aged pristine, hydrophilic, and hydrophobic coated nTiO<sub>2</sub> at 0, 100, 200 and 400 mg/kg. Data are the average of three replicates  $\pm$  SE. Lowercase letters stand for statistical differences between different compounds at the same concentration. Asterisks mean statistical differences between treatments and control ( $p \leq 0.05$ ,  $n = 3$ ).

#### 4.4. CONCLUSION

To our best knowledge, we investigated, for the first time, the effect of aged ENPs with different surface coatings in natural soil on the development of carrot. Although the reactions between the surface coatings and inorganic/bioorganic components in the soil are complex, and NMs are hard to be tracked, this study provided insights to understand the aging process. The pristine, hydrophilic, or hydrophobic surface-coated nTiO<sub>2</sub> may go through different aging pathways, thus, resulted in various responses of carrot plants, compared to the unaged treatments. Different changes in surface charges were detected among the three nTiO<sub>2</sub> after aging. This could be a factor that resulted in the specific Ti uptake patterns: aged pristine nTiO<sub>2</sub> at 400 mg/kg, elicited an increased of Ti uptake by roots, while the accumulation of Ti in hydrophilic-coated nTiO<sub>2</sub>-exposed plants was no longer detected. This may suggest a different change of biocompatibility among the three nTiO<sub>2</sub> after aging. The improved responses of taproot biomass, leaf fresh biomass, plant height and nutrient elements accumulations in roots and leaves, indicated that the aging process alleviated the phytotoxicity caused by the unaged nTiO<sub>2</sub>. Instead, the hydrophilic coated nTiO<sub>2</sub> at 400 mg/kg and the hydrophobic coated nTiO<sub>2</sub> at 100 mg/kg, functioned as plant growth stimulator, which resulted in higher taproot and leaf biomass, taproot length, and the top perimeter compared with control ( $p \leq 0.05$ ). The accumulation of Ca, Zn, K and Fe in carrot roots or leaves, and Mg in taproot flesh and core were increased by the exposure to aged nTiO<sub>2</sub> with hydrophilic or hydrophobic surface coatings; while in the aged pristine nTiO<sub>2</sub> treatments, only the concentration of Ca in roots was enhanced. Several inhibition effects were found in the accumulation of Mn, Ca, Fe, Zn in taproot flesh or core of carrots that were treated by aged hydrophobic nTiO<sub>2</sub>. Moreover, the formation of sugar and starch was reduced by the application of aged surface-coated nTiO<sub>2</sub>. These results provide valuable data to understand how the aging

process affected the interaction between surface-coated nanomaterials and taproot crops. It also suggests a potential strategy to alleviate the phytotoxicity of released surface-coated nanoparticles; and moreover, offers a sustainable method to turn them into potential stimulators for the growth of plants. Instead of direct release into the soil, or direct application to plants, a simple aging process might aid to overcome the detrimental effects that surface-coated nTiO<sub>2</sub> have on belowground vegetables. More studies on nTiO<sub>2</sub> surface coatings characterization, and plants genetic and metabolic changes are needed in the future to better understand plant molecular responses to NPs exposure in soils.

## Chapter 5: Conclusion

In the first study, none of the Cu-based tested concentrations produced visible signs of toxicity. Two-photon microscopy images demonstrated the Cu uptake in nCuO, and bCuO treated roots. At all concentrations, nCuO and CuSO<sub>4</sub> increased leaf allicin compared with control. The antioxidant enzymes were differentially affected by the Cu-based treatments. Although nCuO significantly increased root GPOX and leaf APOX, it reduced CAT in both roots and leaves. Scallion plants exposed to nCuO improved their essential element (Ca, Fe, Mg, Mn, and Ni) contents. Overall, the data suggest that nCuO at concentrations lower than 600 mg/kg may be used as nanofertilizer for green onion production.

In the second and third studies, the content of Ti in plant secondary roots treated with unaged nTiO<sub>2</sub> at 400 mg/kg was in the order of hydrophobic > hydrophilic > pristine regarding the respective treatments. The two-photon microscope images suggested an uptake pathway independent of the surface coating chemistry of nTiO<sub>2</sub>. The growth of taproot was significantly inhibited by all unaged nTiO<sub>2</sub> forms. Remarkably, an abnormal increase of taproot splitting was found. The accumulation of nutrient elements (Mg, Mn, and Zn) was decreased in taproots treated with the unaged surface-coated nTiO<sub>2</sub>. On the other hand, most of these inhibition effects disappeared after nTiO<sub>2</sub> aging in soil. The aged nTiO<sub>2</sub> with surface coatings improved plant agronomic parameters and nutrient element accumulations. More stimulation effects were shown by aged hydrophilic and hydrophobic-coated nTiO<sub>2</sub> than the aged pristine nTiO<sub>2</sub>. These may be related to the changes in surface charges on nTiO<sub>2</sub> after aging. It suggested a potential strategy to alleviate the phytotoxicity of released surface-coated nanoparticles; and moreover, offers a sustainable method to convert them into potential stimulators for the growth of plants.

Taking an overview of the three presented studies, the interaction between NPs and plants depend on nanoparticles type/size, plant varieties, exposed conditions, and NP surface coatings. Results in these studies provided valuable insights into the interaction of nCuO with green onion, and surface-coated nTiO<sub>2</sub> (aged and unaged) with carrot plants. The potential use of nCuO and aged nTiO<sub>2</sub> as nanofertilizers has been suggested in the agrosystem. Meanwhile, the potential risk of releasing unaged nTiO<sub>2</sub> into the environment has been emphasized. More studies at molecular levels and considering the full terrestrial food chain are needed to evaluate the potential effect that plants grown in ENMs-amended soils have on humans.

## Supporting material for Chapter 2-4

**Table S2.1:** Physiochemical characterization of nCuO and bCuO particles

Property	nCuO	bCuO
Primary particle size (nm)	20–100	200–2000
Hydrodynamic diameter <sup>a</sup> (nm)	280 ± 15	376 ± 26
Zeta potential (mV) <sup>a</sup>	-34.4 ± 0.5	-42.7 ± 0.153
Cu content (wt%)	74.3	79.7
Purity (%)	88.3 ± 1.3	92.8 ± 1.1
Other elements present	O, C	O
Shape, morphology	Rhombus, irregular	Prism, irregular
Main copper phase	CuO	CuO
Crystal structure	Monoclinic	Monoclinic

<sup>a</sup> Measurement was performed at pH 7.

**Table S2.2:** The effect of two main independent variables (compound and concentration) and the respective interactions on the uptake of Cu in roots, bulbs and leaves in plants exposed to nCuO, bCuO or CuSO<sub>4</sub> at 0, 75, 150, 300 and 600 mg/kg. (n = 3).

### Tests of Between-Subjects Effects

Dependent Variable: Root Cu

Source	Type III Sum of Squares	df	Mean Square	F	Sig.	Partial Eta Squared
Corrected Model	294115.826 <sup>a</sup>	14	21008.273	43.585	.000	.953
Intercept	357141.035	1	357141.035	740.948	.000	.961
Concentration	272209.112	4	68052.278	141.186	.000	.950
Compounds	6562.306	2	3281.153	6.807	.004	.312
Concentration * Compounds	15344.408	8	1918.051	3.979	.003	.515
Error	14460.166	30	482.006			
Total	665717.028	45				
Corrected Total	308575.992	44				

a. R Squared = .953 (Adjusted R Squared = .931)

Dependent Variable: Leaf Cu

Source	Type III Sum of Squares	df	Mean Square	F	Sig.	Partial Eta Squared
--------	-------------------------	----	-------------	---	------	---------------------



Corrected Model	1193.251 <sup>a</sup>	14	85.232	9.054	.000	.809
Intercept	13820.919	1	13820.919	1468.192	.000	.980
Concentration	451.014	4	112.753	11.978	.000	.615
Compounds	131.209	2	65.604	6.969	.003	.317
Concentration * Compounds	611.029	8	76.379	8.114	.000	.684
Error	282.407	30	9.414			
Total	15296.577	45				
Corrected Total	1475.658	44				

a. R Squared = .809 (Adjusted R Squared = .719)

Dependent Variable: Blub Cu

Source	Type III Sum of Squares	df	Mean Square	F	Sig.	Partial Eta Squared
Corrected Model	581.668 <sup>a</sup>	14	41.548	5.180	.000	.707
Intercept	5092.916	1	5092.916	635.001	.000	.955
Concentration	499.105	4	124.776	15.558	.000	.675
Compounds	31.195	2	15.597	1.945	.161	.115
Concentration * Compounds	51.369	8	6.421	.801	.607	.176
Error	240.610	30	8.020			
Total	5915.194	45				
Corrected Total	822.278	44				

a. R Squared = .707 (Adjusted R Squared = .571)

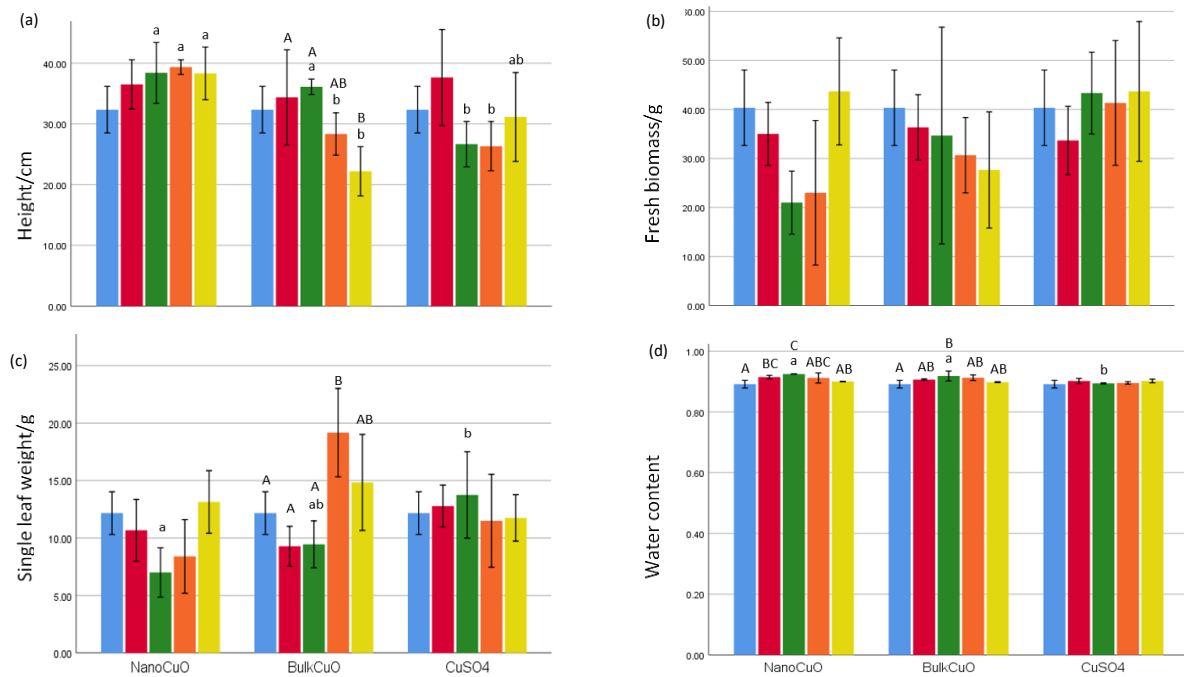


**Fig. S2.1:** Plant height (a), fresh biomass (b), single leaf weight (c) and water content (d) of scallion plants grown under nCuO, bCuO, and CuSO<sub>4</sub> treatments. Data are averages of three replicates  $\pm$  standard error (SE). Lowercase letters stand for statistical differences between among different compounds at same concentration. Uppercase letters represent significant differences among different concentrations of the same compounds ( $p \leq 0.05$ ,  $n = 3$ ).

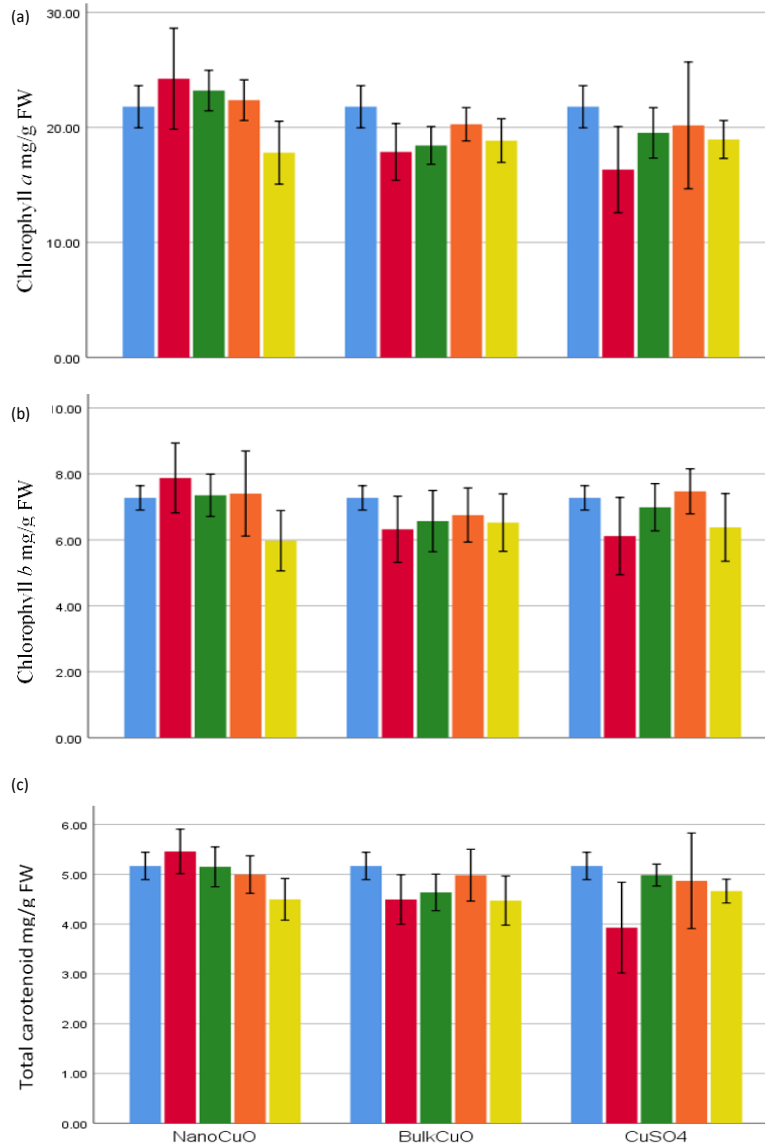


**Fig. S2.2:** Plant leaf chlorophyll *a* (a), chlorophyll *b* (b) and total carotenoid content of scallion plants grown under nCuO, bCuO, and CuSO<sub>4</sub> treatments. Data are averages of three replicates ± standard error (SE). Lowercase letters stand for statistical differences among different compounds at same concentration. Uppercase letters indicate significant differences among different concentrations of the same compounds ( $p \leq 0.05$ ,  $n = 3$ ).

**Table S3.1.** Physical characterization of nano-TiO<sub>2</sub> (Tan et al., 2017).

Properties	Nanoparticles
------------	---------------

	Technique	Pristine TiO <sub>2</sub>	Hydrophobic TiO <sub>2</sub>	Hydrophilic TiO <sub>2</sub>
Size (nm)	TEM	50 ± 25	50 ± 25	50 ± 25
Crystal phase	XRD	Tetragonal, rutile	Tetragonal, rutile	Tetragonal, rutile
Morphology	TEM	Elongated	Elongated	Elongated
Surface area (m <sup>2</sup> /g)	BET	30 ± 10	47.6 ± 1.0	55.7 ± 2.0
Hydrodynamic size (nm)	DLS	341 ± 10	261 ± 5	282 ± 7
Zeta potential in DI water (mV)	DLS	-14.5 ± 0.5	27.0 ± 0.9	26.9 ± 0.5
Purity (wt. %)	TGA	99.9	97.1	95.9

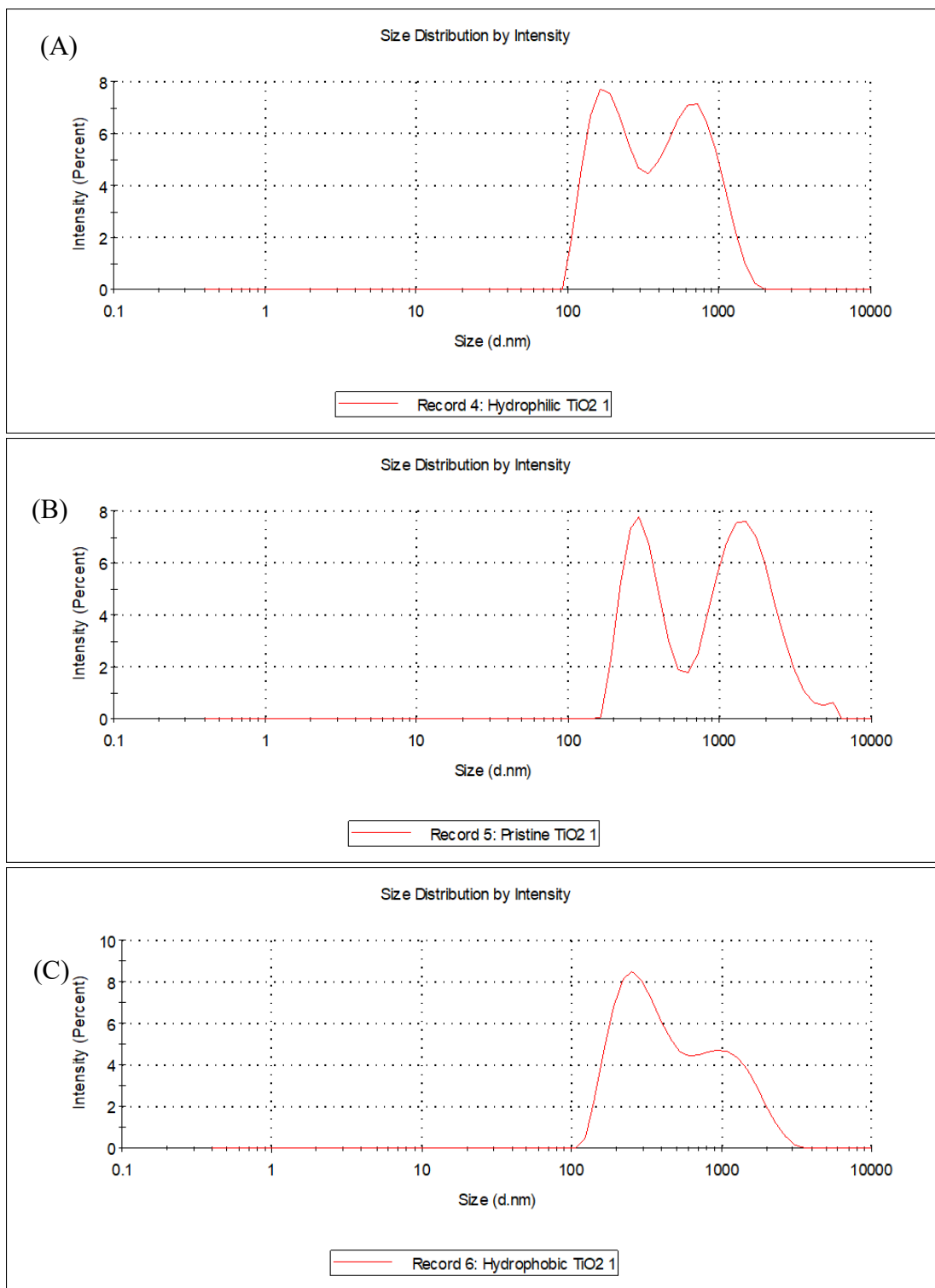


**Fig. S3.1.** Hydrodynamic size distribution of (A) hydrophobic, (B) pristine, and (C) hydrophobic nTiO<sub>2</sub> particles suspended in MW.

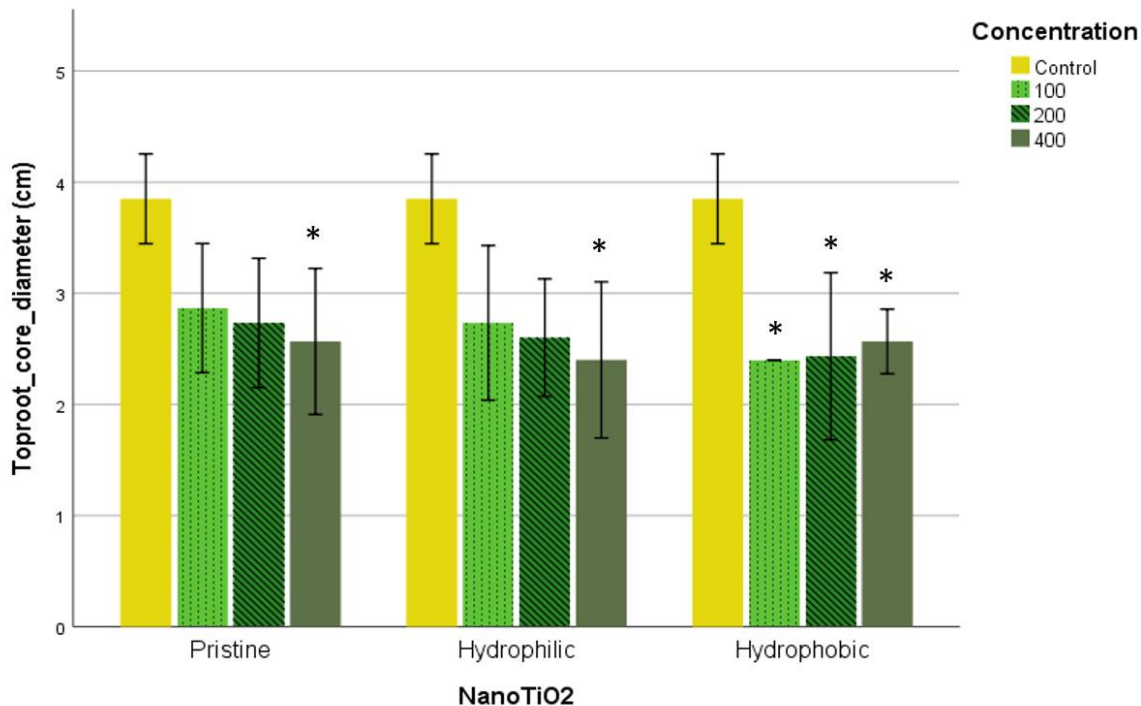


**Fig. S3.2.** Taproot core diameter (cm) of carrots exposed to pristine, hydrophilic, and hydrophobic coated nTiO<sub>2</sub> at 0, 100, 200 and 400 mg/kg. Data are the average of three replicates ± SE. Lowercase letters stand for statistical differences between different compounds at the same concentration. Asterisk represent significant differences with respect to control ( $p \leq 0.05$ ,  $n = 3$ ).

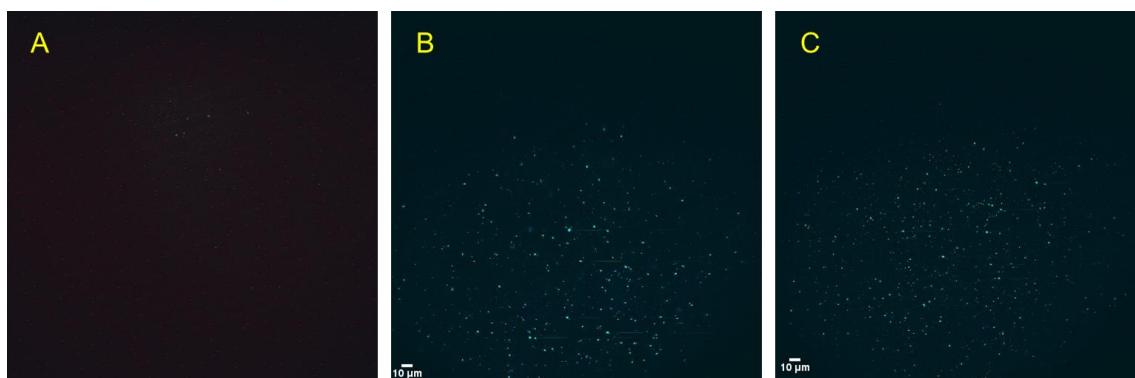


**Fig. S3.3.** The inserted pictures correspond to (A) pure pristine, (B) pure hydrophilic and (C) pure hydrophobic coated nTiO<sub>2</sub> suspension in DI.

## References

### Chapter 2

- Acosta, Y., Zhang, Q., Rahaman, A., Ouellet, H., Xiao, C., Sun, J., Li, C., 2014. Imaging cytosolic translocation of Mycobacteria with two-photon fluorescence resonance energy transfer microscopy. *Biomed. Opt. Express* 5, 3990. <https://doi.org/10.1364/BOE.5.003990>
- Adisa, I.O., Pullagurala, V.L.R., Peralta-Videa, J.R., Dimkpa, C.O., Elmer, W.H., Gardea-Torresdey, J.L., White, J.C., 2019. Recent advances in nano-enabled fertilizers and pesticides: a critical review of mechanisms of action. *Environ. Sci. Nano* 6, 2002–2030. <https://doi.org/10.1039/C9EN00265K>
- Aebi, H., 1974. Catalase. *Methods Enzym. Anal.* 2, 673–684. <https://doi.org/10.1016/B978-0-12-091302-2.50032-3>
- Apodaca, S.A., Tan, W., Dominguez, O.E., Hernandez-Viezcas, J.A., Peralta-Videa, J.R., Gardea-Torresdey, J.L., 2017. Physiological and biochemical effects of nanoparticulate copper, bulk copper, copper chloride, and kinetin in kidney bean (*Phaseolus vulgaris*) plants. *Sci. Total Environ.* 599–600, 2085–2094. <https://doi.org/10.1016/J.SCITOTENV.2017.05.095>
- Beyer, W.F., Fridovich, I., 1987. Assaying for superoxide dismutase activity: Some large consequences of minor changes in conditions. *Anal. Biochem.* 161, 559–566. [https://doi.org/10.1016/0003-2697\(87\)90489-1](https://doi.org/10.1016/0003-2697(87)90489-1)
- Block, E., Naganathan, S., Putman, D., Zhao, S.-H., 1992. Allium Chemistry: HPLC Analysis of Thiosulfinates from Onion. *J. Agric. Food Chem.* 40, 2418–2430.
- Bonilla-Bird, N.J., Paez, A., Reyes, A., Hernandez-Viezcas, J.A., Li, C., Peralta-Videa, J.R., Gardea-Torresdey, J.L., 2018. Two-Photon Microscopy and Spectroscopy Studies to

- Determine the Mechanism of Copper Oxide Nanoparticle Uptake by Sweetpotato Roots during Postharvest Treatment. *Environ. Sci. Technol.* 52, 9954–9963.  
<https://doi.org/10.1021/acs.est.8b02794>
- Bost, M., Houdart, S., Oberli, M., Kalonji, E., Huneau, J.-F., Margaritis, I., 2016. Dietary copper and human health: Current evidence and unresolved issues. *J. Trace Elem. Med. Biol.* 35, 107–115. <https://doi.org/10.1016/J.JTEMB.2016.02.006>
- Cataldo, D.A., Garland, T.R., Wildung, R.E., 1978a. Nickel in plants: I. Uptake kinetics using intact soybean seedlings. *Plant Physiol.* 62, 563–5. <https://doi.org/10.1104/PP.62.4.563>
- Cataldo, D.A., Garland, T.R., Wildung, R.E., Drucker, H., 1978b. Nickel in Plants: II. Distribution and Chemical Form in Soybean Plants. *Plant Physiol.* 62, 566–70.  
<https://doi.org/10.1104/PP.62.4.566>
- Chan, J.Y.-Y., Yuen, A.C.-Y., Chan, R.Y.-K., Chan, S.-W., 2013. A Review of the Cardiovascular Benefits and Antioxidant Properties of Allicin. *Phyther. Res.* 27, 637–646.  
<https://doi.org/10.1002/ptr.4796>
- Deák, M., Horváth, G. V., Davletova, S., Török, K., Sass, L., Vass, I., Barna, B., Király, Z., Dudits, D., 1999. Plants ectopically expressing the ironbinding protein, ferritin, are tolerant to oxidative damage and pathogens. *Nat. Biotechnol.* 17, 192–196.  
<https://doi.org/10.1038/6198>
- Demidchik, V., Shabala, S.N., Davies, J.M., 2007. Spatial variation in H<sub>2</sub>O<sub>2</sub> response of *Arabidopsis thaliana* root epidermal Ca<sup>2+</sup> flux and plasma membrane Ca<sup>2+</sup> channels. *Plant J.* 49, 377–386. <https://doi.org/10.1111/j.1365-313X.2006.02971.x>
- Demidchik, V., Sokolik, A., Yurin, V., Kochian, L. V., Taiz, L., 1999. The Effect of Cu<sup>2+</sup> on Ion Transport Systems of the Plant Cell Plasmalemma. *Plant Physiol.* 114, 1313–1325.



<https://doi.org/10.1104/pp.121.4.1375>

Du, J., Fu, L., Li, H., Xu, S., Zhou, Q., Tang, J., 2019. The potential hazards and ecotoxicity of CuO nanoparticles: an overview. *Toxin Rev.* 1–13.

<https://doi.org/10.1080/15569543.2019.1670211>

Egley, G.H., Paul, R.N., Vaughn, K.C., Duke, S.O., 1983. Role of peroxidase in the development of water-impermeable seed coats in *Sida spinosa* L. *Planta* 157, 224–232.

<https://doi.org/10.1007/BF00405186>

Fatima, A., Singh, S., Prasad, S.M., 2020. Interaction Between Copperoxide Nanoparticles and Plants: Uptake, Accumulation and Phytotoxicity 143–161. [https://doi.org/10.1007/978-3-030-33996-8\\_8](https://doi.org/10.1007/978-3-030-33996-8_8)

Food Composition Databases Show Foods -- Onions, spring or scallions (includes tops and bulb), raw, 2018.

Guo, K.M., Babourina, O., Christopher, D.A., Borsic, T., Rengel, Z., 2010. The cyclic nucleotide-gated channel AtCNGC10 transports  $\text{Ca}^{2+}$  and  $\text{Mg}^{2+}$  in Arabidopsis. *Physiol. Plant.* 139, 303–312. <https://doi.org/10.1111/j.1399-3054.2010.01366.x>

Han, J., Lawson, L., Han, G., Han, P., 1995. Spectrophotometric Method for Quantitative Determination of Allicin and Total Garlic Thiosulfinates. *Anal. Biochem.* 225, 157–160.

<https://doi.org/10.1006/abio.1995.1124>

Hong, J., Rico, C.M., Zhao, L., Adeleye, A.S., Keller, A.A., Peralta-Videa, J.R., Gardea-Torresdey, J.L., 2015. Toxic effects of copper-based nanoparticles or compounds to lettuce (*Lactuca sativa*) and alfalfa (*Medicago sativa*). *Environ. Sci. Process. Impacts* 17, 177–185.

<https://doi.org/10.1039/C4EM00551A>

Huang, Y., Adeleye, A.S., Zhao, L., Minakova, A.S., Anumol, T., Keller, A.A., 2019.

- Antioxidant response of cucumber (*Cucumis sativus*) exposed to nano copper pesticide: Quantitative determination via LC-MS/MS. *Food Chem.* 270, 47–52.  
<https://doi.org/10.1016/J.FOODCHEM.2018.07.069>
- Iavicoli, I., Leso, V., Beezhold, D.H., Shvedova, A.A., 2017. Nanotechnology in agriculture: Opportunities, toxicological implications, and occupational risks. *Toxicol. Appl. Pharmacol.* 329, 96–111. <https://doi.org/10.1016/J.TAAP.2017.05.025>
- Jung, J.-H., Kim, S.-W., Min, J.-S., Kim, Y.-J., Lamsal, K., Kim, K.S., Lee, Y.S., 2010. The Effect of Nano-Silver Liquid against the White Rot of the Green Onion Caused by *Sclerotium cepivorum*. *Mycobiology* 38, 39. <https://doi.org/10.4489/MYCO.2010.38.1.039>
- Keller, A.A., McFerran, S., Lazareva, A., Suh, S., 2013. Global life cycle releases of engineered nanomaterials. *J. Nanoparticle Res.* 15, 1692. <https://doi.org/10.1007/s11051-013-1692-4>
- Lee, D.H., Lee, C.B., 2000. Chilling stress-induced changes of antioxidant enzymes in the leaves of cucumber: in gel enzyme activity assays. *Plant Sci.* 159, 75–85.  
[https://doi.org/10.1016/S0168-9452\(00\)00326-5](https://doi.org/10.1016/S0168-9452(00)00326-5)
- Li, H., Wang, N., Ding, J., Liu, C., Du, H., Huang, K., Cao, M., Lu, Y., Gao, S., Zhang, S., 2017. The maize CorA/MRS2/MGT-type Mg transporter, ZmMGT10, responses to magnesium deficiency and confers low magnesium tolerance in transgenic Arabidopsis. *Plant Mol. Biol.* 95, 269–278. <https://doi.org/10.1007/s11103-017-0645-1>
- Lin, C., Fugetsu, B., Su, Y., Watari, F., 2009. Studies on toxicity of multi-walled carbon nanotubes on Arabidopsis T87 suspension cells. *J. Hazard. Mater.* 170, 578–583.  
<https://doi.org/10.1016/J.JHAZMAT.2009.05.025>
- Majumdar, S., Almeida, I.C., Arigi, E.A., Choi, H., VerBerkmoes, N.C., Trujillo-Reyes, J., Flores-Margez, J.P., White, J.C., Peralta-Videa, J.R., Gardea-Torresdey, J.L., 2015.

- Environmental Effects of Nanoceria on Seed Production of Common Bean (*Phaseolus vulgaris*): A Proteomic Analysis. *Environ. Sci. Technol.* 49, 13283–13293.  
<https://doi.org/10.1021/acs.est.5b03452>
- McGrath, S.P., Chang, A.C., Page, A.L., Witter, E., 1994. Land application of sewage sludge: scientific perspectives of heavy metal loading limits in Europe and the United States. *Environ. Rev.* 2, 108–118. <https://doi.org/10.1139/a94-006>
- Metwally, M.A., Metwally, M.A.A., 2009. Effect of Garlic (*Allium sativum*) on Some Heavy Metal (Copper and Zinc) Induced Alteration in Serum Lipid Profile of *Oreochromis niloticus*. *World J. Fish Mar. Sci.* 1, 1-06.
- Moore-Schiltz, L., Albert, J.M., Singer, M.E., Swain, J., Nock, N.L., 2015. Dietary intake of calcium and magnesium and the metabolic syndrome in the National Health and Nutrition Examination (NHANES) 2001–2010 data. *Br. J. Nutr.* 114, 924–935.  
<https://doi.org/10.1017/S0007114515002482>
- Nakano, Y., Asada, K., 1981. Hydrogen Peroxide is Scavenged by Ascorbate-specific Peroxidase in Spinach Chloroplasts. *Plant Cell Physiol.* 22, 867–880.  
<https://doi.org/10.1093/oxfordjournals.pcp.a076232>
- Nano Copper Oxide Market Size and Industry Forecast - 2022 [WWW Document], 2016. . Allied Mark. Res. URL <https://www.alliedmarketresearch.com/nano-copper-oxide-market> (accessed 4.5.19).
- Österås, A.H., Greger, M., 2006. Interactions between calcium and copper or cadmium in Norway spruce. *Biol. Plant.* 50, 647–652. <https://doi.org/10.1007/s10535-006-0101-6>
- Porra, R.J., 2002. The chequered history of the development and use of simultaneous equations for the accurate determination of chlorophylls a and b. *Photosynth. Res.* 73, 149–156.

<https://doi.org/10.1023/A:1020470224740>

Prasad, K., Laxdal, V.A., Yu, M., Raney, B.L., 1995. Antioxidant activity of allicin, an active principle in garlic. *Mol. Cell. Biochem.* 148, 183–189. <https://doi.org/10.1007/BF00928155>

Prasad, R., Bhattacharyya, A., Nguyen, Q.D., 2017. Nanotechnology in Sustainable Agriculture: Recent Developments, Challenges, and Perspectives. *Front. Microbiol.* 8, 1014. <https://doi.org/10.3389/fmicb.2017.01014>

Rai, M., Ingle, A., 2012. Role of nanotechnology in agriculture with special reference to management of insect pests. *Appl. Microbiol. Biotechnol.* 94, 287–293. <https://doi.org/10.1007/s00253-012-3969-4>

Rastilantie, M.-, Soudek, P., Kotyza, J., Lenikusová, I., Petrová, Š., Benešová, D., Vaněk, T., 2009. Accumulation of heavy metals in hydroponically cultivated garlic (*Allium sativum* L.), onion (*Allium cepa* L.), leek (*Allium porrum* L.) and chive (*Allium schoenoprasum* L.). *J. Food, Agric. Environ.* 7, 761–769.

Rawat, S., Pullagurala, V.L.R., Hernandez-Molina, M., Sun, Y., Niu, G., Hernandez-Viezcas, J.A., Peralta-Videa, J.R., Gardea-Torresdey, J.L., 2018. Impacts of copper oxide nanoparticles on bell pepper (*Capsicum annum* L.) plants: a full life cycle study. *Environ. Sci. Nano* 5, 83–95. <https://doi.org/10.1039/C7EN00697G>

Rico, C.M., Morales, M.I., McCreary, R., Castillo-Michel, H., Barrios, A.C., Hong, J., Tafoya, A., Lee, W.-Y., Varela-Ramirez, A., Peralta-Videa, J.R., Gardea-Torresdey, J.L., 2013. Cerium Oxide Nanoparticles Modify the Antioxidative Stress Enzyme Activities and Macromolecule Composition in Rice Seedlings. *Environ. Sci. Technol.* 47, 14110–14118. <https://doi.org/10.1021/es4033887>

Servin, A.D., White, J.C., 2016. Nanotechnology in agriculture: Next steps for understanding

- engineered nanoparticle exposure and risk. *NanoImpact* 1, 9–12.  
<https://doi.org/10.1016/J.IMPACT.2015.12.002>
- Shang, H., Guo, H., Ma, C., Li, C., Chefetz, B., Polubesova, T., Xing, B., 2019. Maize (*Zea mays* L.) root exudates modify the surface chemistry of CuO nanoparticles: Altered aggregation, dissolution and toxicity. *Sci. Total Environ.* 690, 502–510.  
<https://doi.org/10.1016/j.scitotenv.2019.07.017>
- Stark, W.J., 2011. Nanoparticles in Biological Systems. *Angew. Chemie Int. Ed.* 50, 1242–1258.  
<https://doi.org/10.1002/anie.200906684>
- Tabassum, A., Reitz, S., Rogers, P., Pappu, H.R., 2016. First Report of Iris yellow spot virus Infecting Green Onion (*Allium fistulosum*) in the United States. *Plant Dis.* 100, 2539–2539.  
<https://doi.org/10.1094/PDIS-05-16-0599-PDN>
- Tamez, C., Morelius, E.W., Hernandez-Viezcas, J.A., Peralta-Videa, J.R., Gardea-Torresdey, J., 2019. Biochemical and physiological effects of copper compounds/nanoparticles on sugarcane (*Saccharum officinarum*). *Sci. Total Environ.* 649, 554–562.  
<https://doi.org/10.1016/J.SCITOTENV.2018.08.337>
- The Top 5 Green Onion Producing Countries [WWW Document], 2007. . FAOSTAT data. URL <https://top5ofanything.com/list/0b9685cc/Green-Onion-Producing-Countries> (accessed 4.5.19).
- Trujillo-Reyes, J., Majumdar, S., Botez, C.E., Peralta-Videa, J.R., Gardea-Torresdey, J.L., 2014. Exposure studies of core-shell Fe/Fe<sub>3</sub>O<sub>4</sub> and Cu/CuO NPs to lettuce (*Lactuca sativa*) plants: Are they a potential physiological and nutritional hazard? *J. Hazard. Mater.* 267, 255–263.  
<https://doi.org/10.1016/j.jhazmat.2013.11.067>
- Wang, Z., Xie, X., Zhao, J., Liu, X., Feng, W., White, J.C., Xing, B., 2012. Xylem- and Phloem-

- Based Transport of CuO Nanoparticles in Maize (*Zea mays* L.). *Environ. Sci. Technol.* 46, 4434–4441. <https://doi.org/10.1021/es204212z>
- White, J.C., Gardea-Torresdey, J., 2018. Achieving food security through the very small. *Nat. Nanotechnol.* 13, 627–629. <https://doi.org/10.1038/s41565-018-0223-y>
- Xu, Q.-M., Chen, H., 2011. Antioxidant responses of rice seedling to Ce<sup>4+</sup> under hydroponic cultures. *Ecotoxicol. Environ. Saf.* 74, 1693–1699. <https://doi.org/10.1016/J.ECOENV.2011.04.005>
- Yin, M.-C., Hsu, P.-C., Chang, H.-H., 2003. In Vitro Antioxidant and Antibacterial Activities of Shallot and Scallion. *J. Food Sci.* 68, 281–284. <https://doi.org/10.1111/j.1365-2621.2003.tb14153.x>
- Yue, L., Zhao, J., Yu, X., Lv, K., Wang, Z., Xing, B., 2018. Interaction of CuO nanoparticles with duckweed (*Lemna minor* L): Uptake, distribution and ROS production sites. *Environ. Pollut.* 243, 543–552. <https://doi.org/10.1016/J.ENVPOL.2018.09.013>
- Zhang, Y., Wang, L., Xu, X., Li, F., Wu, Q., 2018. Combined systems of different antibiotics with nano-CuO against *Escherichia coli* and the mechanisms involved. *Nanomedicine* 13, 339–351. <https://doi.org/10.2217/nnm-2017-0290>
- Zuverza-Mena, N., Medina-Velo, I.A., Barrios, A.C., Tan, W., Peralta-Videa, J.R., Gardea-Torresdey, J.L., 2015. Copper nanoparticles/compounds impact agronomic and physiological parameters in cilantro (*Coriandrum sativum*). *Environ. Sci. Process. Impacts* 17, 1783–1793. <https://doi.org/10.1039/C5EM00329F>

### Chapter 3

Acosta, Y., Zhang, Q., Rahaman, A., Ouellet, H., Xiao, C., Sun, J., Li, C., 2014. Imaging

- cytosolic translocation of Mycobacteria with two-photon fluorescence resonance energy transfer microscopy. *Biomed. Opt. Express* 5, 3990. <https://doi.org/10.1364/BOE.5.003990>
- Adisa, I.O., Reddy Pullagurala, V.L., Rawat, S., Hernandez-Viezcas, J.A., Dimkpa, C.O., Elmer, W.H., White, J.C., Peralta-Videa, J.R., Gardea-Torresdey, J.L., 2018. Role of Cerium Compounds in Fusarium Wilt Suppression and Growth Enhancement in Tomato (*Solanum lycopersicum*). *J. Agric. Food Chem.* 66, 5959–5970. <https://doi.org/10.1021/acs.jafc.8b01345>
- Alscher, R.G., Erturk, N., Heath, L.S., 2002. Role of superoxide dismutases (SODs) in controlling oxidative stress in plants. *J. Exp. Bot.* 53, 1331–1341. <https://doi.org/10.1093/jexbot/53.372.1331>
- Andersen, C.P., King, G., Plocher, M., Storm, M., Pokhrel, L.R., Johnson, M.G., Rygiewicz, P.T., 2016. Germination and early plant development of ten plant species exposed to titanium dioxide and cerium oxide nanoparticles. *Environ. Toxicol. Chem.* 35, 2223–2229. <https://doi.org/10.1002/etc.3374>
- ASLI, S., NEUMANN, P.M., 2009. Colloidal suspensions of clay or titanium dioxide nanoparticles can inhibit leaf growth and transpiration via physical effects on root water transport. *Plant. Cell Environ.* 32, 577–584. <https://doi.org/10.1111/j.1365-3040.2009.01952.x>
- Bergamonti, L., Alfieri, I., Lorenzi, A., Predieri, G., Barone, G., Gemelli, G., Mazzoleni, P., Raneri, S., Bersani, D., Lottici, P.P., 2015. Nanocrystalline TiO<sub>2</sub> coatings by sol–gel: photocatalytic activity on Pietra di Noto biocalcarenite. *J. Sol-Gel Sci. Technol.* 75, 141–151. <https://doi.org/10.1007/s10971-015-3684-6>
- Bindraban, P.S., Dimkpa, C., Nagarajan, L., Roy, A., Rabbinge, R., 2015. Revisiting fertilisers

- and fertilisation strategies for improved nutrient uptake by plants. *Biol. Fertil. Soils* 51, 897–911. <https://doi.org/10.1007/s00374-015-1039-7>
- Burke, D., Pietrasiak, N., Situ, S., Abenojar, E., Porche, M., Kraj, P., Lakliang, Y., Samia, A., Burke, D.J., Pietrasiak, N., Situ, S.F., Abenojar, E.C., Porche, M., Kraj, P., Lakliang, Y., Samia, A.C.S., 2015. Iron Oxide and Titanium Dioxide Nanoparticle Effects on Plant Performance and Root Associated Microbes. *Int. J. Mol. Sci.* 16, 23630–23650. <https://doi.org/10.3390/ijms161023630>
- Calia, A., Lettieri, M., Masieri, M., Pal, S., Licciulli, A., Arima, V., 2017. Limestones coated with photocatalytic TiO<sub>2</sub> to enhance building surface with self-cleaning and depolluting abilities. *J. Clean. Prod.* 165, 1036–1047. <https://doi.org/10.1016/J.JCLEPRO.2017.07.193>
- Chen, C., Huang, D., Liu, J., 2009. Functions and Toxicity of Nickel in Plants: Recent Advances and Future Prospects. *CLEAN - Soil, Air, Water* 37, 304–313. <https://doi.org/10.1002/clen.200800199>
- Chen, P., Wei, B., Zhu, X., Gao, D., Gao, Y., Cheng, J., Liu, Y., 2019. Fabrication and characterization of highly hydrophobic rutile TiO<sub>2</sub>-based coatings for self-cleaning. *Ceram. Int.* 45, 6111–6118. <https://doi.org/10.1016/J.CERAMINT.2018.12.085>
- Colangiuli, D., Lettieri, M., Masieri, M., Calia, A., 2019. Field study in an urban environment of simultaneous self-cleaning and hydrophobic nanosized TiO<sub>2</sub>-based coatings on stone for the protection of building surface. *Sci. Total Environ.* 650, 2919–2930. <https://doi.org/10.1016/J.SCITOTENV.2018.10.044>
- Cooper GM., 2000. Structure of the Plasma Membrane, in: *The Cell: A Molecular Approach*. Sinauer Associates, Sunderland (MA). <https://doi.org/10.1038/nchembio.2067>
- Cornelis, G., Hund-Rinke, K., Kuhlbusch, T., van den Brink, N., Nickel, C., 2014. Fate and



- Bioavailability of Engineered Nanoparticles in Soils: A Review. *Crit. Rev. Environ. Sci. Technol.* 44, 2720–2764. <https://doi.org/10.1080/10643389.2013.829767>
- Deák, M., Horváth, G. V., Davletova, S., Török, K., Sass, L., Vass, I., Barna, B., Király, Z., Dudits, D., 1999. Plants ectopically expressing the ironbinding protein, ferritin, are tolerant to oxidative damage and pathogens. *Nat. Biotechnol.* 17, 192–196. <https://doi.org/10.1038/6198>
- Deng, C., Wang, Y., Cota-Ruiz, K., Reyes, A., Sun, Y., Peralta-Videa, J., Hernandez-Viezcas, J.A., Turley, R.S., Niu, G., Li, C., Gardea-Torresdey, J., 2020. Bok choy (*Brassica rapa*) grown in copper oxide nanoparticles-amended soils exhibits toxicity in a phenotype-dependent manner: Translocation, biodistribution and nutritional disturbance. *J. Hazard. Mater.* 398, 122978. <https://doi.org/10.1016/j.jhazmat.2020.122978>
- Du, W., Sun, Y., Ji, R., Zhu, J., Wu, J., Guo, H., 2011. TiO<sub>2</sub> and ZnO nanoparticles negatively affect wheat growth and soil enzyme activities in agricultural soil. *J. Environ. Monit.* 13, 822. <https://doi.org/10.1039/c0em00611d>
- Ebbs, S.D., Bradfield, S.J., Kumar, P., White, J.C., Musante, C., Ma, X., 2016. Accumulation of zinc, copper, or cerium in carrot (*Daucus carota*) exposed to metal oxide nanoparticles and metal ions. *Environ. Sci. Nano* 3. <https://doi.org/10.1039/c5en00161g>
- Foltête, A.-S., Masfaraud, J.-F., Bigorgne, E., Nahmani, J., Chaurand, P., Botta, C., Labille, J., Rose, J., Férard, J.-F., Cotelle, S., 2011. Environmental impact of sunscreen nanomaterials: Ecotoxicity and genotoxicity of altered TiO<sub>2</sub> nanocomposites on *Vicia faba*. *Environ. Pollut.* 159, 2515–2522. <https://doi.org/10.1016/J.ENVPOL.2011.06.020>
- Frazier, T.P., Burklew, C.E., Zhang, B., 2014. Titanium dioxide nanoparticles affect the growth and microRNA expression of tobacco (*Nicotiana tabacum*). *Funct. Integr. Genomics* 14,

75–83. <https://doi.org/10.1007/s10142-013-0341-4>

Gao, F., Hong, F., Liu, C., Zheng, L., Su, M., Wu, X., Yang, F., Wu, C., Yang, P., 2006.

Mechanism of Nano-anatase TiO<sub>2</sub> on Promoting Photosynthetic Carbon Reaction of Spinach: Inducing Complex of Rubisco-Rubisco Activase. *Biol. Trace Elem. Res.* 111, 239–254. <https://doi.org/10.1385/BTER:111:1:239>

Ge, Y., Schimel, J.P., Holden, P.A., 2011. Evidence for negative effects of TiO<sub>2</sub> and ZnO nanoparticles on soil bacterial communities. *Environ. Sci. Technol.* 45, 1659–1664.

<https://doi.org/10.1021/es103040t>

Gottschalk, F., Sonderer, T., Scholz, R.W., Nowack, B., 2009. Modeled Environmental Concentrations of Engineered Nanomaterials (TiO<sub>2</sub>, ZnO, Ag, CNT, Fullerenes) for Different Regions. *Environ. Sci. Technol.* 43, 9216–9222.

<https://doi.org/10.1021/es9015553>

Guo, K.M., Babourina, O., Christopher, D.A., Borsic, T., Rengel, Z., 2010. The cyclic nucleotide-gated channel AtCNGC10 transports Ca<sup>2+</sup> and Mg<sup>2+</sup> in *Arabidopsis*. *Physiol. Plant.* 139, 303–312. <https://doi.org/10.1111/j.1399-3054.2010.01366.x>

Hepler, P.K., 2005. Calcium: A central regulator of plant growth and development. *Plant Cell.*

<https://doi.org/10.1105/tpc.105.032508>

Hong, F., Yang, F., Liu, C., Gao, Q., Wan, Z., Gu, F., Wu, C., Ma, Z., Zhou, J., Yang, P., 2005a.

Influences of nano-TiO<sub>2</sub> on the chloroplast aging of spinach under light. *Biol. Trace Elem. Res.* 104, 249–260. <https://doi.org/10.1385/BTER:104:3:249>

Hong, F., Zhou, J., Liu, C., Yang, F., Wu, C., Zheng, L., Yang, P., 2005b. Effect of Nano-TiO<sub>2</sub> on Photochemical Reaction of Chloroplasts of Spinach. *Biol. Trace Elem. Res.* 105, 269–

279. <https://doi.org/10.1385/BTER:105:1-3:269>

- Hrubý, M., Cígler, P., Kuzel, S., 2002. Contribution to understanding the mechanism of titanium action in plant. *J. Plant Nutr.* 25, 577–598. <https://doi.org/10.1081/PLN-120003383>
- Jacob, D.L., Borchardt, J.D., Navaratnam, L., Otte, M.L., Bezbaruah, A.N., 2013. Uptake and Translocation of Ti From Nanoparticles in Crops and Wetland Plants. *Int. J. Phytoremediation* 15, 142–153. <https://doi.org/10.1080/15226514.2012.683209>
- Jiang, F., Shen, Y., Ma, C., Zhang, X., Cao, W., Rui, Y., 2017. Effects of TiO<sub>2</sub> nanoparticles on wheat (*Triticum aestivum* L.) seedlings cultivated under super-elevated and normal CO<sub>2</sub> conditions. *PLoS One* 12, e0178088. <https://doi.org/10.1371/journal.pone.0178088>
- Keller, A.A., Lazareva, A., 2013. Predicted Releases of Engineered Nanomaterials: From Global to Regional to Local. *Environ. Sci. Technol. Lett.* 1, 65–70. <https://doi.org/10.1021/ez400106t>
- Kinraide, T.B., Wang, P., 2010. The surface charge density of plant cell membranes ( $\sigma$ ): An attempt to resolve conflicting values for intrinsic  $\sigma$ . *J. Exp. Bot.* 61, 2507–2518. <https://doi.org/10.1093/jxb/erq082>
- Larue, C., Castillo-Michel, H., Sobanska, S., Trcera, N., Sorieul, S., Cécillon, L., Ouerdane, L., Legros, S., Sarret, G., 2014. Fate of pristine TiO<sub>2</sub> nanoparticles and aged paint-containing TiO<sub>2</sub> nanoparticles in lettuce crop after foliar exposure. *J. Hazard. Mater.* 273, 17–26. <https://doi.org/10.1016/J.JHAZMAT.2014.03.014>
- Larue, C., Castillo-Michel, H., Stein, R.J., Fayard, B., Pouyet, E., Villanova, J., Magnin, V., Pradas del Real, A.-E., Trcera, N., Legros, S., Sorieul, S., Sarret, G., 2016. Innovative combination of spectroscopic techniques to reveal nanoparticle fate in a crop plant. *Spectrochim. Acta Part B At. Spectrosc.* 119, 17–24. <https://doi.org/10.1016/J.SAB.2016.03.005>

- Larue, C., Laurette, J., Herlin-Boime, N., Khodja, H., Fayard, B., Flank, A.-M., Brisset, F., Carriere, M., 2012. Accumulation, translocation and impact of TiO<sub>2</sub> nanoparticles in wheat (*Triticum aestivum* spp.): Influence of diameter and crystal phase. *Sci. Total Environ.* 431, 197–208. <https://doi.org/10.1016/J.SCITOTENV.2012.04.073>
- Lindsay, W.L., 1972. Zinc in Soils and Plant Nutrition, *Advances in Agronomy*. Academic Press. [https://doi.org/10.1016/S0065-2113\(08\)60635-5](https://doi.org/10.1016/S0065-2113(08)60635-5)
- Magnesium | Linus Pauling Institute | Oregon State University [WWW Document], n.d. [https://doi.org/Oregon State University](https://doi.org/Oregon%20State%20University)
- Majumdar, S., Almeida, I.C., Arigi, E.A., Choi, H., VerBerkmoes, N.C., Trujillo-Reyes, J., Flores-Margez, J.P., White, J.C., Peralta-Videa, J.R., Gardea-Torresdey, J.L., 2015. Environmental Effects of Nanoceria on Seed Production of Common Bean (*Phaseolus vulgaris*): A Proteomic Analysis. *Environ. Sci. Technol.* 49, 13283–13293. <https://doi.org/10.1021/acs.est.5b03452>
- Mandeh, M., Omidi, M., Rahaie, M., 2012. In Vitro Influences of TiO<sub>2</sub> Nanoparticles on Barley (*Hordeum vulgare* L.) Tissue Culture. *Biol. Trace Elem. Res.* 150, 376–380. <https://doi.org/10.1007/s12011-012-9480-z>
- Mitrano, D.M., Motellier, S., Clavaguera, S., Nowack, B., 2015. Review of nanomaterial aging and transformations through the life cycle of nano-enhanced products. *Environ. Int.* 77, 132–147. <https://doi.org/10.1016/J.ENVINT.2015.01.013>
- Pancrecius, J.K., Ulaeto, S.B., Ramya, R., Rajan, T.P.D., Pai, B.C., 2018. Metallic composite coatings by electroless technique – a critical review. *Int. Mater. Rev.* 63, 488–512. <https://doi.org/10.1080/09506608.2018.1506692>
- Piccinno, F., Gottschalk, F., Seeger, S., Nowack, B., 2012. Industrial production quantities and

- uses of ten engineered nanomaterials in Europe and the world. *J. Nanoparticle Res.* 14, 1109. <https://doi.org/10.1007/s11051-012-1109-9>
- Pošćić, F., Mattiello, A., Fellet, G., Miceli, F., Marchiol, L., Poščić, F., Mattiello, A., Fellet, G., Miceli, F., Marchiol, L., 2016. Effects of Cerium and Titanium Oxide Nanoparticles in Soil on the Nutrient Composition of Barley (*Hordeum vulgare* L.) Kernels. *Int. J. Environ. Res. Public Health* 13, 577. <https://doi.org/10.3390/ijerph13060577>
- Rafique, R., Arshad, M., Khokhar, M.F., Qazi, I.A., Hamza, A., Virk, N., 2015. Growth Response of Wheat to Titania Nanoparticles Application. *NUST J. Eng. Sci.* 7, 42–46. <https://doi.org/10.24949/NJES.V7I1.133.G71>
- Raliya, R., Nair, R., Chavalmane, S., Wang, W.-N., Biswas, P., 2015. Mechanistic evaluation of translocation and physiological impact of titanium dioxide and zinc oxide nanoparticles on the tomato (*Solanum lycopersicum* L.) plant. *Metallomics* 7, 1584–1594. <https://doi.org/10.1039/C5MT00168D>
- Robichaud, C.O., Uyar, A.E., Darby, M.R., Zucker, L.G., Wiesner, M.R., 2009. Estimates of Upper Bounds and Trends in Nano-TiO<sub>2</sub> Production As a Basis for Exposure Assessment. *Environ. Sci. Technol.* 43, 4227–4233. <https://doi.org/10.1021/es8032549>
- Rubatzky, V.E., Quiros, C.F., Simon, P.W., 1999. Carrots and related vegetable Umbelliferae., Carrots and related vegetable Umbelliferae. CABI Publishing.
- Septian, 2017. 15 Health Benefits of Carrot Leaves [WWW Document]. <https://doi.org/DrHeben-DrHealthBenefits.com>
- Servin, A.D., Castillo-Michel, H., Hernandez-Viezcas, J.A., Diaz, B.C., Peralta-Videa, J.R., Gardea-Torresdey, J.L., 2012. Synchrotron Micro-XRF and Micro-XANES Confirmation of the Uptake and Translocation of TiO<sub>2</sub> Nanoparticles in Cucumber (*Cucumis sativus*) Plants.

- Environ. Sci. Technol. 46, 7637–7643. <https://doi.org/10.1021/es300955b>
- Sharma, H.K., 2018. Carrots Production, Processing, and Nutritional Quality, in: Handbook of Vegetables and Vegetable Processing. John Wiley & Sons, Ltd, Chichester, UK, pp. 589–608. <https://doi.org/10.1002/9781119098935.ch25>
- Song, G., Gao, Y., Wu, H., Hou, W., Zhang, C., Ma, H., 2012. Physiological effect of anatase TiO<sub>2</sub> nanoparticles on *Lemna minor*. Environ. Toxicol. Chem. 31, 2147–2152. <https://doi.org/10.1002/etc.1933>
- Sors, T.G., Ellis, D.R., Salt, D.E., 2005. Selenium uptake, translocation, assimilation and metabolic fate in plants. Photosynth. Res. 86, 373–389. <https://doi.org/10.1007/s11120-005-5222-9>
- Tan, W., Du, W., Barrios, A.C., Armendariz, R., Zuverza-Mena, N., Ji, Z., Chang, C.H., Zink, J.I., Hernandez-Viezcas, J.A., Peralta-Videa, J.R., Gardea-Torresdey, J.L., 2017a. Surface coating changes the physiological and biochemical impacts of nano-TiO<sub>2</sub> in basil (*Ocimum basilicum*) plants. Environ. Pollut. 222, 64–72. <https://doi.org/10.1016/J.ENVPOL.2017.01.002>
- Tan, W., Du, W., Barrios, A.C., Armendariz, R., Zuverza-Mena, N., Ji, Z., Chang, C.H., Zink, J.I., Hernandez-Viezcas, J.A., Peralta-Videa, J.R., Gardea-Torresdey, J.L., 2017b. Surface coating changes the physiological and biochemical impacts of nano-TiO<sub>2</sub> in basil (*Ocimum basilicum*) plants. Environ. Pollut. 222, 64–72. <https://doi.org/10.1016/J.ENVPOL.2017.01.002>
- Tan, W., Peralta-Videa, J.R., Gardea-Torresdey, J.L., 2018. Interaction of titanium dioxide nanoparticles with soil components and plants: current knowledge and future research needs – a critical review. Environ. Sci. Nano 5, 257–278. <https://doi.org/10.1039/C7EN00985B>

- Tumburu, L., Andersen, C.P., Rygiewicz, P.T., Reichman, J.R., 2017. Molecular and physiological responses to titanium dioxide and cerium oxide nanoparticles in *Arabidopsis*. *Environ. Toxicol. Chem.* 36, 71–82. <https://doi.org/10.1002/etc.3500>
- Tumburu, L., Andersen, C.P., Rygiewicz, P.T., Reichman, J.R., 2015. Phenotypic and genomic responses to titanium dioxide and cerium oxide nanoparticles in *Arabidopsis* germinants. *Environ. Toxicol. Chem.* 34, 70–83. <https://doi.org/10.1002/etc.2756>
- Vittori Antisari, L., Carbone, S., Gatti, A., Vianello, G., Nannipieri, P., 2015. Uptake and translocation of metals and nutrients in tomato grown in soil polluted with metal oxide (CeO<sub>2</sub>, Fe<sub>3</sub>O<sub>4</sub>, SnO<sub>2</sub>, TiO<sub>2</sub>) or metallic (Ag, Co, Ni) engineered nanoparticles. *Environ. Sci. Pollut. Res.* 22, 1841–1853. <https://doi.org/10.1007/s11356-014-3509-0>
- Wang, Y., Deng, C., Cota-Ruiz, K., Peralta-Videa, J.R., Sun, Y., Rawat, S., Tan, W., Reyes, A., Hernandez-Viezcas, J.A., Niu, G., Li, C., Gardea-Torresdey, J.L., 2020. Improvement of nutrient elements and allicin content in green onion (*Allium fistulosum*) plants exposed to CuO nanoparticles. *Sci. Total Environ.* 725, 138387. <https://doi.org/10.1016/j.scitotenv.2020.138387>
- Wu, B., Zhu, L., Le, X.C., 2017. Metabolomics analysis of TiO<sub>2</sub> nanoparticles induced toxicological effects on rice (*Oryza sativa* L.). *Environ. Pollut.* 230, 302–310. <https://doi.org/10.1016/J.ENVPOL.2017.06.062>
- Yang, F., Hong, F., You, W., Liu, C., Gao, F., Wu, C., Yang, P., 2006. Influences of Nano-anatase TiO<sub>2</sub> on the Nitrogen Metabolism of Growing Spinach. *Biol. Trace Elem. Res.* 110, 179–190. <https://doi.org/10.1385/BTER:110:2:179>
- Yang, F., Liu, C., Gao, F., Su, M., Wu, X., Zheng, L., Hong, F., Yang, P., 2007. The Improvement of Spinach Growth by Nano-anatase TiO<sub>2</sub> Treatment Is Related to Nitrogen

Photoreduction. *Biol. Trace Elem. Res.* 119, 77–88. <https://doi.org/10.1007/s12011-007-0046-4>

Zahra, Z., Arshad, M., Rafique, R., Mahmood, A., Habib, A., Qazi, I.A., Khan, S.A., 2015. Metallic Nanoparticle (TiO<sub>2</sub> and Fe<sub>3</sub>O<sub>4</sub>) Application Modifies Rhizosphere Phosphorus Availability and Uptake by *Lactuca sativa*. *J. Agric. Food Chem.* 63, 6876–6882. <https://doi.org/10.1021/acs.jafc.5b01611>

Zahra, Z., Waseem, N., Zahra, R., Lee, H., Badshah, M.A., Mehmood, A., Choi, H.-K., Arshad, M., 2017. Growth and Metabolic Responses of Rice (*Oryza sativa* L.) Cultivated in Phosphorus-Deficient Soil Amended with TiO<sub>2</sub> Nanoparticles. *J. Agric. Food Chem.* 65, 5598–5606. <https://doi.org/10.1021/acs.jafc.7b01843>

Zheng, L., Hong, F., Lu, S., Liu, C., 2005. Effect of Nano-TiO<sub>2</sub> on Strength of Naturally Aged Seeds and Growth of Spinach.

#### Chapter 4

Abadía, J., 2012. Iron Nutrition in Soils and Plants: Proceedings of the Seventh International Symposium on Iron Nutrition and Interactions in Plants. Springer, Science & Business Media, Zaragoza, Spain.

Adisa, I.O., Reddy Pullagurala, V.L., Rawat, S., Hernandez-Viezcas, J.A., Dimkpa, C.O., Elmer, W.H., White, J.C., Peralta-Videa, J.R., Gardea-Torresdey, J.L., 2018. Role of Cerium Compounds in Fusarium Wilt Suppression and Growth Enhancement in Tomato (*Solanum lycopersicum*). *J. Agric. Food Chem.* 66, 5959–5970. <https://doi.org/10.1021/acs.jafc.8b01345>



- Alexander†, M., 2000. Aging, Bioavailability, and Overestimation of Risk from Environmental Pollutants. <https://doi.org/10.1021/ES001069+>
- Alscher, R.G., Erturk, N., Heath, L.S., 2002. Role of superoxide dismutases (SODs) in controlling oxidative stress in plants. *J. Exp. Bot.* 53, 1331–1341. <https://doi.org/10.1093/jxb/53.372.1331>
- Auffan, M., Pedoutour, M., Rose, J., Masion, A., Ziarelli, F., Borschneck, D., Chaneac, C., Botta, C., Chaurand, P., Labille, J., Bottero, J.-Y., 2010. Structural Degradation at the Surface of a TiO<sub>2</sub>-Based Nanomaterial Used in Cosmetics. *Environ. Sci. Technol.* 44, 2689–2694. <https://doi.org/10.1021/es903757q>
- Bergamonti, L., Alfieri, I., Lorenzi, A., Predieri, G., Barone, G., Gemelli, G., Mazzoleni, P., Raneri, S., Bersani, D., Lottici, P.P., 2015. Nanocrystalline TiO<sub>2</sub> coatings by sol–gel: photocatalytic activity on Pietra di Noto biocalcarene. *J. Sol-Gel Sci. Technol.* 75, 141–151. <https://doi.org/10.1007/s10971-015-3684-6>
- Calia, A., Lettieri, M., Masieri, M., Pal, S., Licciulli, A., Arima, V., 2017. Limestones coated with photocatalytic TiO<sub>2</sub> to enhance building surface with self-cleaning and depolluting abilities. *J. Clean. Prod.* 165, 1036–1047. <https://doi.org/10.1016/J.JCLEPRO.2017.07.193>
- Chen, G., Liu, X., Su, C., 2012. Distinct effects of humic acid on transport and retention of TiO<sub>2</sub> rutile nanoparticles in saturated sand columns. *Environ. Sci. Technol.* 46, 7142–7150. <https://doi.org/10.1021/es204010g>
- Chen, P., Wei, B., Zhu, X., Gao, D., Gao, Y., Cheng, J., Liu, Y., 2019. Fabrication and characterization of highly hydrophobic rutile TiO<sub>2</sub>-based coatings for self-cleaning. *Ceram. Int.* 45, 6111–6118. <https://doi.org/10.1016/J.CERAMINT.2018.12.085>
- Colangiuli, D., Lettieri, M., Masieri, M., Calia, A., 2019. Field study in an urban environment of

- simultaneous self-cleaning and hydrophobic nanosized TiO<sub>2</sub>-based coatings on stone for the protection of building surface. *Sci. Total Environ.* 650, 2919–2930.  
<https://doi.org/10.1016/J.SCITOTENV.2018.10.044>
- Cooper GM., 2000. Structure of the Plasma Membrane, in: *The Cell: A Molecular Approach*. Sinauer Associates, Sunderland (MA). <https://doi.org/10.1038/nchembio.2067>
- Coutris, C., Joner, E.J., Oughton, D.H., 2012. Aging and soil organic matter content affect the fate of silver nanoparticles in soil. *Sci. Total Environ.* 420, 327–333.  
<https://doi.org/10.1016/j.scitotenv.2012.01.027>
- de Boer, A., 1999. Potassium Translocation into the Root Xylem. *Plant Biol.* 1, 36–45.  
<https://doi.org/10.1055/s-2007-978486>
- DuBois, M., Gilles, K.A., Hamilton, J.K., Rebers, P.A., Smith, F., 1956. Colorimetric Method for Determination of Sugars and Related Substances. *Anal. Chem.* 28, 350–356.  
<https://doi.org/10.1021/ac60111a017>
- Godinez, I.G., Darnault, C.J.G., 2011. Aggregation and transport of nano-TiO<sub>2</sub> in saturated porous media: Effects of pH, surfactants and flow velocity. *Water Res.* 45, 839–851.  
<https://doi.org/10.1016/J.WATRES.2010.09.013>
- Gottschalk, F., Sonderer, T., Scholz, R.W., Nowack, B., 2009. Modeled environmental concentrations of engineered nanomaterials (TiO<sub>2</sub>, ZnO, Ag, CNT, fullerenes) for different regions. *Environ. Sci. Technol.* 43, 9216–9222.
- Hajra, A., Mondal, N.K., 2017. Effects of ZnO and TiO<sub>2</sub> nanoparticles on germination, biochemical and morphoanatomical attributes of *Cicer arietinum* L. *Energy, Ecol. Environ.* 2, 277–288. <https://doi.org/10.1007/s40974-017-0059-6>
- Jaberzadeh, A., Moaveni, P., Tohidi Moghadam, H.R., Zahedi, H., 2013. Influence of bulk and

- nanoparticles titanium foliar application on some agronomic traits, seed gluten and starch contents of wheat subjected to water deficit stress. *Not. Bot. Horti Agrobot. Cluj-Napoca* 41, 201–207. <https://doi.org/10.15835/NBHA4119093>
- Jiang, F., Shen, Y., Ma, C., Zhang, X., Cao, W., Rui, Y., 2017. Effects of TiO<sub>2</sub> nanoparticles on wheat (*Triticum aestivum* L.) seedlings cultivated under super-elevated and normal CO<sub>2</sub> conditions. *PLoS One* 12, e0178088. <https://doi.org/10.1371/journal.pone.0178088>
- Judy, J.D., Unrine, J.M., Rao, W., Wirick, S., Bertsch, P.M., 2012. Bioavailability of gold nanomaterials to plants: Importance of particle size and surface coating. *Environ. Sci. Technol.* 46, 8467–8474. <https://doi.org/10.1021/es3019397>
- Keller, A.A., Lazareva, A., 2013. Predicted Releases of Engineered Nanomaterials: From Global to Regional to Local. *Environ. Sci. Technol. Lett.* 1, 65–70. <https://doi.org/10.1021/ez400106t>
- Koelmel, J., Leland, T., Wang, H., Amarasiriwardena, D., Xing, B., 2013. Investigation of gold nanoparticles uptake and their tissue level distribution in rice plants by laser ablation-inductively coupled-mass spectrometry. *Environ. Pollut.* 174, 222–228. <https://doi.org/10.1016/j.envpol.2012.11.026>
- Labille, J., Feng, J., Botta, C., Borschneck, D., Sammut, M., Cabie, M., Auffan, M., Rose, J., Bottero, J.Y., 2010. Aging of TiO<sub>2</sub> nanocomposites used in sunscreen. Dispersion and fate of the degradation products in aqueous environment. *Environ. Pollut.* 158, 3482–3489. <https://doi.org/10.1016/j.envpol.2010.02.012>
- Lapied, E., Nahmani, J.Y., Moudilou, E., Chaurand, P., Labille, J., Rose, J., Exbrayat, J.-M., Oughton, D.H., Joner, E.J., 2011. Ecotoxicological effects of an aged TiO<sub>2</sub> nanocomposite measured as apoptosis in the anecic earthworm *Lumbricus terrestris* after exposure through

- water, food and soil. *Environ. Int.* 37, 1105–1110.  
<https://doi.org/10.1016/J.ENVINT.2011.01.009>
- Larue, C., Castillo-Michel, H., Sobanska, S., Trcera, N., Sorieul, S., Cécillon, L., Ouerdane, L., Legros, S., Sarret, G., 2014a. Fate of pristine TiO<sub>2</sub> nanoparticles and aged paint-containing TiO<sub>2</sub> nanoparticles in lettuce crop after foliar exposure. *J. Hazard. Mater.* 273, 17–26.  
<https://doi.org/10.1016/J.JHAZMAT.2014.03.014>
- Larue, C., Castillo-Michel, H., Sobanska, S., Trcera, N., Sorieul, S., Cécillon, L., Ouerdane, L., Legros, S., Sarret, G., 2014b. Fate of pristine TiO<sub>2</sub> nanoparticles and aged paint-containing TiO<sub>2</sub> nanoparticles in lettuce crop after foliar exposure. *J. Hazard. Mater.* 273, 17–26.  
<https://doi.org/10.1016/J.JHAZMAT.2014.03.014>
- Larue, C., Castillo-Michel, H., Stein, R.J., Fayard, B., Pouyet, E., Villanova, J., Magnin, V., del Real, A.-E.P., Trcera, N., Legros, S., 2016. Innovative combination of spectroscopic techniques to reveal nanoparticle fate in a crop plant. *Spectrochim. Acta Part B At. Spectrosc.* 119, 17–24.
- Lyu, S., Wei, X., Chen, J., Wang, C., Wang, X., Pan, D., 2017. Titanium as a Beneficial Element for Crop Production. *Front. Plant Sci.* 8, 597. <https://doi.org/10.3389/fpls.2017.00597>
- Majumdar, S., Almeida, I.C., Arigi, E.A., Choi, H., VerBerkmoes, N.C., Trujillo-Reyes, J., Flores-Margez, J.P., White, J.C., Peralta-Videa, J.R., Gardea-Torresdey, J.L., 2015. Environmental Effects of Nanoceria on Seed Production of Common Bean (*Phaseolus vulgaris*): A Proteomic Analysis. *Environ. Sci. Technol.* 49, 13283–13293.  
<https://doi.org/10.1021/acs.est.5b03452>
- Mandeh, M., Omid, M., Rahaie, M., 2012. *In Vitro* Influences of TiO<sub>2</sub> Nanoparticles on Barley (*Hordeum vulgare* L.) Tissue Culture. *Biol. Trace Elem. Res.* 150, 376–380.

<https://doi.org/10.1007/s12011-012-9480-z>

- Mitrano, D.M., Motellier, S., Clavaguera, S., Nowack, B., 2015. Review of nanomaterial aging and transformations through the life cycle of nano-enhanced products. *Environ. Int.* 77, 132–147. <https://doi.org/10.1016/j.envint.2015.01.013>
- Mudunkotuwa, I.A., Pettibone, J.M., Grassian, V.H., 2012. Environmental implications of nanoparticle aging in the processing and fate of copper-based nanomaterials. *Environ. Sci. Technol.* 46, 7001–7010. <https://doi.org/10.1021/es203851d>
- Naftaly, A., Dror, I., Berkowitz, B., 2016. Measurement and modeling of engineered nanoparticle transport and aging dynamics in a reactive porous medium. *Water Resour. Res.* 52, 5473–5491. <https://doi.org/10.1002/2016WR018780>
- Pancrecius, J.K., Ulaeto, S.B., Ramya, R., Rajan, T.P.D., Pai, B.C., 2018. Metallic composite coatings by electroless technique – a critical review. *Int. Mater. Rev.* 63, 488–512. <https://doi.org/10.1080/09506608.2018.1506692>
- Peijnenburg, W., Praetorius, A., Scott-Fordsmand, J., Cornelis, G., 2016. Fate assessment of engineered nanoparticles in solids dominated media – Current insights and the way forward. *Environ. Pollut.* 218, 1365–1369. <https://doi.org/10.1016/J.ENVPOL.2015.11.043>
- Piccinno, F., Gottschalk, F., Seeger, S., Nowack, B., 2012. Industrial production quantities and uses of ten engineered nanomaterials in Europe and the world. *J. Nanoparticle Res.* 14, 1109. <https://doi.org/10.1007/s11051-012-1109-9>
- Pošćić, F., Mattiello, A., Fellet, G., Miceli, F., Marchiol, L., Poščić, F., Mattiello, A., Fellet, G., Miceli, F., Marchiol, L., 2016. Effects of Cerium and Titanium Oxide Nanoparticles in Soil on the Nutrient Composition of Barley (*Hordeum vulgare* L.) Kernels. *Int. J. Environ. Res. Public Health* 13, 577. <https://doi.org/10.3390/ijerph13060577>

- Rawat, S., Pullagurala, V.L.R., Adisa, I.O., Wang, Y., Gardea-Torresdey, J.L., 2018. Factors affecting fate and transport of engineered nanomaterials in terrestrial environments. *Curr. Opin. Environ. Sci. Heal.* 6, 47–53. <https://doi.org/10.1016/J.COESH.2018.07.014>
- Robichaud, C.O., Uyar, A.E., Darby, M.R., Zucker, L.G., Wiesner, M.R., 2009. Estimates of Upper Bounds and Trends in Nano-TiO<sub>2</sub> Production As a Basis for Exposure Assessment. *Environ. Sci. Technol.* 43, 4227–4233. <https://doi.org/10.1021/es8032549>
- Servin, A.D., Morales, M.I., Castillo-Michel, H., Hernandez-Viezcas, J.A., Munoz, B., Zhao, L., Nunez, J.E., Peralta-Videa, J.R., Gardea-Torresdey, J.L., 2013. Synchrotron Verification of TiO<sub>2</sub> Accumulation in Cucumber Fruit: A Possible Pathway of TiO<sub>2</sub> Nanoparticle Transfer from Soil into the Food Chain. *Environ. Sci. Technol.* 47, 11592–11598. <https://doi.org/10.1021/es403368j>
- Sharma, H.K., 2018. Carrots Production, Processing, and Nutritional Quality, in: *Handbook of Vegetables and Vegetable Processing*. John Wiley & Sons, Ltd, Chichester, UK, pp. 589–608. <https://doi.org/10.1002/9781119098935.ch25>
- Tan, W., Du, W., Barrios, A.C., Armendariz, R., Zuverza-Mena, N., Ji, Z., Chang, C.H., Zink, J.I., Hernandez-Viezcas, J.A., Peralta-Videa, J.R., Gardea-Torresdey, J.L., 2017a. Surface coating changes the physiological and biochemical impacts of nano-TiO<sub>2</sub> in basil (*Ocimum basilicum*) plants. *Environ. Pollut.* 222, 64–72. <https://doi.org/10.1016/J.ENVPOL.2017.01.002>
- Tan, W., Du, W., Barrios, A.C., Armendariz, R., Zuverza-Mena, N., Ji, Z., Chang, C.H., Zink, J.I., Hernandez-Viezcas, J.A., Peralta-Videa, J.R., Gardea-Torresdey, J.L., 2017b. Surface coating changes the physiological and biochemical impacts of nano-TiO<sub>2</sub> in basil (*Ocimum basilicum*) plants. *Environ. Pollut.* 222, 64–72.

<https://doi.org/10.1016/J.ENVPOL.2017.01.002>

Wang, Y., Deng, C., Cota-Ruiz, K., Peralta-Videa, J.R., Sun, Y., Rawat, S., Tan, W., Reyes, A., Hernandez-Viezcas, J.A., Niu, G., Li, C., Gardea-Torresdey, J.L., 2020a. Improvement of nutrient elements and allicin content in green onion (*Allium fistulosum*) plants exposed to CuO nanoparticles. *Sci. Total Environ.* 725, 138387.

<https://doi.org/10.1016/j.scitotenv.2020.138387>

Wang, Y., Deng, C., Cota-ruiz, K., Tan, W., Reyes, A., Peralta-Videa, J.R., Li, C., Gardea-Torresdey, J.L., 2020b. Effects of different surface-coated nTiO<sub>2</sub> on full-life grown carrot plants : impacts on root splitting , essential elements , and Ti uptake. *J. Hazard. Mater.* (Submitted and in review).

White, J.C., Gardea-Torresdey, J., 2018. Achieving food security through the very small. *Nat. Nanotechnol.* 13, 627–629. <https://doi.org/10.1038/s41565-018-0223-y>

Wu, J.-C., Qiu, H.-M., Yang, G.-Q., Dong, B., Gu, H., 2003. Nutrient Uptake of Rice Roots in Response to Infestation of *Nilaparvata lugens* (Stål) (Homoptera: Delphacidae). *J. Econ. Entomol.* 96, 1798–1804. <https://doi.org/10.1093/jee/96.6.1798>

Yechezkel, Y., Dror, I., Berkowitz, B., 2016. Transport of engineered nanoparticles in partially saturated sand columns. *J. Hazard. Mater.* 311, 254–262.

<https://doi.org/10.1016/J.JHAZMAT.2016.03.027>

## Vita

Yi Wang was born in Nanjing, Jiangsu, China. She received her Bachelor of Science in University of Science and Technology of China (USTC), 2012. Then, she joined the Doctoral Program in the Department of Chemistry and Biochemistry at The University of Texas at El Paso. Her research project has been under the supervision of Dr. Jorge Gardea Torresdey.

During her Ph.D. studies, she has published two peer-review journal articles as the first author. Also, she has published five peer-review journal articles, one peer-review book chapter and one journal review article, all of them as a co-author. She recently submitted a research article to a high-impact journal that is under review. Moreover, she is preparing three more manuscripts that will be submitted soon. She is also a member of the University of California's Center for Environmental Implications of Nanotechnology (UC CEIN) and the American Chemical Society (ACS). She has presented her research at four different local or national conference meetings.

While pursuing her Ph.D., Mrs. Yi Wang worked as a Teaching Assistant in the Department of Chemistry and Biochemistry. Also, she was the president (2016-2018) of UTEP Chinese Students and Scholars Association (CSSA). She also served as a volunteer in several campus research events, such as research expo and COURI.

Contact Information: 208 Argonaut Dr

El Paso, TX 79912

[ywang10@miners.utep.edu](mailto:ywang10@miners.utep.edu)